MASTER OF SCIENCE

Exploring Parkinson's disease associated LRRK2 and PINK1/Parkin signal transduction pathways within immune cells

Joseph, Theresita

Award date:
2019

Exploring Parkinson's disease associated LRRK2 and PINK1/Parkin signal transduction pathways within immune cells

Theresita Joseph

Thesis submitted for degree of Masters of Research (MRes)

May 2019 (original submission), October 2019 (revised)

<u>Project Supervisors:</u>

Professor Dario Alessi (1) & Professor Miratul Muqit (2)

I. ACKNOWLEDGMENTS:

First and foremost, I am immensely grateful to my supervisors, Professor Miratul Muqit and Professor Dario Alessi, for providing me with the opportunity to undertake this Masters of Research (MRes) degree, and for the continual support, advice and encouragement they have provided me throughout my time at the MRC PPU in Dundee.

Importantly, the work I conducted within this project would not have been possible without the technical guidance, moral support, inspiration, (and voluntary blood donation!) provided by numerous members of the MM and DRA laboratories. In particular, special thanks to Prosenjit Pal, with whom I conducted several *P. aeruginosa* infection experiments with, and to Pawel Lis for his initial teaching on key laboratory techniques used within this project. In addition, specific thanks to Alexia Kalogeropulou, Anna Tasegian, Francesca Tonelli, Kirsten Balk, Elena Purtle, Odetta Antico, Holly Keir, Andy Waddell and Andy Shaw, for their teaching and guidance in several experiments I conducted. I am also grateful to Dr Esther Sammler, Professor James Chalmers, and the Cystic fibrosis (CF) respiratory nurses at Ninewells Hospital for their assistance in helping me obtain sputum samples. Furthermore, I am thankful for the administrative assistance provided by Alison Hart (especially for organising the many Ninewells taxi journeys), and to Emma Mitchell, whose support, chats and joyful personality made me excited to be a part of the MRC PPU from Day 1.

I could not have wished for a better experience of research or for a more enjoyable and rewarding year out of medical school, and for this I am forever thankful for the friends I made both within and outside of the MRC PPU. In particular, I am indebted to the kindness and friendship provided by my flatmate Holly Lennie, who made Dundee very quickly become a home for me. In addition, I am grateful for the friends I made at the University of Dundee Medical School, including Erin Timmoney, Rachel Gordon and Adele Harris, who provided me with encouragement during this degree. My gratitude always extends to my parents, who have constantly supported me throughout every decision, especially with my acceptance to undertake this MRes degree, and for the faith they have instilled within me.

And last but not least, to my uncle, Prince Casinader, whose dignity and grace throughout his experience of Parkinson’s disease (PD) created a deep desire within me to help fight this disabling condition in my future career; and to whom every step I take in PD research will be in dedication to.

It has been a great privilege to undertake this Masters project at the MRC PPU, and I look forward to hearing of future findings made in the laboratory from areas I worked on during my time here.

II. DECLARATION:

I hereby declare that the following thesis is based on the result of investigations performed by myself, or shared with another lab member, Prosenjit Pal, where stated within this thesis. This thesis is of my own composition, and all references from work other than my own is clearly stated within the text. The work within this thesis has not been previously accepted for a higher degree.

Theresita Joseph

III. ABSTRACT

Introduction

Parkinson's disease (PD) is the second most common neurodegenerative disorder in the world[1]. Whilst the majority of PD patients have no known cause of the disease ('sporadic'), around 5-10% of PD patients have genetic, familial forms of the disease[2]. *LRRK2* and *PINK1* are two independent genes that respectively cause autosomal dominant and autosomal recessive forms of PD. They both encode protein kinases, which control signal transduction pathways through reversible phosphorylation of target proteins[3]. Current research aims to better understand and visualise the activation of both proteins and their associated pathways, to help uncover their role in PD pathogenesis.

Aims

The work detailed within this thesis is divided into two main projects 'A' and 'B', which respectively concern experiments I conducted in the LRRK2 and PINK1 signal transduction pathways.

The main aim of Project A was to explore the activation of LRRK2 during infection of immune cells, in which I specifically focused on human peripheral blood neutrophils and mouse bone marrow derived macrophages (BMDMs). All infection experiments were conducted using *P. aeruginosa*, a Gram-negative opportunistic bacterium. In addition, I aimed to explore LRRK2 activation within neutrophils isolated from the sputum samples of cystic fibrosis (CF) patients, who are frequently infected with strains of *P. aeruginosa.*

The main aim of Project B was to investigate if activation of the PINK1/Parkin pathway could be detected within peripheral blood neutrophils, which would provide a quickly accessible and valuable human bio-source to interrogate PINK1 activity.

Methods

For Project A, I directly isolated peripheral blood neutrophils from whole blood donated by healthy volunteers, and extracted BMDMs from the femurs of sacrificed mice. I subsequently cultured and infected both cell types with standardised (PAO1) or uncharacterised clinical isolate strains of *P. aeruginosa*, over a time-course of 0-4 hours. In subsequent immunoblot analysis of cell lysates, I measured LRRK2 activity through use of the highly specific MJFF-pRab10 antibody, which detects Rab10 phosphorylated by LRRK2 at Thr73. I also directly isolated neutrophils from the sputum of CF patients with chronic *P. aeruginosa* infection, and similarly analysed them for LRRK2 activity, using the MJFF-pRab10 antibody.

For Project B, I isolated peripheral blood neutrophils and treated them with the mitochondrial uncoupler CCCP for durations of 3-20 hours, and analysed neutrophil lysates for PINK1 stabilisation through immunoblotting with the PINK1 (Novus) antibody. I also conducted PINK1 immuno-precipitation (IP) experiments to confirm the presence of endogenous PINK1 in peripheral blood neutrophils.

Results

My results in Project A revealed an increase in LRRK2-dependent Rab10 phosphorylation during infection of human peripheral blood neutrophils with *P. aeruginosa* infection. Furthermore, sputum neutrophils isolated from CF patients revealed markedly elevated levels of LRRK2-dependent Rab10 phosphorylation compared to controls, suggesting that LRRK2 activity may play an important role in human neutrophils during infection. In contrast, infection of mouse BMDMs with *P. aeruginosa* resulted in a progressive increase in LRRK2 Ser935 phosphorylation, but did not result in any observable LRRK2-dependent Rab10 phosphorylation. Further investigation into LRRK2 Ser935 phosphorylation in BMDMs following *P. aeruginosa* infection was shown to be mediated by the IKK family of kinases.

My results in Project B revealed that endogenous PINK1 could not be defected in stimulated peripheral blood neutrophils with CCCP between 3-20 hour time-courses.

Conclusions

The results I obtained in Project A collectively indicated that the LRRK2 kinase is influenced by *P. aeruginosa* infection, of which key differences in its activation and phosphorylation of serine residues exist depending on immune cell type and human/mouse species. My results support future work which aims to explore the mechanisms behind *P. aeruginosa* infection and LRRK2 activity. Furthermore, my preliminary findings of LRRK2 activation within sputum neutrophils of CF patients with *P. aeruginosa* infection provides the basis for a future clinical study to assess the natural course of LRRK2 activation during CF infective exacerbations.

Whilst my results in Project B did not demonstrate that PINK1 could be activated within peripheral blood neutrophils, future work could consider the use of different mitochondrial uncouplers, fractionation experiments, or more sensitive antibody readouts of the PINK1/Parkin pathway, to validate the current findings.

IV. ABBREVIATIONS

α	Alpha
β	Beta
ε	Epsilon
μ	Micro
aa	Amino acid
AD	Autosomal dominant
AR	Autosomal recessive
BSA	Bovine serum albumin
BMDM	Bone marrow derived macrophages
°C	Degrees Celsius
CCCP	Carbonyl cyanide m-chlorophenyl hydrazone
CF	Cystic Fibrosis
CISD1	CDGSH iron-sulfur domain-containing protein 1
CL2	Contamination level 2
COR	C-terminal of Roc
Da	Dalton
DA	Dopamine
DIFP	Disopropyl fluorophosphate
DMEM	Dulbecco's Modified Eagle Medium
DMSO	Dimethyl sulfoxide DNA Deoxyribonucleic acid
ECL	Enhanced chemiluminescence
EDTA	Ethylenediaminetetraacetic acid
EGTA	Ethylene glycol tetraacetic acid
EO	Early-onset
FBS	Foetal bovine serum
GAPDH	Glycerinaldehyd-3-phosphat-Dehydrogenase
GWAS	Genome wide association studies
GTP	Guanosine-5'-triphosphate
hr	Hour
HEPES	4-(2-hydroxyethyl)-1-piperazineethanesulfonic acid
IL	Interleukin
IMM	Inner mitochondrial membrane
IP	Immunoprecipitation
KO	Knock-out
LB	Luria Bertani
LRRK2	Leucine-repeat rich kinase-2
m	Milli
M	Molar
MAPK	Mitogen activated protein kinase
min	Minute
MLi2	cis-2,6-dimethyl-4-(6-(5-(1-methylcyclopropoxy)-1H-indazol-3-yl)pyrimidin-4-yl)morpholine
mol	Mole
MPP	Mitochondrial processing peptidase

MTS	Mitochondrial targeting sequence
MyD88	Myeloid differentiation primary response 88
NFκB	Nuclear Factor-KappaB
OMM	Outer mitochondrial membrane
PD	Parkinson's disease
P.aeruginosa	Pseudomonas aeruginosa
PAGE	Polyacrylamide gel electrophoresis
PAMP(s)	Pathogen-associated molecular pattern(s)
PARL	Presenilin-associated rhomboid-like protein
PBS	Phosphate buffered saline
PINK1	PTEN-induced kinase 1
PTEN	Phosphatase and tensin homologue
RIPK	Receptor interacting protein kinases
ROC	Ras-of-complex
rpm	Revolutions per minute
RPMI	Roswell Park Memorial Institute medium
SDS	Sodium dodecyl sulphate
Ser	Serine
SNpc	Substantia nigra pars compacta
TAK1	Transforming growth factor beta-activated kinase 1
TBK1	Tank-binding kinase 1
TBS	Tris buffered saline
TBST	TBS + Tween
TEMED	N,N,N′,N′-Tetramethylethane-1,2-diamine
Thr	Threonine
TM	Transmembrane domain
TIM	Translocase of the inner membrane
TLR	Toll-like-receptor
TNFα	Tumour Necrosis Factor-alpha
TRAF	TNF receptor-associated factor
TOM	Translocase of the outer membrane
U	Unit
Ubl	Ubiquitin like domain
WT	Wild-type

V. TABLE OF CONTENTS

VI. LIST OF FIGURES AND TABLES

TABLES:

FIGURES:

1. *CHAPTER 1* - INTRODUCTION

1.1 Parkinson's Disease (PD)

Parkinson's disease (PD) is a progressive, age-related condition that is currently the second most common neurodegenerative disorder in the world[4], affecting 2-3% of the population over 65 years of age. Whilst it was first described over 200 years ago by James Parkinson within his landmark '*Essay on the Shaking Palsy'* **(Figure 1.1A)**, the understanding of PD continues to evolve[5]. At its core, PD is pathologically hallmarked by selective neurodegeneration of dopaminergic neurones projecting from the ventro-lateral tier of the substantia nigra pars compacta (SNpc) to the striatum, leading to continual depletion of the neurotransmitter dopamine (DA)[6] **(Figure 1.1B)**. In addition, autopsy findings reveal widespread accumulation of proteinaceous intracytoplasmic inclusions known as Lewy bodies and Lewy neurites, composed of α-Synuclein, within the few spared dopaminergic neurones[7] **(Figure 1.1C).**

Clinically, PD is diagnosed by the presence of cardinal motor symptoms corresponding to 'parkinsonism', which according to the Movement Disorder Society (MDS) diagnostic criteria require the presence of bradykinesia (slowness of movement), in combination with at least one of rigidity and/or resting tremor[8]. In addition, other forms of parkinsonism must be excluded for a confirmed PD diagnosis, including atypical or drug-induced parkinsonism, as well as the presence of supportive PD criteria, and red flag exclusions[8]. Motor symptom onset usually begins in the late 50s and is commonly unilateral, with persistence of asymmetry throughout the disease. However, several systemic non-motor symptoms such as reduction or loss of smell (hyposmia), constipation, depression and sleep disturbances are also part of the PD prodrome[9], and can precede the onset of motor symptoms by several years or even decades. Progressive PD disability and worsening quality of life is thus driven by a combination of continuing motor and non-motor symptoms, eventually resulting in cognitive decline and dementia in some individuals (**Figure 1.1D**).

Sadly, there are still no curative treatments available to slow or prevent PD, thus current approaches aim to provide symptomatic benefit and improve quality of life. Key PD treatments include pharmacological substitution of striatal dopamine with 'L-DOPA', in addition to non-dopaminergic approaches to address both motor and non-motor symptoms[10]. However, given the progressive nature of PD, the efficacy of pharmacological treatments eventually wear-off, and can additionally lead to disabling 'off-target' effects including unwanted dyskinetic movements. Deep brain stimulation (DBS) is an invasive interventional option available for those with L-DOPA related motor complications or drug refractory tremor, however is not without its own risks[11]. Moreover, it addresses only the symptoms of PD, rather than the underlying disease process.

FIGURE 1.1

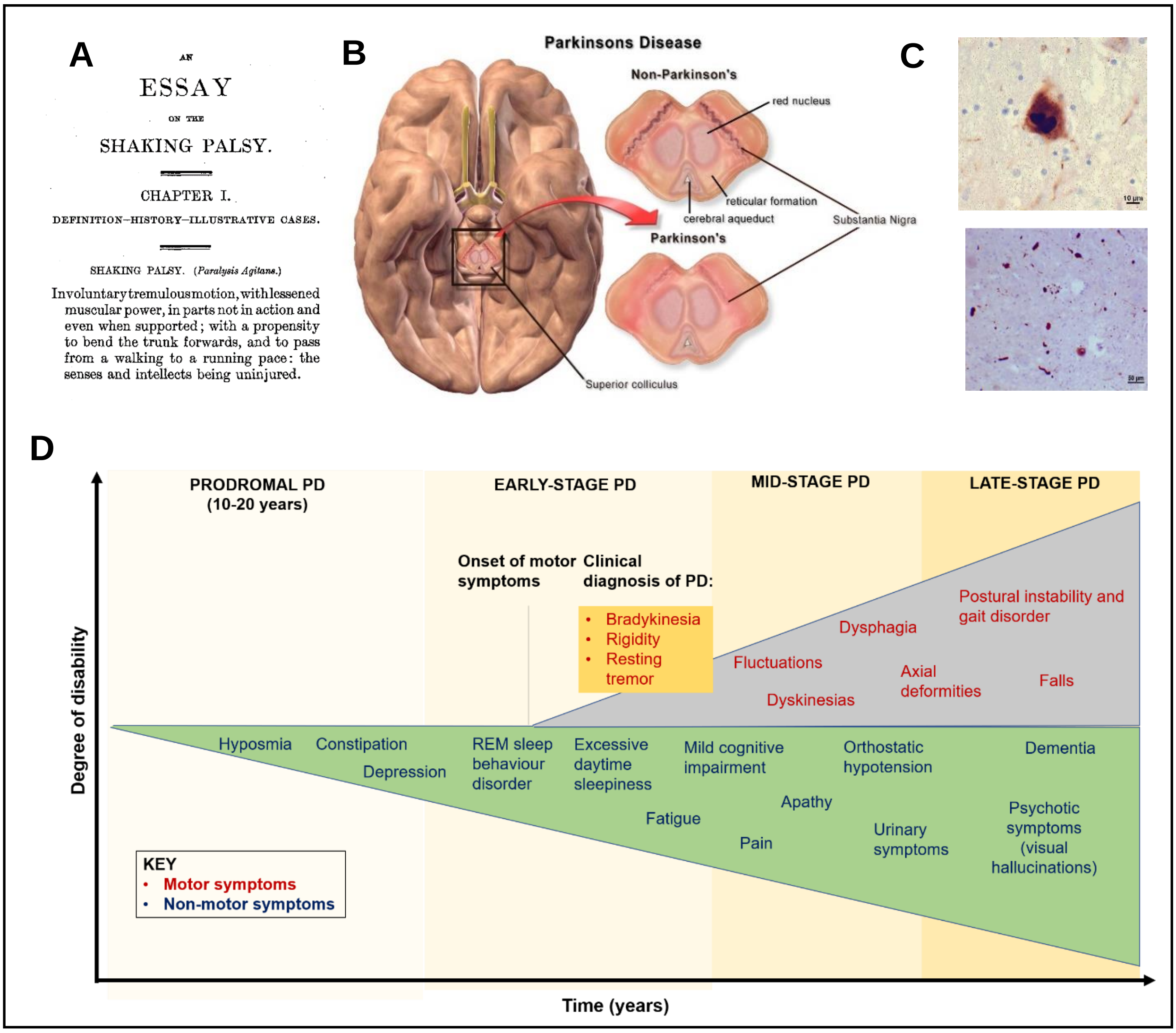

FIGURE 1.1: Combined schematic of Parkinson's disease (PD) background, histopathology and timescale

(A) First published description of PD as the '*Shaking Palsy'* by James Parkinson in 1817.

(B) PD neuropathology: Illustration of transverse midbrain sections of the basal ganglia, with particular focus on the substantia nigra pars compacta (SNpc) in a healthy individual (top) compared to an individual with PD (bottom). Top illustration shows healthy pigmentation of the SNpc from dopaminergic neurones, whilst bottom illustration shows significant depigmentation of the SNpc due to dopaminergic neurone loss, leading to PD symptoms.

(C) PD histopathology: Photomicrograph of Lewy bodies (top) and Lewy neurites (bottom) found in remaining dopaminergic neurones within regions of the SNpc from a PD patient. Lewy bodies and neurites are intraneuronal inclusions predominantly formed of the protein alpha-synuclein. Top micrograph shows a 60-times magnification of Lewy bodies whilst the bottom micrograph shows a 20-times magnification of Lewy neurites. Neuromelanin laden cells of the substantia nigra are seen in the background.

(D) PD clinical progression: Schematic of the onset and progression of non-motor and motor PD symptoms over time in years (x-axis) against the degree of disease disability (y-axis), revealing growing disability with increasing years of PD. It should be noted that this timescale can considerably vary between PD individuals, and not all PD individuals will experience these symptoms.

***Figures 1.1A-C** were publicly available for reuse and reproduction. **Figure 1.1D** is adapted upon **Figure 5** published in Poewe, W. et al. (2017) Parkinson disease.*

1.1.1 PD genetics

Considerable years of research has revealed that PD is a clearly complex and multifactorial disease. The underlying molecular pathogenesis of PD is still being uncovered, however is thought to involve a myriad of pathways and mechanisms including mitochondrial dysfunction, oxidative stress, calcium homeostasis, α-Synuclein proteostasis and neuroinflammation[6].

Whilst the majority of PD patients are 'sporadic' with unknown aetiology, around 5-10% of patients have an inherited monogenetic form of the disease with Mendelian inheritance ('familial PD'), which can be inherited in an autosomal dominant (AD) or autosomal recessive (AR) manner[12]. Generally, AD PD patients are characterised by late PD symptomatic onset in the late 50s (similar to sporadic PD patients), whilst AR PD patients tend to have an earlier PD onset <45 years[13]. So far, linkage analysis and genome wide association studies (GWAS) have identified 23 loci (PARK1-23) associated with PD, of which 13 have shown to be causal for PD, 3 which increase PD risk, and 7 in which the relationship with PD is currently unclear **(Table 1)**. In addition, a further 92 common genetic risk loci and variants in sporadic PD patients have been revealed through GWAS studies[14]. Thus, a culminative combination of multiple common and rare genetic variants in addition to several environmental and stochastic factors are likely to be behind the majority of 'sporadic' PD patients.

In the timeline of PD gene discovery, 2004 heralded ground-breaking findings of mutations in two independent genes, *LRRK2* (PARK8)[15] and *PINK1* (PARK6)[16], to be causally linked to PD (**Table 1**). Both genes encode a group of enzymes termed protein kinases, which cause post-translational modifications (PTMs) of target proteins through the reversible addition of a covalently bound phosphate group onto the side chains of one of three amino acids; serine (Ser), threonine (Thr) or tyrosine (Tyr)[17] (**Figure 1.2**). This integral process termed 'phosphorylation' results in a conformational and functional change of the target protein, which can affect the regulation of downstream cellular processes including the cell cycle, growth, apoptosis and signal transduction pathways[18]. Research into the functional and biological importance of LRRK2 and PINK1 kinases and their signal transduction pathways have provided key insights into the PD molecular pathogenesis, which will be explored below.

FIGURE 1.2

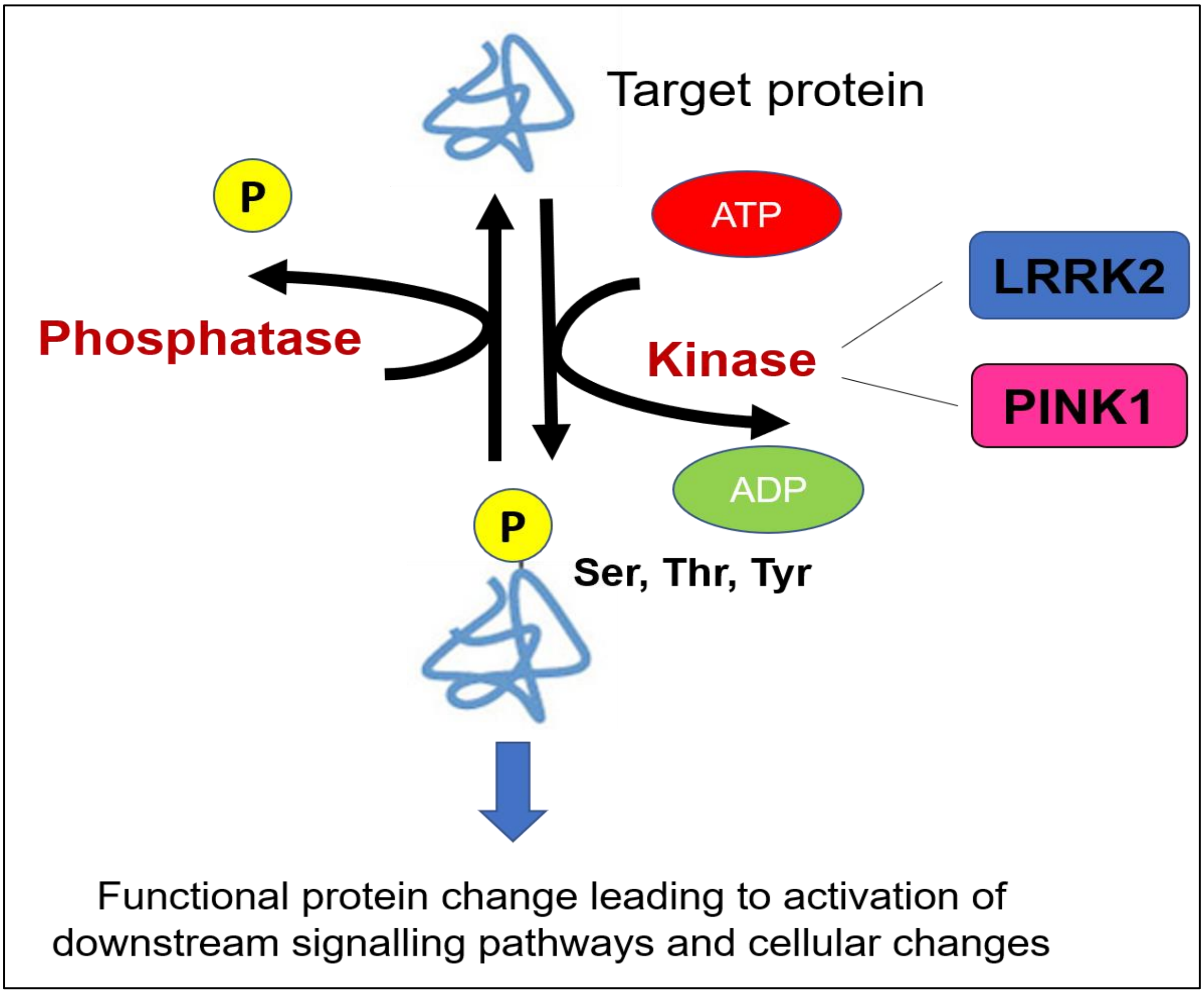

FIGURE 1.2: Schematic of protein phosphorylation by protein kinases

Both LRRK2 and PINK1 are protein kinases which catalyse the phosphorylation of target proteins through the addition of a phosphate group onto side chains of one of three amino acids (Serine, Threonine, Tyrosine). This process can be reversed by a separate group of enzymes known as phosphatases. Protein phosphorylation is a crucial cellular event leading to downstream signalling pathway activation which triggers different cellular processes.

Original image

TABLE 1

LOCUS SYMBOL	GENE LOCUS	GENE	GENE SYMBOL (OMIM)	DISEASE ONSET
Autosomal dominant PD (late onset)				
PARK1/4	4q22.1	alpha synuclein (α-Syn)	*SNCA* (163890)	Early-onset, late-onset*
PARK8	12q12	Leucine rich repeat kinase 2	*LRRK2* (609007)	Late-onset
PARK17	16q11.2	VPS35, retromer complex component	*VPS35* (601501)	Late-onset
Autosomal recessive PD (early onset)				
PARK2	6q26	Parkin RBR E3 ubiquitin protein ligase (Parkin)	*PRKN* (602544)	Early-onset
PARK6	1p36	PTEN induced putative kinase 1	*PINK1* (608309)	Early-onset
PARK7	1p36.23	Parkinsonism associated deglycase	*PARK7* (602533)	Early-onset
PARK19	1p31.3	DnaJ heat shock protein family (Hsp40) member C6	*DNAJC6* (608375)	Early-onset
Autosomal recessive PD (complex genetic forms)				
PARK9	1p36.13	ATPase 13A2	*ATP13A2* (610513)	Early-onset
PARK14	22q13.1	Phospholipase A2 group VI	*PLA2G6* (603604)	Early-onset
PARK15	22q12.3	F-box protein 7	*FBXO7* (605648)	Early-onset
PARK20	21q22.1	Synaptojanin 1	*SYNJ1* (604297)	Early-onset
PARK23	15q22.2	Vacuolar protein sorting 13 homolog C	*VPS13C* (608879)	Early-onset
PD Risk loci				
PARK10	1p32	Parkinson disease 10	*PARK10*	Late-onset
PARK12	Xq21-q25	Parkinson disease 12	*PARK12*	Late-onset
PARK16	1q32	Parkinson disease 16	*PARK16*	Late-onset
Loci with current unconfirmed relationship to PD (thought to be autosomal dominant)				
PARK3	2p13	Parkinson disease 3	*PARK3* (Unclear)	Late-onset
PARK5	4p13	Ubiquitin C-terminal hydrolase L1	*UCHL1* (191342)	Early-onset, late-onset*
PARK11	2q37.1	GRB10 interacting GYF protein 2	*GIGYF2* (612003)	Late-onset
PARK13	2p13.1	HtrA serine peptidase 2	*HTRA2* (606441)	Late-onset, early-onset*
PARK18	3q27.1	Eukaryotic translation initiation factor 4 gamma 1	*EIF4G1* (600495)	Late-onset
PARK21	20p13	Transmembrane protein 230	*TMEM230*(617019)	Late-onset, early-onset*
PARK22	7p11.2	Coiled-coil-helix-coiled-coil-helix domain containing 2	*CHCHD2* (616244)	Late-onset, early-onset*

TABLE 1: Current updated list of PARK1-23. The symbol, gene locus, official gene name, gene symbol and disease onset according to the Human Genome Nomenclature Committee (HGNC) for all PARK1-23 loci are displayed, separated according to mode of inheritance and complex genetic forms. 3 PARK risk loci and 7 PARK loci with unconfirmed relationship to PD are also included. Late-onset refers to PD onset >50 years, and early-onset <50 years. *Indicates few cases in which alternate disease onset has been recorded. Highlighted genes (*LRRK2 and PINK1*). indicate the two genes of focus within the work in this thesis.

Table adapted according to Table 1 published within Poewe, W. et al. (2017) Parkinson disease

1.2 LRRK2

Missense mutations in the leucine-rich repeat kinase 2 (*LRRK2*) gene, within the PARK8 locus (**Table 1**), were found to cause PD by two independent studies in 2004[15,19]. Currently, *LRRK2* mutations comprise the main genetic cause of PD[20], and are dominantly inherited in familial PD patients, or appear sporadically. In particular, G2019S is the most common *LRRK2* mutation, accounting for 4% of familial and 1-2% of sporadic PD cases worldwide[21,22]. Notably, G2019S prevalence varies with ethnic background, and is particularly high within individuals of Ashkenazi Jewish (29% familial, 10% sporadic PD) and North African Berbers ancestry (40% familial and 30% sporadic PD)[23]. GWAS studies have also revealed that risk of sporadic PD is moderately increased by common protein-coding and non-protein coding variants at the *LRRK2* locus[24].

Clinically, the phenotype of PD patients with *LRRK2* mutations closely resembles those with sporadic PD (late-onset, tremor dominant), however differs by certain non-motor features such as improved smell, reduced frequency sleep behaviour disorder (RBD), and several atypical features such as dementia[25]. Different *LRRK2* mutations can also produce varying neuropathology with and without Lewy bodies, as well as with hyperphosphorylated tau or ubiquitin-inclusions[26]. Of the G2019S mutation, Lewy bodies have been observed in most post-mortem samples[27].

1.2.1 LRRK2 protein structure

The *LRRK2* gene encodes a large (2527-amino acid) multi-domain protein, containing two enzymatic regions at its core; a Ras-of-complex (ROC) GTPase domain ending with a C-terminal of Roc (COR) spacer domain, and a serine/threonine (Ser/Thr) kinase domain[28]. Several protein-protein interaction domains surround this enzymatic core, including a leucine-rich-repeat (LRR) region (N-terminus), an ankyrin-like repeat region (ANK), an Armadillo repeat region, and a WD40 domain (C-terminus) **(Figure 1.3)**[22].

LRRK2 is auto-phosphorylated at Ser1292, which resides between the LRR and GTPase domains, and is also phosphorylated constitutively at a cluster of serine residues (Ser910, Ser935, Ser955 and Ser973), which reside in a non-catalytic region between the ANK domain and LRR region[29] (**Figure 1.3**). Phosphorylation of Ser910 and Ser935 sites regulate 14-3-3 binding and LRRK2 cytosolic localisation[30]. Use of several diverse LRRK2 kinase inhibitors, such as MLi2, as well as several PD mutations in the enzymatic core of LRRK2, cause dephosphorylation of these sites[29]. Previous work has identified protein phosphatase 1 (PP1) as a phosphatase behind LRRK2 dephosphorylation of its serine resiudes[31]. However, it is still unclear how LRRK2 kinase activity itself influences phosphorylation of these sites.

The most common confirmed *LRRK2* mutations cluster within the enzymatic core of *LRRK2*; R1441C/G/H and N1437H (GTPase ROC domain); Y1699C (COR domain); G2019S and I2020T (kinase domain)[21] (**Figure 1.3**). Regardless of mutation position, all pathogenic mutations cause an increase in *LRRK2* kinase activity[32], thus associating kinase activity with PD pathogenicity. Furthermore, there is clear communication between both GTPase and kinase domains, given that mutations within the GTPase ROC domain of *LRRK2* increase kinase activity by 4-fold, compared a 2-fold increase by kinase domain mutations themselves[22]. Therefore, LRRK2 represents an attractive therapeutic target for PD, in which LRRK2 kinase inhibitors are being developed and tested by several pharmaceutical and biotechnological companies for their use as potential novel PD treatments[22].

FIGURE 1.3

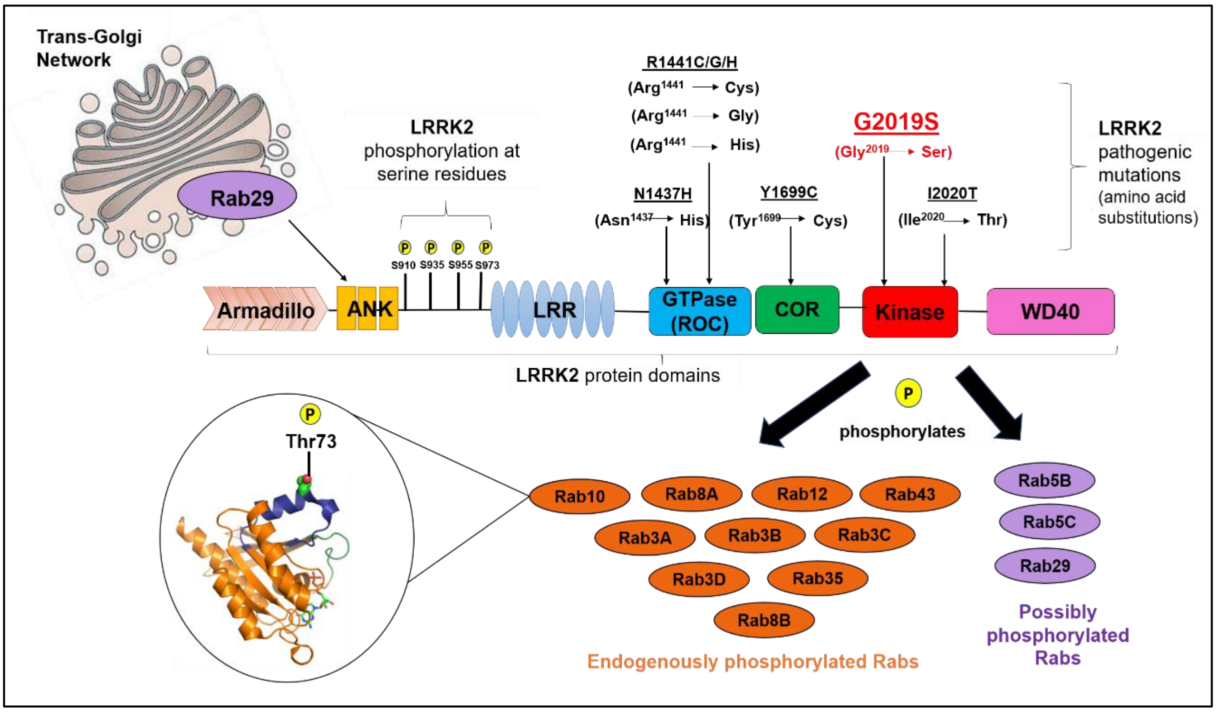

FIGURE 1.3: Schematic of LRRK2 protein domains, confirmed pathogenic mutations, and phosphorylation of its Rab substrates following kinase activation.

LRRK2 is a large multi-domain protein containing several protein-protein interaction domains surrounding a double enzymatic core; consisting of a GTPase ROC domain ending with a COR domain, and a serine/threonine (Ser/Thr) kinase domain. All 7 pathogenic confirmed LRRK2 mutations cluster within all 3 domains of the double enzymatic core, with G2019S, located within the kinase domain, being the most common LRRK2 mutation. In addition, the serine sites of LRRK2 (Ser910, Ser935, Ser955, Ser973), are depicted between the ANK and LRR LRRK2 domains. LRRK2 phosphorylates a subgroup of Rab GTPases, of which endogenous phosphorylation for 10 Rab GTPases (orange) have been confirmed, whilst 3 (purple) are possibly phosphorylated[32,33]. Rab10 is phosphorylated at a highly conserved Thr73 residue within the effector binding region switch II domain, whereby its crystal structure is shown in more detail. In a predicted model of LRRK2 activation, Rab29 binds to the ANK domain of LRRK2, and acts as an upstream master regulator by recruiting LRRK2 to the trans-Golgi network[36].

Original image, based upon published findings in Steger, M, et al (2017)

1.2.2 LRRK2 phosphorylation of Rab proteins

Important work within the Alessi lab revealed that LRRK2 directly phosphorylates a subset of 14 Rab GTPases, including Rab8A, Rab10 and Rab29/Rab7L1, which are its first validated physiological substrates[32,33] (**Figure 1.3**). This phosphorylation occurs on a conserved Ser/Thr residue located within the effector binding switch-II region of their GTPase domains (Thr72 in Rab8A and Thr73 in Rab10)[33,34]. Recent work revealed that Rab7L1/Rab29 also functions as an upstream master regulator of LRRK2[35]. In a predicted model of LRRK2 activation, Rab29 binds to the ANK domain of LRRK2 and recruits it to the trans-Golgi network, which greatly stimulates its kinase activity[36]. Moreover, pathogenic LRRK2 mutants including R1441G/C and Y1699C are preferentially activated by Rab29 in comparison to wild-type LRRK2[36], providing further association between increased LRRK2 kinase activity and PD pathogenesis.

Rab GTPases (~70 Rabs within humans) constitute the largest branch of the Ras superfamily, and are critical regulators of intracellular trafficking within eukaryotic cells[37]. They cyclically switch between inactive (GDP-bound) or active (GTP-bound) states, which are respectively activated by Rab guanine nucleotide exchange factors (GEFs), or inactivated through the hydrolysis of bound GTP by GTPase activating proteins (GAPs)[38]. Active GTP-bound Rabs associate with membranes, where they interact with a carefully orchestrated downstream sequence of Rab effectors (e.g. tethering factors, molecular motors), which facilitate induction of diverse pathways; including vesicle formation, movement, docking and membrane fusion[38].

LRRK2 mediated phosphorylation of Rab isoforms decreases their interaction with other known regulatory proteins or exchange factors that promote their activation and insertion into target membranes, such as guanosine nucleotide dissociation inhibitors (GDI); GDI1/2[33]. However, LRRK2 phosphorylated forms of Rab isoforms (Rab8A, 10, 12) are able to interact with other effector proteins termed RILPL1 and RILPL2, which are regulators of primary ciliogenesis[32]. In the context of PD, pathogenic *LRRK2* mutations located within the GTPase (R1441G/C) and COR (Y1C99C) domains, as well as the kinase domain (G2019S/I2020T), have shown to markedly enhance Rab8A and Rab10 isoform phosphorylation in vivo[39], indicating an important role of these proteins and their downstream signalling pathways in PD pathogenesis.

1.2.3 LRRK2 role during infection and inflammation

Whilst the physiological role(s) of LRRK2 are still being uncovered, a growing amount of evidence points to its involvement during infection and inflammation[40,41]. Indeed, LRRK2 is part of the family of receptor interacting protein kinases (RIPK 1-7), of which different members play key roles in the inflammatory response to infection and apoptosis of infected cells[42].

Supportively, whilst LRRK2 is ubiquitously expressed, its expression is significantly elevated within cells of the innate and adaptive immune system[43], as well as in glial cells. LRRK2 expression is further increased by multiple pro-inflammatory signals such as lipopolysaccharide (LPS) and interferon-γ (IFN-γ)[43,44], and is also increased in the immune cells of PD patients[41]. Mutations in *LRRK2* have also been associated with several inflammatory diseases, including leprosy[45], Crohn's disease[46], SLE[47], and cancer[48]. Thus, LRRK2 appears to lie at a unique nexus of neurodegeneration and inflammation.

Mechanistically, several studies have aimed to understand how LRRK2 is activated or modulated in response to infection or inflammation. Notably, previous work within the Alessi lab found a key connection between Toll-like receptor (TLR) activation and LRRK2 phosphorylation within mouse bone marrow derived macrophages (BMDMs)[49]. TLRs have a vital role in recognising specific pathogen-associated molecular patterns (PAMPs) present on invading pathogens, which lead to the induction of downstream intracellular signalling pathways responsible for inflammatory immune responses[50]. Specifically, activation of TLR's 1,2,5,6,7,8 and 9 signals through the MyD88-dependent pathway, which promotes TRAF6-dependent activation of the TAK1 kinase. Subsequently, TAK1 phosphorylates and promotes the activation of "canonical" IKKα and IKKβ kinases, which induce the transcription of NFκB dependent genes, including TNFα and IL-6, that are key for the inflammatory response. In addition, "non-canonical" TBK1 and IKKε kinases are also activated by the MyD88 pathway, which have a negative regulatory effect on "canonical" IKK activation. TLR3 activation leads to stimulation of the MyD88-independent pathway (TRIF), leading to downstream activation of "non-canonical" IKK kinases, whilst TLR4 activation uniquely signals through both MyD88-dependent and independent pathways. **Figure 1.4** illustrates a summary of both TLR-activated immune signalling pathways, and the key findings from the Alessi lab[49].

Specifically, the experiments performed within the Alessi lab revealed that activating several TLRs with various MyD88-dependent pathway agonists in mouse BMDMs led to increased LRRK2 phosphorylation at several serine residues, including Ser910, Ser935 and Ser955[49]. This phosphorylation was found to be controlled by both "canonical" IKKα and IKKβ, and "non-canonical" (TBK1 and IKKε) kinases, whereby a combination of pharmacological inhibitors against both sets of kinases prevented TLR-mediated LRRK2 phosphorylation[49] **(Figure 1.4 and Figure 1.5).** It is still not established however what the role of TLR-mediated LRRK2 phosphorylation is on macrophage immune response, or how this phosphorylation affects LRRK2 cellular kinase activity. Indeed, the authors revealed that LRRK2 KO macrophages still possessed a normal pro-inflammatory cytokine secretion in response to TLR2 or TLR4 stimulation[49], suggesting that LRRK2 phosphorylation in response to TLR signalling may not impact downstream cytokine responses.

FIGURE 1.4

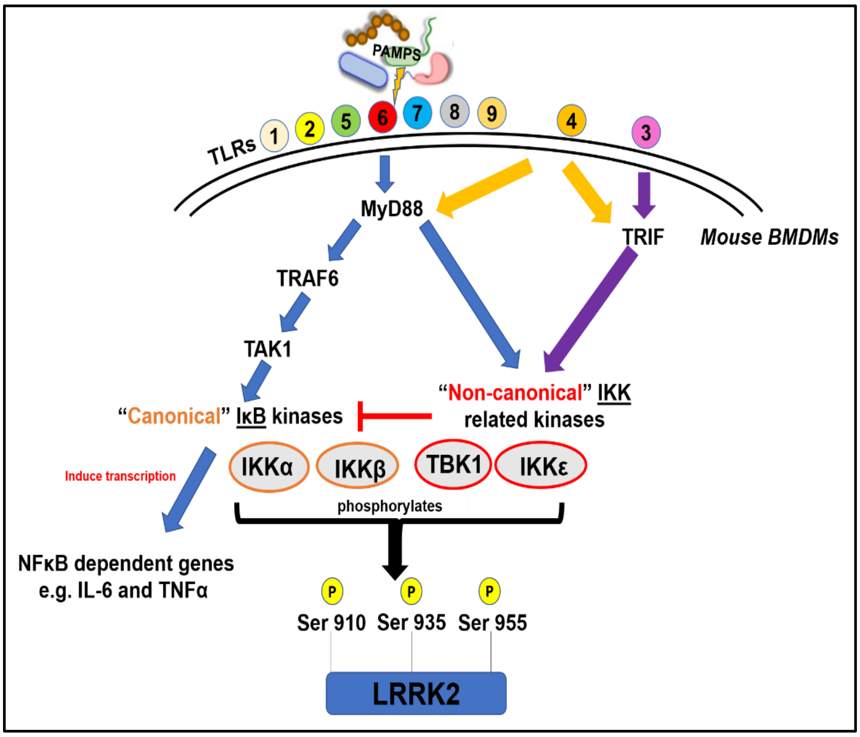

FIGURE 1.4: Schematic of activation of Toll-like receptors (TLRs) by pathogen associated molecular patterns (PAMPs) in mouse BMDMs, based on published work from Dzamko *et al.,* 2012.

Downstream activation of both 'canonical' and 'non-canonical' IKK related kinases following use of MyD88-dependent agonists in mouse BMDMs was shown to phosphorylate LRRK2 at serine sites including Ser910, 935 and 955.

Original image

FIGURE 1.5

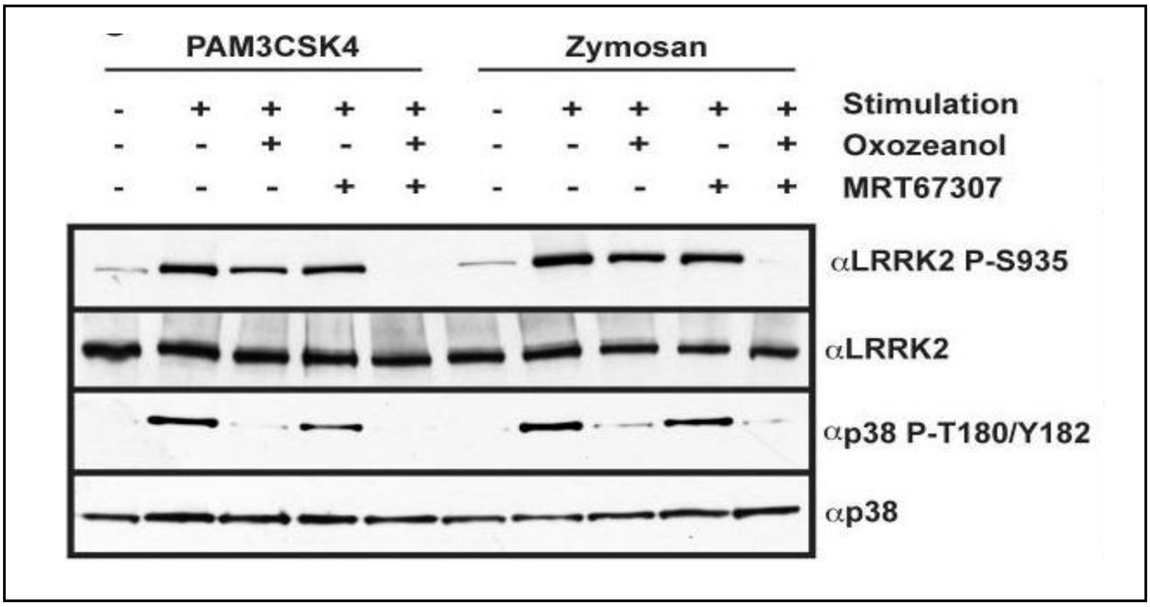

FIGURE 1.5: Immunoblot from published data (Dzamko *et al*., 2012)

Immunoblot analysis demonstrating that activation of the MyD88-dependent pathway by TLR agonists PAM3CSK4 (1µg/ml) and Zymosan (200µg/ml) in wild-type BMDMs led to LRRK2 phosphorylation at Ser935. Significantly, Ser935 phosphorylation was abolished only through combination of MRT67307 and Oxozeaenol inhibitors, which inhibit TBK1**/** IKKε and TAK1 kinases respectively, thus demonstrating that both sets of kinases are needed for LRRK2 Ser935 phosphorylation.

Several studies have also shed insight into the activation and specific response of LRRK2 upon cellular infection of macrophages with different pathogens. During *S. Typhimurium* infection in mice, LRRK2 co-localises with infected macrophages and helps clear the infection[51], and is also required for mucosal immunity against *Listeria monocytogenes* in another mouse model[52]. In contrast, during *M. Tuberculosis* (*M. Tb*) infection, LRRK2 negatively regulates phagosome maturation in both human and mouse macrophages, reducing *M. Tb* degradation by lysosomes and hence supporting its replication[53]. Therefore, the specific role of LRRK2 during macrophage infection intriguingly appears to be either beneficial or deleterious to the host response depending on the pathogen and cell host in question.

1.3 *Pseudomonas aeruginosa*

Pseudomonas aeruginosa (*P. aeruginosa*) is a Gram-negative opportunistic bacterium, ubiquitously found in soil and ground water. Its large and hypermutable genome (~5500 genes) enables colonization and survival within a diverse range of conditions and species, including humans, where it can infect several sites of the body including the respiratory tract, urinary tract, eyes, and skin[54]. Several hundred strains *of P. aeruginosa* have been characterized, of which the common reference strain is PAO1, a spontaneous resistant mutant of the original PAO strain, isolated from a wound from a patient in Australia in 1954[55].

P. aeruginosa is traditionally regarded as an extracellular pathogen, indicating that it avoids phagocytosis and multiplies extracellularly. However, it has also shown signs of intracellular activity, including its invasion and survival inside host cells, adding to its complexity[56,57]. Its mechanism of pathogenicity is directly associated with several virulence factors, including structural cell-associated determinants such as lipopolysaccharide (LPS) within the outer membrane, pili and flagellin, as well as several extra-cellular factors, including proteases, exotoxins and haemolysins[58] (**Figure 1.6A**). Both LPS and flagellin act as PAMPs, and have shown to activate TLR2/TLR4 and TLR5 respectively[59]. Importantly, *P. aeruginosa* utilizes the type III secretion system (T3SS), which expresses one or more of four known exotoxins (ExoS, ExoU, ExoT and ExoY)[60]. These exotoxins are translocated into host cells and promote invasion and/or intracellular trafficking through modulating interaction with epithelial cells, immune cells and host tissues. The T3SS itself increases inflammation and neutrophil recruitment[61], as well as inhibiting internalization of *P. aeruginosa* into macrophages[62].

1.3.1 *P. aeruginosa* and Cystic fibrosis (CF)

Although healthy individuals are rarely affected by *P. aeruginosa*, severe infections occur in immunocompromised individuals, as well as those vulnerable to nosocomial hospital-acquired infections, including patients with burn wounds, urinary tract infections or pneumonia[63]. In particular, *P. aeruginosa* infection is the predominant cause of morbidity and mortality in individuals with cystic fibrosis (CF)[64], an autosomal recessive genetic disorder caused by mutations within the cystic fibrosis transmembrane conductance regulator (*CFTR*) gene, located on chromosome 7[65]. All CFTR mutations cause defective transport of chloride ions and water across epithelial surfaces, leading to thick and sticky mucus hyper-production within the respiratory, digestive and reproductive systems[65] (**Figure 1.6B**).

Whilst CF is clearly a multi-system disorder, the effects of mucus accumulation in the respiratory system are currently the best studied due to the severity of breathing problems experienced by individuals, as well as the notorious problem of poly-microbial airway colonization over their lifetime. Indeed, CF individuals frequently suffer from repeated respiratory tract infections punctuated by acute episodes of pulmonary 'exacerbations', which contribute to worsening inflammation and damage of their airway linings[66]. The prevalence of bacteria infecting the airways in CF varies with age. Typically, CF patients are infected with *P. aeruginosa* in early childhood (~20% <2 years), and harbor the pathogen through subsequent years, whereby more than 70% of CF adults are chronically infected with *P. aeruginosa* by age 25[67]. Some studies have revealed that whilst bacterial diversity in CF airways decreases as severity increases, *P. aeruginosa* remains as the dominant organism[68].

Several genotypic and phenotypic adaptations of *P. aeruginosa* are thought to explain for its persistence in CF, including its intrinsic resistance to several antibiotics and antiseptics[69], its ability to form diverse hypermutable strains[70], and its creation of biofilms[71]; where micro-colonies of bacteria grow in a self-produced extracellular matrix. Specifically, *P. aeruginosa* strains in CF appear to convert into an exopolysaccharide alginate-producing mucoid phenotype over time, which is associated with an accelerated loss of pulmonary function and increased morbidity[72]. In addition, previous work revealed that novel *P. aeruginosa* strains isolated from the sputum of CF patients showed marked upregulation of several drug resistant proteins (MexY, MexB, MexC) and downregulation of chemotaxis and aerotaxis proteins (PA1561, PctA, PctB), compared to the standard PAO1 strain[73]. Thus, it is likely that different *P. aeruginosa* strains provide alternate mechanisms of virulence and drug-resistance required for survival, depending on the unique lung environment of each CF individual. As a result, CF patients are often isolated in their clinic appointments to minimise spread of these multi-drug resistant *P. aeruginosa* strains, for which their underlying mechanisms are still unknown.

FIGURE 1.6

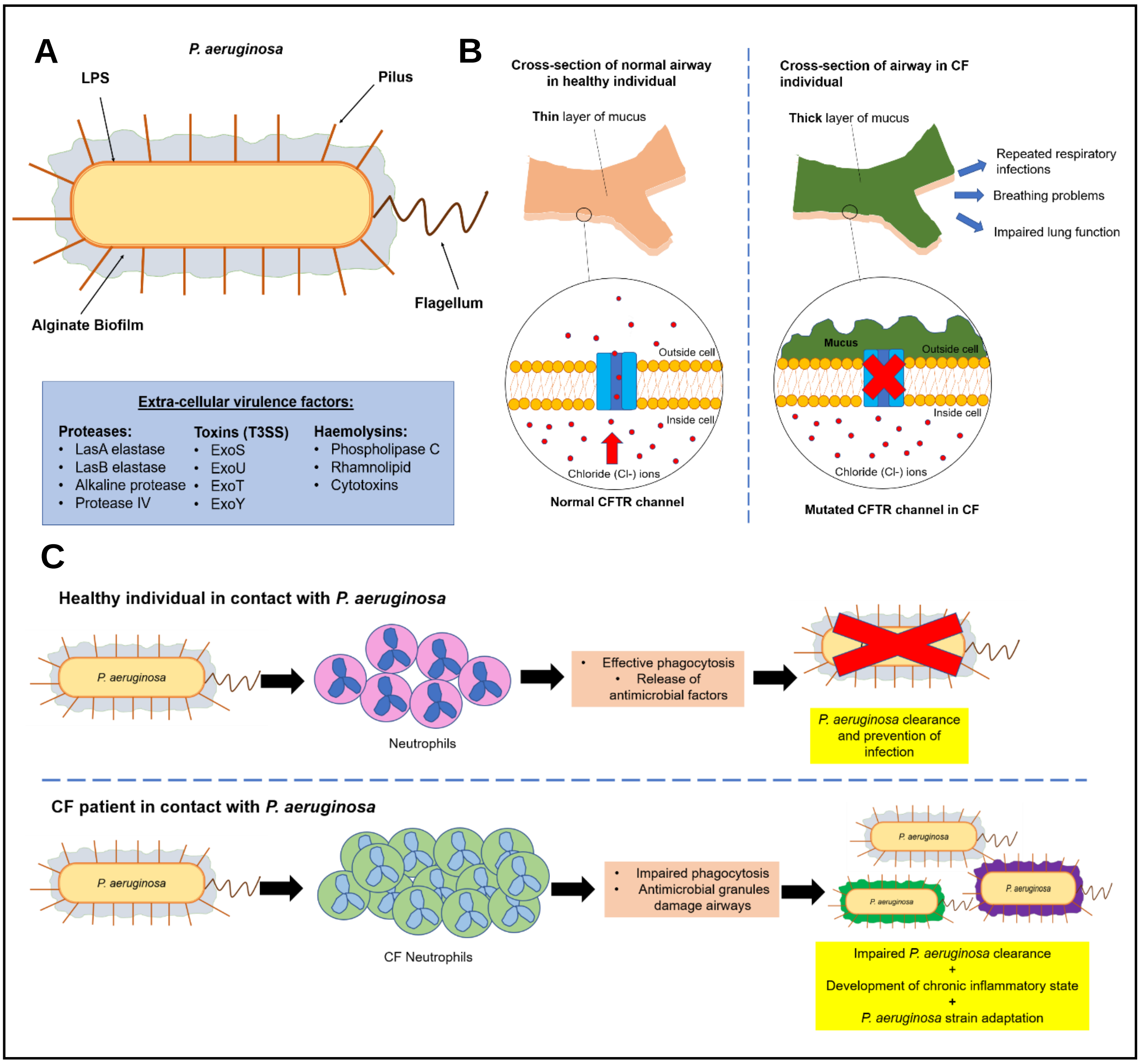

FIGURE 1.6: Combined schematic of (A) simplified *P. aeruginosa* structure, (B) CF pathobiology within the lung architecture

(A) *P. aeruginosa* is a gram-negative rod-shaped bacterium, with specific structural characteristics including the flagellum, pili, lipopolysaccharide (LPS) and alginate biofilm, of which the latter forms in differentiated strains. Extra-cellular virulence factors, including several proteases, T3SS exotoxins and haemolysins are also outlined.

(B) Illustration depicting the normal CFTR channel, which allows movement of chloride ions into the extra-cellular space in mucus-secreting glands, contrasted with impaired chloride movement within the mutant CFTR channel in cystic fibrosis (CF). The airways cross-section above reveals thick mucus in CF individuals with mutant CFTR channels, which is responsible for the breathing problems and recurrent infections.

(C) Illustration showing the clearance of *P. aeruginosa* from healthy individuals through effective phagocytosis by healthy neutrophils (top image), contrasted with the impaired *P. aeruginosa* clearance in CF individuals despite the large efflux of neutrophils. CF neutrophils appear defective, and additionally cause damage to the CF airways. *P. aeruginosa* persistence in CF individuals facilitates further strain adaptation for survival, allowing the development of a chronic inflammatory state.

Original images

1.3.2 Neutrophils, LRRK2 and *P. aeruginosa*

As a general immune defence mechanism, neutrophils are key for the elimination of *P. aeruginosa* and prevention of infection in healthy individuals (**Figure 1.6C**), thus neutropenic patients have higher frequencies of *P. aeruginosa* infection[63]. Neutrophils are the most common type of white blood cell, and are usually the first immune cells to arrive at the site of inflammation. They provide essential non-specific host defence via releasing several proteases, reactive oxygen species (ROS) and metabolites, and can be stimulated to synthesise and secrete several cytokines and chemokines required for activating inflammatory pathways against *P. aeruginosa*[74].

Paradoxically, the large infiltration of neutrophils across the airway epithelium of CF patients during infection appears a key factor behind pulmonary exacerbations and the persistence of *P. aeruginosa* (**Figure 1.6C**). CF neutrophils appear to have a reduced phagocytic capacity and impaired function for host defense against *P. aeruginosa*, which is further impeded by the thick inflammatory environment of the CF mucus[75,76]. Furthermore, proteases including elastase and matrix metalloproteinases (MMPs) released from neutrophil toxic granules cause irreversible tissue damage and structural remodeling of the CF airways, which worsens prognosis[77]. Currently, it is not known whether defects in the CFTR channel influence the migration or function of neutrophils[78], or whether there are any other genes which may be involved in the excessive inflammatory response in CF.

Interestingly, neutrophils have been reported to demonstrate a high expression level of both LRRK2 and Rab10 (**Figure 1.7**). A considerable advantage of the use of neutrophils for experimentation is that they can be readily isolated from human blood in around 30 minutes, of which isolated cells are 98-99% homogenous[79]. With this knowledge, the Alessi lab has recently employed a robust assay to interrogate LRRK2 kinase pathway activity and assess molecular changes within human peripheral blood neutrophils[79]. Crucially, this work has been facilitated through use of the newly developed highly specific and sensitive MJFF-pRab10 rabbit monoclonal antibody, which detects Rab10 phosphorylated at Thr73 by LRRK2[39], hence can be used as a direct readout of LRRK2 activity. In addition, neutrophils within the sputum of CF patients comprise of the major cell type, and can be quickly isolated by established techniques. Hence, human neutrophils provide an ideal source to explore the role of LRRK2 during the course of infection.

FIGURE 1.7

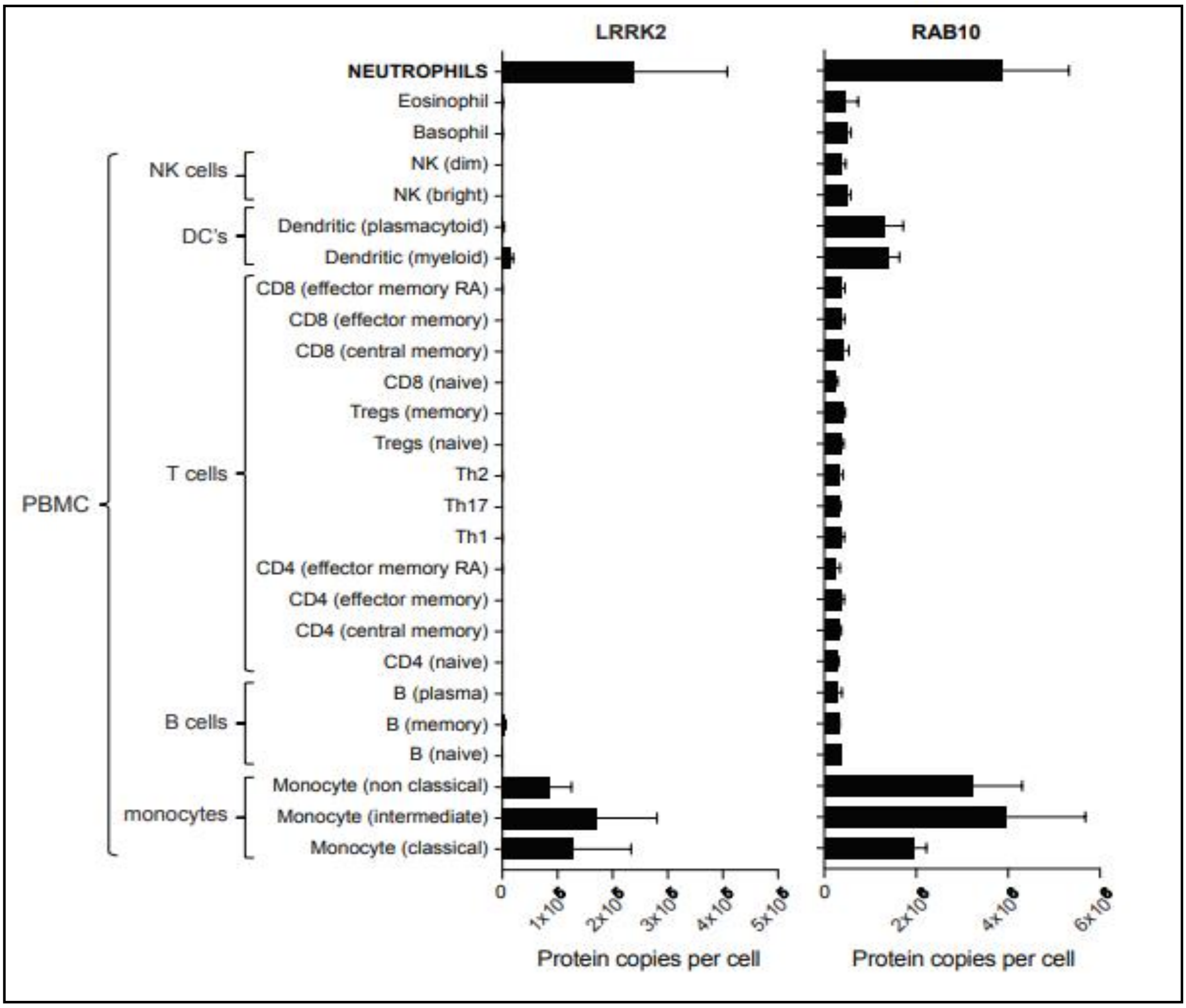

Abundance of LRRK2 and Rab10 within immune cells isolated from human peripheral blood, based on data from Immprot database (http://www.immprot.org)

Graphical display of high numbers of protein copies per cell for of both LRRK2 and Rab10 within neutrophils and several types of monocytes. To obtain this data, the study used fluorescence-activated cell sorting (FACS) to isolate pure populations of immune cells isolated from human blood. Histone rule was used to estimate the protein copy numbers per cells.

Image published as Figure 1 in Fan, Y et al., 2018 and reproduced with permission from authors.

1.4 PINK1 and Parkin

Two other important genes linked to PD are *PINK1* (PTEN-induced kinase 1; human PARK6), which encodes a serine/threonine protein kinase, and *Parkin* (human PARK2), encoding a ubiquitin E3 ligase (**Table 1**). Loss-of-function homozygous or compound heterozygous mutations, as well as rearrangements in these genes, are the most common causes of autosomal recessive early-onset PD (below age of 45)[23]. PD patients with either mutation have clinically indistinguishable phenotypes, with largely restricted nigrostriatal pathology that can interestingly be spared of Lewy body inclusions, in reported cases[80].

Notably, the PINK1 and Parkin enzymes respectively encoded by each gene converge on an evolutionarily conserved signal transduction pathway which regulates mitochondrial homeostasis and quality control, including the selective elimination of damaged mitochondria from cells through a process known as mitophagy. These findings enhanced the growing hypothesis that mitochondrial dysfunction is one of the key mechanisms underlying Parkinson's pathogenesis[7]. Indeed, PD-related *PINK1* mutations have shown to inhibit PINK1 kinase activity and prevent mitophagy initiation in cells with mitochondrial damage, leading to reactive oxygen species accumulation and neuronal loss[81]. Furthermore, experiments using Drosophila models of PINK1 have revealed that neurodegeneration could be rescued in only wild-type (WT) versions of the *PINK1* gene compared to kinase-inactive versions[82]. Thus, better understanding of the connection between PINK1/Parkin pathway dysfunction and dopaminergic neurodegeneration provides important insights into PD, and may help with future development of neuroprotective treatments.

1.4.1 PINK1/Parkin signalling pathway

Considerable work in cell culture over the last decade has helped shed light on the mechanisms by which the PINK1/Parkin pathway normally regulates mitochondrial homeostasis and mitophagy[80]. PINK1 is unique amongst all other kinases due to the presence of an N-terminal mitochondrial targeting sequence (MTS). In addition, it contains a transmembrane domain, and three insertional loops (Ins1-3) within its catalytic kinase domain[83] **(Figure 1.8A)**.

Under basal conditions within healthy mitochondria, PINK1 is synthesised at the ribosome as its full-length 63kDa form. It is targeted from the cytosol to the mitochondria through its N-terminal MTS, and is then translocated from the outer mitochondrial membrane (OMM) to the inner mitochondrial membrane (IMM) through the Translocase of the Outer Membrane (TOM) and Translocase of the Inner Membrane (TIM) complexes, respectively[84]. Once at the mitochondrial matrix, PINK1 is sequentially cleaved in two steps; first by the mitochondrial processing peptidase (MPP) to its 60kDa intermediate form, and then by presenilin-associated rhomboid-like protein (PARL) to its 52kDa mature form[85]. Following cleavage, the 52kDa mature form is exported back into the cytosol, where it is rapidly degraded by the N-end rule pathway[86].

However, upon mitochondrial depolarisation or conditions of stress/damage (which can be induced by mitochondrial uncouplers), full-length PINK1 becomes activated and stabilised on the OMM of mitochondria through inhibition of its mitochondrial import and cleavage[87]. Herein, PINK1 phosphorylates ubiquitin (Ub) present on proteins within the OMM at Serine 65 (Ser 65) (becoming 'phospho-ubiquitin', pUb), which stimulates recruitment of Parkin to the mitochondria. The subsequent binding of Parkin with phosphorylated ubiquitin molecules results in a conformational change that primes Parkin for its phosphorylation by PINK1 at its Ser65 residue within its N-terminal ubiquitin-like domain (Ubl)[87]. Parkin Ser65 phosphorylation is essential for activation of Parkin E3 ligase activity[88,89], which polyubiquitylates multiple proteins at the OMM, leading to their de novo assembly and elongation. The ubiquitin chains on these proteins are in turn phosphorylated by PINK1, which are then targeted for degradation in the lysosome. This promotes a feedforward loop amplification for the completion of mitophagy, thus promoting cell survival and protection against apoptosis **(Figure 1.8B).**

Additional findings have revealed that activated PINK1 indirectly regulates phosphorylation of a subset of Rab proteins including Rab8A, 8B and 13 at Serine 111 (Ser111), which appears independent of its direct activation of Parkin E3 ligase activity **(Figure 1.8B)** [90]. Excitingly, recent work has revealed that whilst Ser111 phosphorylation does not alter Rab8A structure, it does disrupt LRRK2-mediated phosphorylation of Rab8A at Thr72 (unpublished work).

FIGURE 1.8

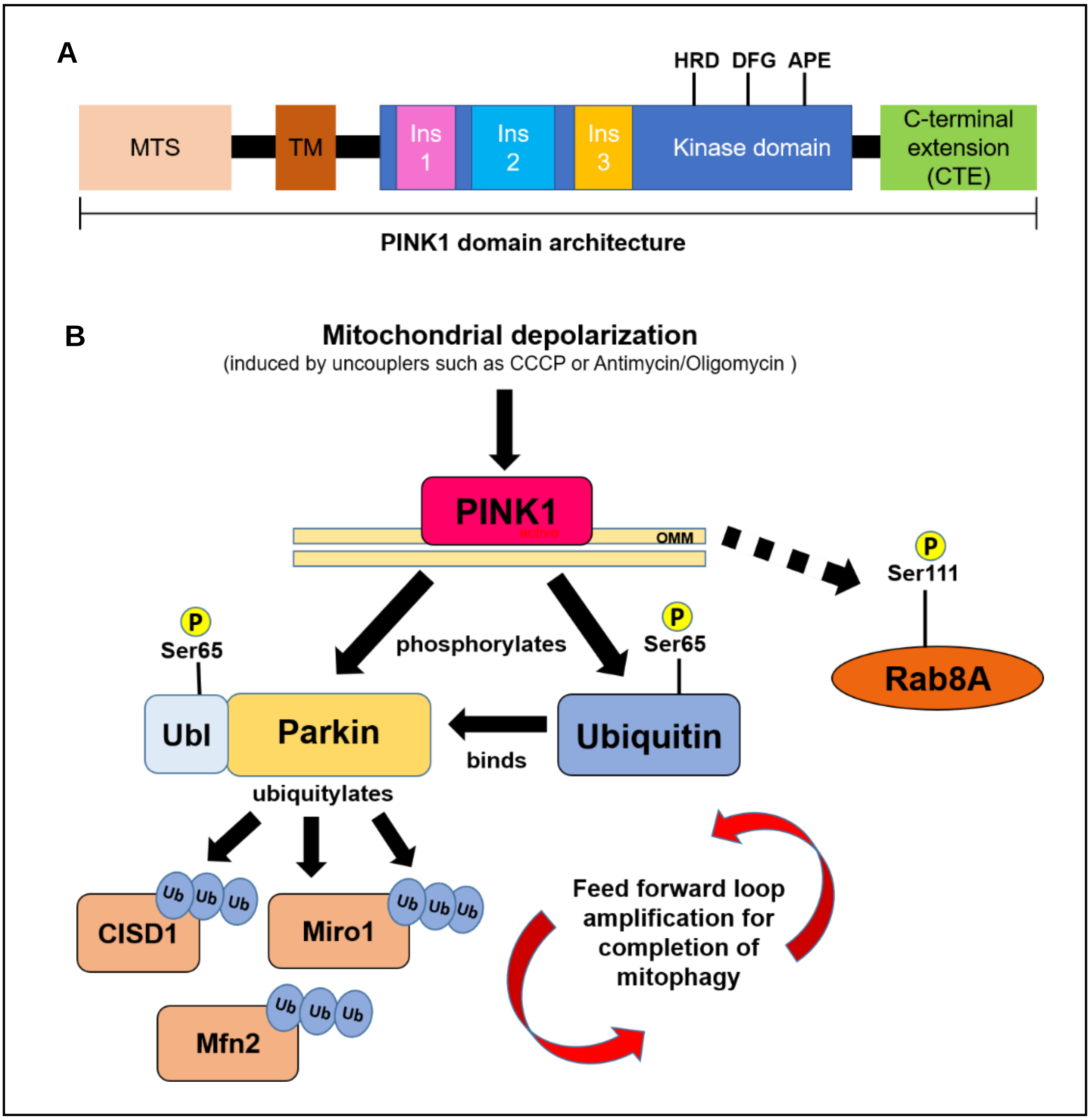

FIGURE 1.8: PINK1 structure and pathway

(1.8A) Human PINK1 domain architecture, showing an N-terminal mitochondrial targeting domain, a kinase domain containing 3 insertional loops (Ins1-3), a catalytic motif (HRD) and activation loop motifs (DFG, APE) and a C-terminal extension (CTE).

(1.8B) Schematic diagram of PINK1/Parkin pathway activation following mitochondrial depolarisation. PINK1 is stabilised at the outer mitochondrial membrane (OMM) and prevented from degradation. Here, it phosphorylates Parkin and Ubiquitin at their respective Ser65 residues. This is crucial for Parkin activation, leading to poly-ubiquitylation of several substrates, including CISD1, Miro1 and Mfn2. These ubiquitin chains are subsequently phosphorylated by PINK1, contributing to the feed forward amplification of the cycle to complete the mitophagy process. PINK1 also indirectly regulates the phosphorylation of Rab8A at Ser111.

Original images

1.4.2 Detecting PINK1 expression and activity in human cells

Detection and analysis of endogenous PINK1/Parkin signalling and mitophagy in mammalian tissues has been challenging due to the high turnover of PINK1 under normal conditions, coupled with previous limitations in available antibody tools to sensitively and specifically detect PINK1 at its low levels. Hence, most understanding of the role and activation of PINK1 has been derived from in vitro observations and cell culture studies using highly overexpressed exogenous PINK1 and/or Parkin and artificially induced mitochondrial depolarisation through uncoupling agents[91].

Whilst PINK1 mRNA is ubiquitously expressed in humans, its expression is highest within metabolically active human tissues and organs; including cardiac and skeletal muscles, the testes and the brain[92], which is consistent with its role in mitophagy. Within the brain, higher PINK1 expression is observed in neuronal cells of the substantia nigra, hippocampus, and cerebellar Purkinje cells[93]. Obtaining bio-samples of these cells from living patients to investigate PINK1/Parkin activity provides obvious limitations. However, recent work within the Muqit lab provided the first direct analysis of PINK1/Parkin pathway activity in primary fibroblast cultures established from human skin biopsies[89,94]. Specifically, 3-hour treatment with the mitochondrial uncoupler CCCP (carbonyl cyanide 3-chlorophenylhydrazone) in fibroblasts derived from PD patients harbouring PINK1 mutations/Parkin Ser65N homozygous mutations, compared to in those from a healthy subject, abolished Parkin Ser65 phosphorylation and activation. This was associated with a substantial reduction in CISD1 ubiquitylation and reduced accumulation of pUb as readouts of Parkin E3 ligase activity in CCCP-treated Ser65N mutated fibroblasts.

Notably, recent work within the Alessi lab promoted the suggestion to consider neutrophils as a key bioresource in Parkinson’s bio-repositories[79]. As discussed above, peripheral blood neutrophils can be quickly isolated from whole blood through the robust assay developed, and has successfully been used to measure endogenous LRRK2 activity through the highly sensitive and specific pRab10 antibodies employed. Using the current antibody tools available to interrogate PINK1/Parkin activity, it would thus be beneficial to investigate if PINK1 activity can similarly be detected in this readily obtainable human blood cell type.

1.5 Project aims

The first aim of my project (**Project A**) was to explore if I could activate LRRK2 during infection of immune cells with *P. aeruginosa*. The *P. aeruginosa* strains I used within this project included the characterised (PAO1) strain, as well as several uncharacterised strains isolated from the sputum of chronically infected CF patients (Strains 'A-D'). I directly isolated neutrophils from human peripheral blood, as well as from sputum samples provided by *P. aeruginosa* infected CF patients. I used both human neutrophil cell types to investigate LRRK2 activity through assessing LRRK2-dependent Rab10 phosphorylation. I also isolated, cultured and infected mouse bone marrow derived macrophages with *P. aeruginosa* strains to investigate the resultant impact on LRRK2 Ser935 phosphorylation, as well as for LRRK2-dependent Rab10 phosphorylation.

The second aim of my project (**Project B**) was to investigate if I could detect PINK1 in human peripheral blood neutrophils, following induction of mitochondrial depolarisation over several time courses using the mitochondrial uncoupler CCCP. I used immunoblotting and immunoprecipitation (IP) experiments with the PINK1 (Novus) antibody to confirm the detection of stabilised PINK1 in peripheral blood neutrophils. If successful, my project findings would indicate that peripheral blood neutrophils could be utilised as useful cell type to directly and quickly assess for PINK1/Parkin pathway dysfunctions in PD patients. This could promote future exploration into the overall role in which this pathway plays in PD pathogenesis for both sporadic and familial PD patients.

2. *CHAPTER 2* – MATERIALS AND METHODS

2.1 Materials

2.1.1 Reagents

Signal transduction inhibitors of LRRK2 (MLi2), TBK1/IKKε (MRT67307) and TAK1 (NG25), as well as Protein G Sepharose beads for immuno-precipitation were provided by the MRC Reagents and Services, University of Dundee. Tissue culture reagents were obtained from Life Technologies. CCCP was obtained commercially through Sigma (#C2759), and stocks kept frozen at -20^{0}C.

2.1.2 Antibodies

Primary antibodies used include in-house antibodies produced by the MRC Reagents and Services, or commercially available antibodies, which are respectively listed in in **Table 2.**

TABLE 2: In-house generated antibodies with the Michael J. Fox foundation (MJFF) and Commercial antibodies utilised within the project

Antibodies	Identifier	Company	Host
Michael J. Fox foundation			
p(Ser935)-LRRK2	UDD2	MRC Reagents and Services	Rabbit
Total LRRK2 (C-terminus)	N241A/34	Neuromab	Mouse
p(Thr73)-Rab10	MJF-R21	Abcam	Rabbit
Total Rab10	Clone- 605B11	Nanotools	Mouse
p-Rab8	MJF-20-25-5	Abcam	Rabbit
p(Thr71)-Rab7L1 (Rab29)	S877D (sheep number)	MRC Reagents and Services	Mouse
Total Rab7	9367	Cell signalling	Rabbit
Commercial			
Total Rab8A	6975	Cell signalling	Rabbit
p-p38 MAPK	9211	Cell signalling	Rabbit
GAPDH	2118	Cell signalling	Rabbit
Tubulin	5174	Cell signalling	Mouse
PINK1 human	BC-100-494	Novus	Rabbit
Parkin human	Sc-32282	SantaCruz	Mouse
p(Ser65)-Ubiquitin	PR3322	(in-house made with 21st century)	Rabbit

2.2 Study participants

2.2.1 Blood and sputum sample collection

For experiments utilising human peripheral blood neutrophils, members of the School of Life Sciences at the University of Dundee kindly donated 20ml blood per experiment, which was collected into BD Vacutainer tubes (BD Vacutainer Haemogard Closure K2-EDTA Tubes).

For experiments utilising sputum neutrophils, naturally expectorated sputum samples were obtained from CF patients who were attending clinic appointments at the Respiratory department of Ninewells hospital following a recent infective exacerbation. Before samples were collected, explanation of the project and informed consent from each patient was obtained, in accordance with hospital procedures. Although no formal sputum culture analysis was obtained from each patient at the time of sputum collection, all CF patients had confirmed *P. aeruginosa* cultures previously detected in sputum samples. No demographic or clinical information from CF patients was obtained and samples were kept anonymised.

Given that healthy individuals cannot naturally produce sputum, a neutrophil sputum control sample was obtained from a patient with Primary Ciliary Dyskinesia (PCD). PCD is an inherited autosomal-recessive disorder characterised by impaired muco-ciliary clearance mechanisms due to abnormal ciliary beating, thus leading to copious sputum production[95]. Whilst no formal sputum culture could be obtained for this patient, the patient was not reported to be suffering from an infection during the time of sputum collection, nor had previous culture positive for *P. aeruginosa* infection, hence was utilised as a 'non-infected' control for sputum neutrophil preliminary assessment. As above, a neutrophil blood control was obtained from a healthy blood donor at the School of Life Sciences.

2.3 Cell isolation

2.3.1 Peripheral blood neutrophil isolation

The peripheral blood neutrophil isolation procedure was commenced within 30 minutes of blood collection, through immune-magnetic negative isolation with the Direct Human Neutrophil Isolation Kit (STEMCELL Technologies, #19666), which had been previously purchased for work within the Alessi lab. The established neutrophil isolation Dundee protocol is summarised below[79], with **Figure 2.1** illustrating the main mechanism behind neutrophil isolation.

20ml freshly collected blood samples from each donor was transferred into individual 50ml falcon tubes, and 1ml of "*Isolation cocktail*" from the Neutrophil Isolation Kit was added to each tube. "*Rapid-Spheres magnetic beads*" from the isolation kit were vortexed for 30 seconds and

1ml added to the blood sample, mixed by gently inverting the blood tube, and left to incubate at room temperature for 5 minutes. “EDTA Stock Solution 2” (1mM EDTA-PBS solution) was added to each tube to the 50ml mark, and mixed by gently pipetting up and down. Each blood tube was carefully placed into an *EasySep magnet* (STEMCELL Technologies, #18002), and left for 10 minutes at room temperature. The enriched cell suspension containing neutrophils in the middle of each falcon tube was pipetted using a 20ml pipette and transferred into a new 50ml falcon tube, with care taken not to touch the sides of the tube in contact with the magnet. Around 10ml of red blood cell suspension was left at the bottom of each tube. 1ml of *Rapid-Spheres magnetic beads* were added again to the new enriched cell suspension, mixed gently through inversion, and left to incubate at room temperature for a further 5 minutes. Each tube was placed again into the magnet and left for 5 minutes at room temperature. The enriched cell suspension was taken up by pipette and transferred into a new 50ml falcon tube, which was placed immediately into the magnet for a final time, and left for 10 minutes. The final suspension contained pure neutrophils, which was transferred into a new 50ml falcon tube. Each tube was topped up with 1mM EDTA stock solution 2 to a final volume of 40ml, gently mixed, and centrifuged at 335xg for 5 minutes. Immediately after centrifugation, the supernatant from each tube was carefully discarded to leave the neutrophil pellet. Neutrophil pellets were resuspended in 10ml of RPMI medium at room temperature by gently pipetting cells. A cell count was performed and viability determined with Trypan blue.

FIGURE 2.1

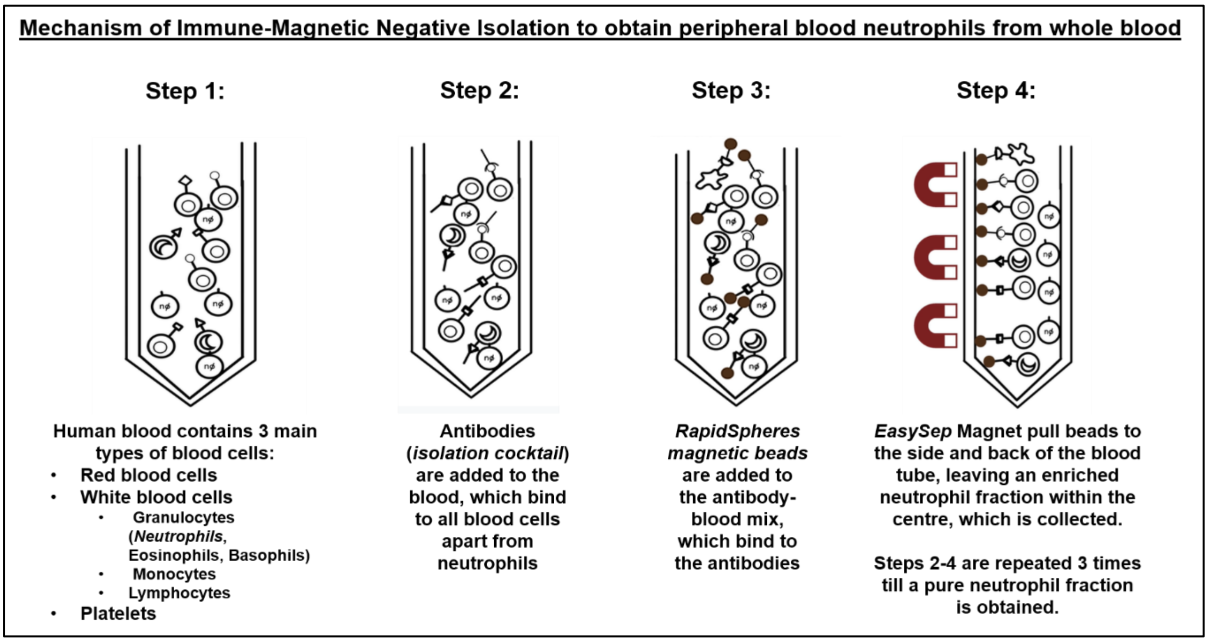

FIGURE 2.1: Schematic of key mechanisms behind immune-magnetic negative isolation using the EasySep Direct Human Neutrophil Isolation Kit to obtain a pure enriched fraction of peripheral blood neutrophils.

Figures adapted with permission from the Dundee Neutrophil Isolation Video developed by Dr Ying Fan, MRC PPU

2.3.2 Sputum neutrophil isolation

Sputum neutrophil isolation was commenced within 2 hours of sputum collection, and was performed according to the protocol advised by Professor James Chalmers, Ninewells Hospital. 1g of each freshly expectorated sputum sample was weighed, transferred into 15ml sterile centrifuge tube, and resuspended in 8ml of PBS. Each resuspended sputum sample was agitated on ice for 15 minutes, prior to centrifugation at 335 x g for 10 minutes at 4^0C. After centrifugation, 4ml of PBS supernatant was removed from each tube to leave sputum samples dissolved in the remaining supernatant. *Sputolysin* (Dithiothreitol, Concentration 9-11mg/Ml, #578517) was provided by Professor James Chalmers, and made to a 1:5 dilution with sterile water. 4ml of *Sputolysin* dilution was added to each sputum sample, vortexed for 2 minutes, and agitated for 15 minutes at 4^0C. Each sputum sample was filtered through a 48mm nylon gauze pre-dampened in PBS, into a second tube. Sputum filtrates were centrifuged at 335 x g for 5 mins, supernatants discarded, and sputum pellets resuspended in 10ml of RPMI medium at room temperature.

2.3.3 Bone Marrow Derived Mouse Macrophages (BMDM) isolation

Preparation of the culture medium used for BMDM growth included the addition of 5ml of stock Penicillin/Streptomycin (P/S) and L-glutamine to a 500ml bottle of DMEM. 150ml of DMEM + P/S+ L-glutamine solution was removed and replaced with 50ml of heat-inactivated fetal bovine serum (FBS) and 100ml of L929-cell conditioned medium.

Bone marrow precursor cells were isolated from sacrificed mouse femurs and tibiae under sterile conditions, and red cells removed using ammonium chloride lysis buffer. Bone marrow cells were flushed with PBS, diluted in pre-prepared BMDM culture media at 10^6 cells/ml, plated into normal tissue culture (TC) 10cm Petri dishes (10ml each), and placed within an incubator set at 37°C. Primary macrophages remained within the supernatant, whilst resident macrophages and fibroblasts adhered to the TC plastic. On Day 3, suspended cells were transferred into 10cm bacteriological dishes and returned to the at 37°C incubator. On Day 6, 5ml bone marrow growth medium was added to each 10cm dish. By Day 8, bone marrow cells had finished proliferating and were ready to be harvested, and were re-plated at $1x10^6$ per well (6 well plate), for which they were viable to use till Day 12. 24 hours before experimentation with *P. aeruginosa* strains, current medium was replaced with bone marrow growth medium without P/S, to ensure *P. aeruginosa* growth was not impaired. In some initial experiments, the impact of using original medium with P/S on *P. aeruginosa* growth was tested.

Rab29 knockout (KO) mouse BMDM cells were provided by Alexia Kalogeropulou from the Alessi lab, and cells cultured as described above.

2.3.4 HEK293 and HeLa cell culture

HEK293 FLP In T-Rex PINK1 knockout cells and PINK1 knockout with stably re-expressed PINK1-3X FLAG cells, and HeLa Wild-Type (WT)/PINK1 Knockout (KO) cells were gifted by Dr Richard Youle to the lab, which were used for control experiments. Both cell types were cultured in DMEM (Dulbecco's Modified Eagle's Medium) supplemented with 10% FBS, 2 mM L-glutamine and P/S. Cells were plated in 10cm tissue culture dishes, and kept at 37 °C.

2.4 Inhibitor treatments

2.4.1 MLi2 and kinase inhibitor treatments

Peripheral blood neutrophils and sputum neutrophils resuspended in RPMI medium were divided equally into two tubes labelled 'MLi2' and 'DMSO', and respectively treated for 30 minutes with 200nM MLi-2, a potent and highly selective LRRK2 inhibitor, or DMSO. Each tube was inverted every 10 minutes during the 30 minutes. Following 30 minutes incubation, sputum neutrophils were immediately lysed according to the procedure described below in **A.2.5.1,** whilst peripheral blood neutrophils were utilised for *P. aeruginosa* experiments, and were thus subsequently plated into sterile tissue culture 60mm dishes (~5 $x10^6$ neutrophils per dish).

BMDMs were treated with 200nM MLi2 (LRRK2) inhibitor, or DMSO as a control, for 1 hour before infection with *P. aeruginosa*. In later experiments, BMDMs were treated with either 2µM NG25 (TAK1 inhibitor), 2µM MRT67307 (TBK1/IKKε inhibitor), 200nM MLi2, or DMSO alone or specified combinations for 1 hour before *P. aeruginosa* infection.

2.4.2 CCCP treatments

Peripheral blood neutrophils were stimulated with 10µM CCCP for 3,6,9, 12 and 20-hour durations, and left to incubate at 37 °C during treatments.

HEK293 cells were first treated with 0.1ug/ml Doxycycline for 24 hours, followed by 3-hour treatment of 10µM CCCP. HeLa cells were directly stimulated with 10µM CCCP, or 10µM Antimycin A (Sigma) and 1 µM Oligomycin dissolved in DMSO for 22 hours.

2.5 *P. aeruginosa* infection experiments

Of note, the procedures outlined in **2.5.1-2.5.3** were carried out as part of a shared collaborative project with Prosenjit Pal, a member of the Alessi lab.

2.5.1 *P. aeruginosa* strains and media

P. aeruginosa laboratory strain PAO1 (characterised) and clinical isolate (uncharacterised) strains 'A-D' were provided by Professor James Chalmers, Ninewells Hospital. Clinical isolate strains were obtained from sputum samples of Cystic Fibrosis (CF) patients with chronic *P. aeruginosa* infection in the NHS Microbiology department of Ninewells hospital. Strains were stored on beads and kept frozen -80 °C.

Luria Bertani (LB) media and plates were supplied by the Media Kitchen of the University of Dundee.

2.5.2 *P. aeruginosa* plating, serial dilution protocol

P. aeruginosa cultures were prepared 1 day prior to performing infection experiments. In brief, one bead from each *P. aeruginosa* strain was inoculated into LB media without antibiotics, and grown overnight (16 hours) in the 37°C incubator on a shaker at 200rpm. The next day, 100µl from each overnight culture was added into 900µl 50% glycerol within Eppendorf tubes to make a stock solution, and were vortexed. Serial dilutions were performed from stock solutions; 100µl of stock solution was added into 900µl 50% glycerol stock within an Eppendorf, vortexed (10^{-1}), and the procedure repeated up to 10^{-8} dilution. 20µl of serial dilutions 10^{-5} -10^{-8} were streaked onto individual sterile agar plates without antibiotics using sterile applicator sticks, and left to incubate at 37°C for 16 hours. All serial dilutions, including the original stock solution, were left within the fridge at 5°C.

The next day, the number of bacterial colonies grown on each plate were counted and estimations of the bacterial concentration/ml within the original stock calculated for same day use in peripheral blood neutrophil/ mouse BMDM infection experiments.

2.5.3 *P. aeruginosa* infection procedure

Infection experiments were conducted under CL2 conditions in the molecular microbiology department (prior approval obtained). Peripheral blood neutrophils pre-treated for 30 minutes with MLi2/DMSO were infected with *P. aeruginosa* PAO1 and clinical isolates strains at a calculated multiplicity of infection (MOI) factor of 10. BMDMs pre-treated with 1 hour of MLi2/DMSO or NG25/MRT67307/MLi2/DMSO inhibitor treatments were infected with *P.*

aeruginosa PAO1 initially at MOI 10 or 50, and then future experiments utilising either PAO1 or *P. aeruginosa* clinical isolate strain 'A' at MOI 10. Given that all *P. aeruginosa* infection durations were 0, 0.5, 1, 2 or 4 hour treatments, cells were treated at staggered timepoints and lysed together. In between infections, all cells were kept incubated at 37°C.

2.6 Cell lysis

2.6.1 Peripheral blood and sputum neutrophil cell lysis

Lysis buffer used contained 50 mM Tris-HCL pH 7.5, 1 mM EGTA, 1 mM EDTA, 1 mM sodium orthovanadate, 10 mM β-glycerophosphate, 50 mM NAF, 5 mM sodium pyrophosphate, 0.27 M sucrose, 0.1% (v/v) 2-mercaptoethanol and 1% (v/v) Triton X-100. Importantly, lysis buffer used for neutrophil experiments also contained DIFP, a toxic protease inhibitor, which was needed to suppress the intrinsic serine protease activity that is high in neutrophils[79]. Pre-prepared lysis buffer aliquots were kept frozen at -80^{0}C, and defrosted on ice immediately before use.

Slightly different lysis procedures were required for neutrophil and BMDMs in order to maximise cell collection, given that neutrophils do not adhere to TC plate surfaces compared to BMDMs. Hence, peripheral blood neutrophils from each plate were gently scraped off and transferred into a separate 15ml falcon tube using a pipette, to ensure that all neutrophils collected remained within the media. All tubes were centrifuged at 335xg for 5 minutes at room temperature, and supernatants immediately discarded. 100µl chilled lysis buffer was added to each neutrophil pellet, resuspended, and transferred to Eppendorf tubes. Neutrophil pellets were left to lyse on ice for 10 minutes, and lysates clarified by centrifugation at 800g for 15 minutes at 4^{0}C. Supernatants were transferred into labelled Eppendorf tubes and used for protein quantification by Bradford assay (Thermo Scientific), and samples prepared for immunoblotting. Excess lysate was snap-frozen and stored at −80°C for future work.

For lysis of sputum neutrophils, the same procedure beginning from the centrifugation of neutrophils within tubes was carried out following completion of 30-minute MLi2/DMSO treatment.

For lysis of BMDMs, culture media was aspirated from each dish to leave the cells adhered to the bottom of the plate. BMDMs were gently washed with 1ml of phosphate-buffered saline, prior to addition of the lysis buffer. Cells were lysed on ice in standard lysis buffer without DIFP, and the same procedure as above administered.

2.7 Quantitative Immunoblot (IB) analysis

Cell lysates were mixed with 4x SDS-PAGE loading buffer to a final protein concentration of 1µg/ul and heated at 90 degrees for 5 minutes. Samples (10-40µg) were loaded onto commercial 4-12% Bis-Tris gels, electrophoresed at 130V for 2 hours and electrophorectically transferred onto nitrocellulose membrane at for 90V for 90 minutes.

Transferred membrane was blocked with 5% (w/v) skim milk powder dissolved in TBST for 1 hour, and then cropped at relevant molecular weight levels for overnight incubation at 4 degrees with the relevant primary antibodies, which were all diluted in 2% BSA in TBST at a final concentration of 1µg/ml for each antibody (**Table 2**). The following day, membranes were washed three times with TBST for 10 minutes each, followed by 1-hour secondary antibody incubation at room temperature (goat anti-mouse IRDye 680LT multiplexed with goat anti-rabbit IRDye 800CW secondary antibodies diluted in TBST at a 1:10,000 dilution). Membranes were washed again with TBST 3 times for 10 minutes each, imaged using infrared fluorescent detection with the Odyssey CLx Licor imaging system, and quantified with the Image Studio Software. For parts of **Project B** requiring higher sensitivity for detection of PINK1, membranes were developed using ECL.

2.8 PINK1 Immuno-precipitation (IP) experiments

For immunoprecipitation (IP) of PINK1 from control cell lysates and peripheral blood neutrophils, 1mg of whole-cell lysate was incubated overnight at 4°C with 10µg of Protein G Sepharose pre-bound to 10µg PINK1 (in-house S085D, 3rd bleed) antibody. The next day, immunoprecipitations were washed 3 times with high salt (150mM NaCl) lysis buffer, then once with 50mM Tris-HCl Ph 7.5, and eluted by resuspending in 25µl of 2x SDS sample buffer. Samples were agitated at 50°C within a Thermo-Mixer for 20 minutes, followed by 5 minutes at 75°C, before transferral to Spin X centrifuge filters. 75% of IP sample was loaded into 8% Bis-Tris commercial gels, and subjected subsequent Western blot procedure as described above. Any remaining lysates were snap-frozen and stored at -20°C till further analysis.

3. *CHAPTER 3* – PROJECT A RESULTS

3.1 Investigating LRRK2 activity following *P. aeruginosa* infection in neutrophils

For **Project A**, my aim was to investigate the effect of *P. aeruginosa* infection in immune cells on LRRK2 activity, using Rab10 phosphorylation at Thr73 (pThr73-Rab10) detected through the highly sensitive MJFF-pRab10 antibody as an indirect readout. Human neutrophils have high expression of LRRK2 and Rab10, (**Figure 1.5**), hence I first investigated the impact of *P. aeruginosa* infection on peripheral blood neutrophils over a 4-hour time-course. Specifically, I directly isolated neutrophils from the blood of healthy donors, and pre-treated them for 30 minutes with/without MLi2 prior *P. aeruginosa* infection, in order to confirm LRRK2-dependent pRab10 findings. Given that *P. aeruginosa* strains have shown key phenotypic and genotypic differences, I also investigated for any differences in LRRK2 activation by *P. aeruginosa* strains. For this, I utilised both the standard characterised PAO1 strain, as well as 4 uncharacterised clinical isolate strains obtained from sputum samples of chronically infected CF patients with *P. aeruginosa.* Of note, work conducted and presented within **Figures 3.1-3.3** were part of a shared project with Prosenjit Pal, a member of the Alessi lab.

3.1.1 Increased LRRK2-mediated Rab10 phosphorylation following *P. aeruginosa* infection within human peripheral blood neutrophils

The results in **Figure 3.1** demonstrate a progressive increase in pThr73-Rab10 levels within peripheral blood neutrophils during PAO1 infection over a 4-hour time-course. The MLi2 dependent elimination of pThr73-Rab10 signal, as well as p.S935-LRRK2 signal, confirmed that the phosphorylation observed was LRRK2-dependent. Interestingly, at the 4-hour infection time-point, a band-shift was observed in total Rab10, as well as in several other Rab proteins including Rab8A, 7, and p-Rab8 (MJFF-20-25-2). The band-shifts were also present with MLi2 treatment, therefore were independent of LRRK2 activity. Hence, the shifts could be indicative of post-translation modifications (PTMs) of Rab proteins by PAO1, of which future work is required to further investigate this possibility.

Activation of the p38 mitogen activated protein kinase (MAPK) signalling pathway results in phosphorylation of MAPK and nuclear translocation, and occurs in response to several cellular stresses[96]. Thus, levels of phosphorylated p38 (p.p38) were used as a marker of cellular response to infection. In **Figure 3.1**, an increase in p.p38 levels was observed in peripheral blood neutrophils infected with PAO1 at 1-2 hours duration, indicating a response to infection. The decreased p.p38 levels observed by 4 hours may have been due to protein degradation at longer infection time-points. More accurate assessment of p38 MAPK activation in response to *P. aeruginosa* infection would require comparison of p.p38 against total levels of p38, which was not performed in this work.

Figures 3.2 and 3.3 demonstrate results of peripheral blood neutrophils infected with several uncharacterised *P. aeruginosa* clinical isolate strains (Strains A-D), which were obtained from sputum samples of chronically infected CF patients. As for **Figure 3.1**, the results reveal an increase in LRRK2-dependent Rab10 phosphorylation over the time-course of each *P. aeruginosa* clinical isolate infection, although quantitative analysis revealed variability in the rate and amount of Rab10 phosphorylation between strains and between donors. For example, whilst the pThr73-Rab10/Total Rab10 ratio is highest at 4 hours in both donors for Strains A and C, Strain D showed a reduced ratio in Donor 1 at 4 hours of infection. Conversely, 4 hours of infection with Strain B resulted in considerable neutrophil death, revealed through the reduced GAPDH signal in both donors.

Strain C appeared to show a similar time-course of increased Rab10 phosphorylation in neutrophils to the PAO1 strain (**Figure 3.1**), possibly suggesting similar properties of the strains. However, the band-shift of several Rab proteins at 4 hours of infection with PAO1 (**Figure 3.1**) was not observed with any of the clinical isolate strains, which may suggest specific differences of PAO1 strain interaction with Rab proteins. Explanations for the reasons behind *P. aeruginosa* strain differences, as well as future methods to better interrogate the impact of these differences on LRRK2 biology, is explored within the discussion (**5.1.1**)

In all experiments (**Figures 3.1-3.3**), use of MLi2 led to LRRK2 Ser935 dephosphorylation, confirming the ability of LRRK2 kinase inhibitors to control LRRK2 phosphorylation. On analysis of total LRRK2, whilst the molecular weight of full-length LRRK2 resides around 250kDa, use of the LRRK2 antibody recognising the C-terminal domain of LRRK2 in **Figures 3.2 and 3.3** revealed a strong band above 150kDa (~170kDa) in both Donor 1 and Donor 2, corresponding to an N-terminally truncated form of LRRK2. Previous work on peripheral blood neutrophils using this antibody have similarly reported the presence of this truncated LRRK2 170kDa species, which showed higher abundance compared to the full-length 250kDa form[79]. This truncated form is thought to result from proteolysis of LRRK2 in neutrophils, which have very high levels of the elastase protease.

FIGURE 3.1

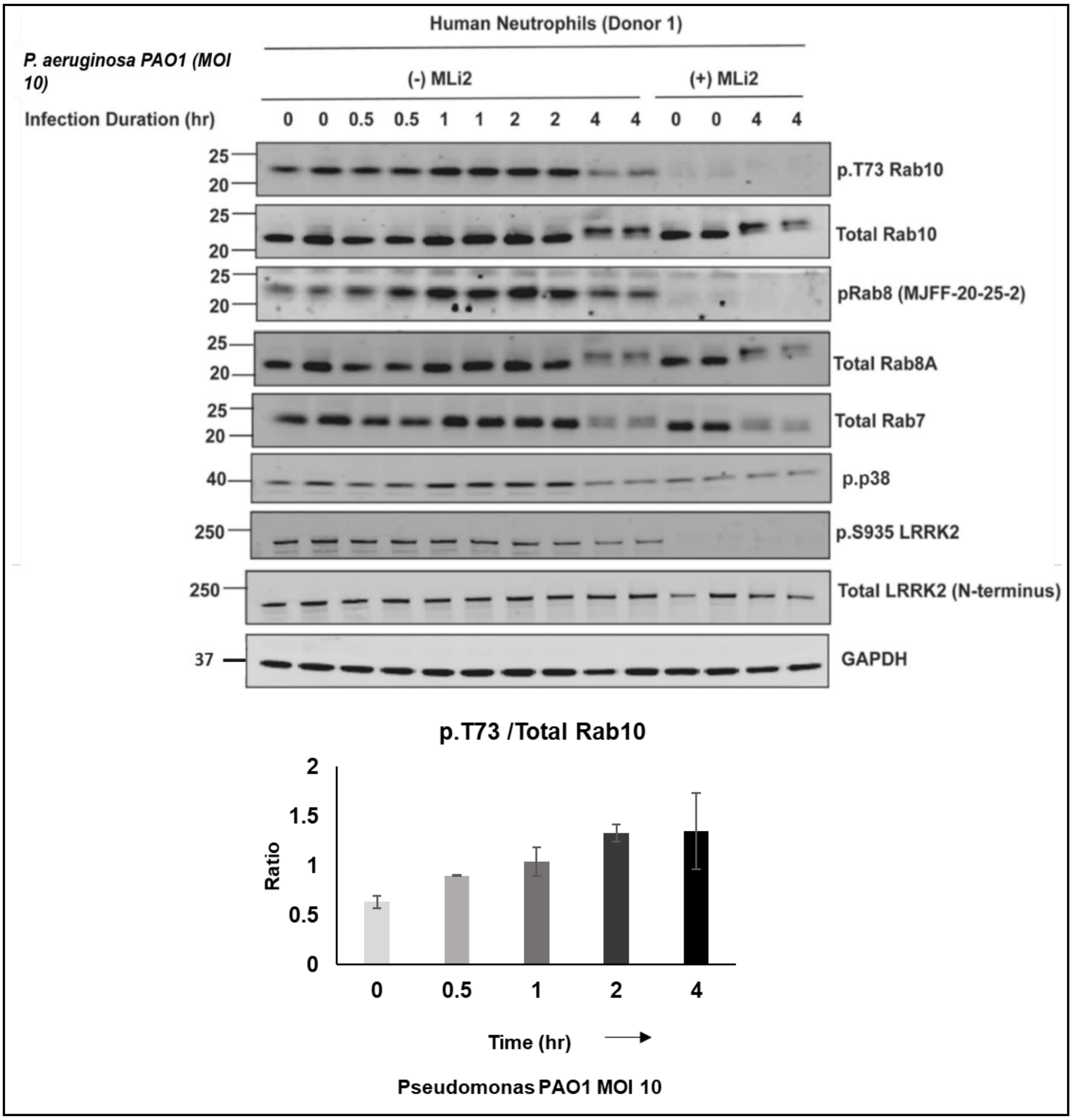

FIGURE 3.1: Increased LRRK2-mediated Rab10 phosphorylation following *P. aeruginosa* PA01 infection of human peripheral blood neutrophils

(Top) Immunoblot analysis of peripheral blood neutrophils infected with characterised PAO1 *P. aeruginosa* strain. Peripheral blood neutrophils were isolated from whole blood samples from healthy donors. Neutrophils were pre-treated with +/- 200nM MLi2 for 30 minutes, prior to infection with PAO1 over a time course of 0-4 hours (MOI 10). Membranes were probed with indicated antibodies (1µg/ml antibody) within **Table 2**; pT73 Rab-10 and Total Rab10 to investigate LRRK2 activity, as well as additional antibodies for the following Rab proteins: Rab 8A, Rab7 (total), p-Rab8 (MJFF-20-25-2). MLi2 treatment was verified by immunoblotting with pS935-LRRK2 antibody, and *P. aeruginosa* infection verified through probing against p.p38. GAPDH was used as an internal loading control. **(Bottom)** Quantification of immunoblots analysed through pThr73-Rab10 /Total Rab10 ratio.

FIGURE 3.2

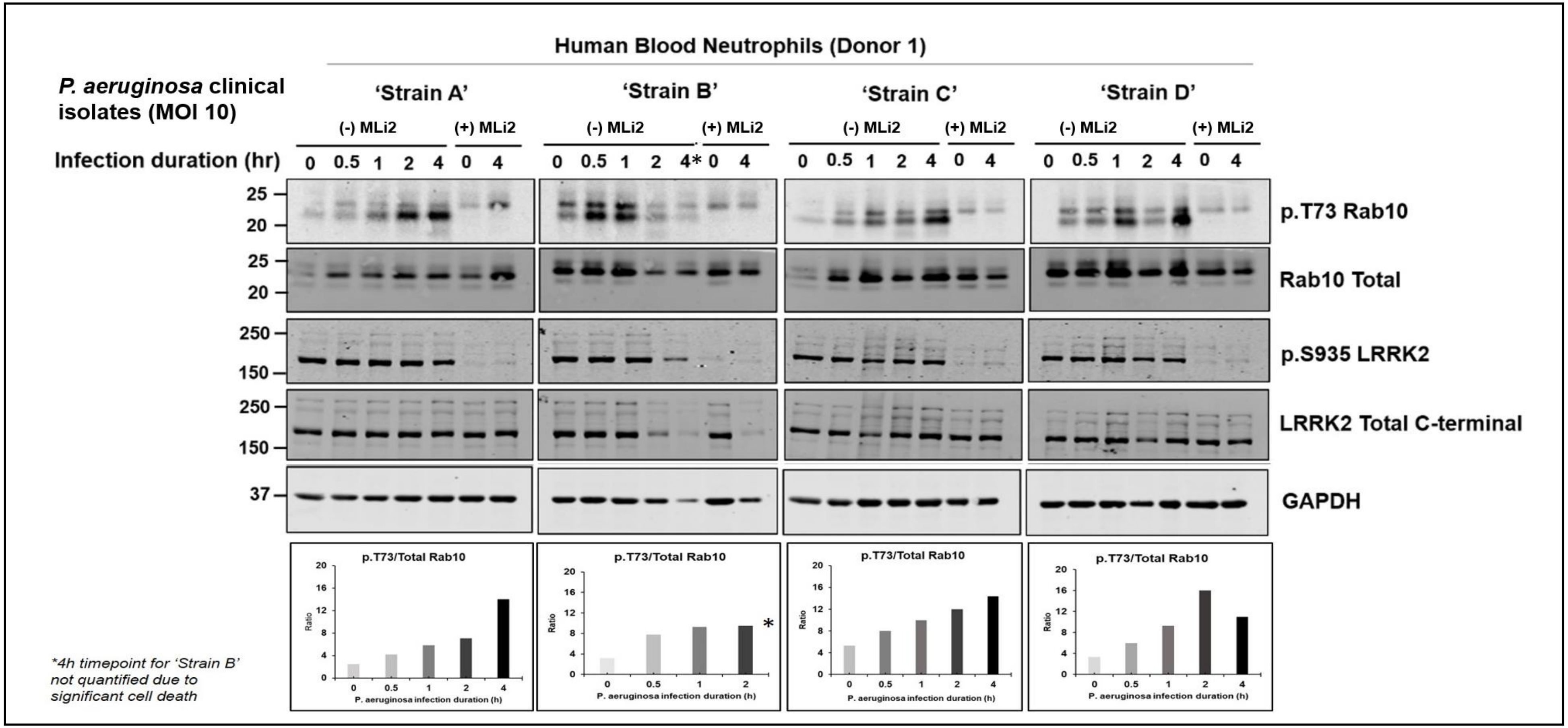

FIGURE 3.2: Increased LRRK2-mediated Rab10 phosphorylation following infection of human peripheral blood neutrophils (Donor 1) with *P. aeruginosa* clinical isolates (uncharacterised Strains 'A-D')

(Top) MLi2 treatment and infection time-courses in peripheral blood neutrophils isolated from Donor 1 were repeated as described above in legend for **Figure 3.1.** Each *P. aeruginosa* strain (A-D) was obtained from the sputum of different chronically infected cystic fibrosis (CF) patients. Membranes were probed with indicated antibodies (1µg/ml antibody), using pThr73-Rab10 and Total Rab10 to investigate LRRK2 activity resulting from *P. aeruginosa* strain infection. MLi2 treatment was verified by immunoblotting with pS935-LRRK2 antibody. GAPDH was used as an internal loading control. **(Bottom)** Quantification of immunoblots analysed through pT7-Rab10/ total Rab10 ratio shown for each strain. As significant cell death was observed at 4h upon infection of neutrophils with Strain B, pT73-Rab10 /Total Rab10 ratio was not quantified at this time-point (* indicated in Figure).

FIGURE 3.3

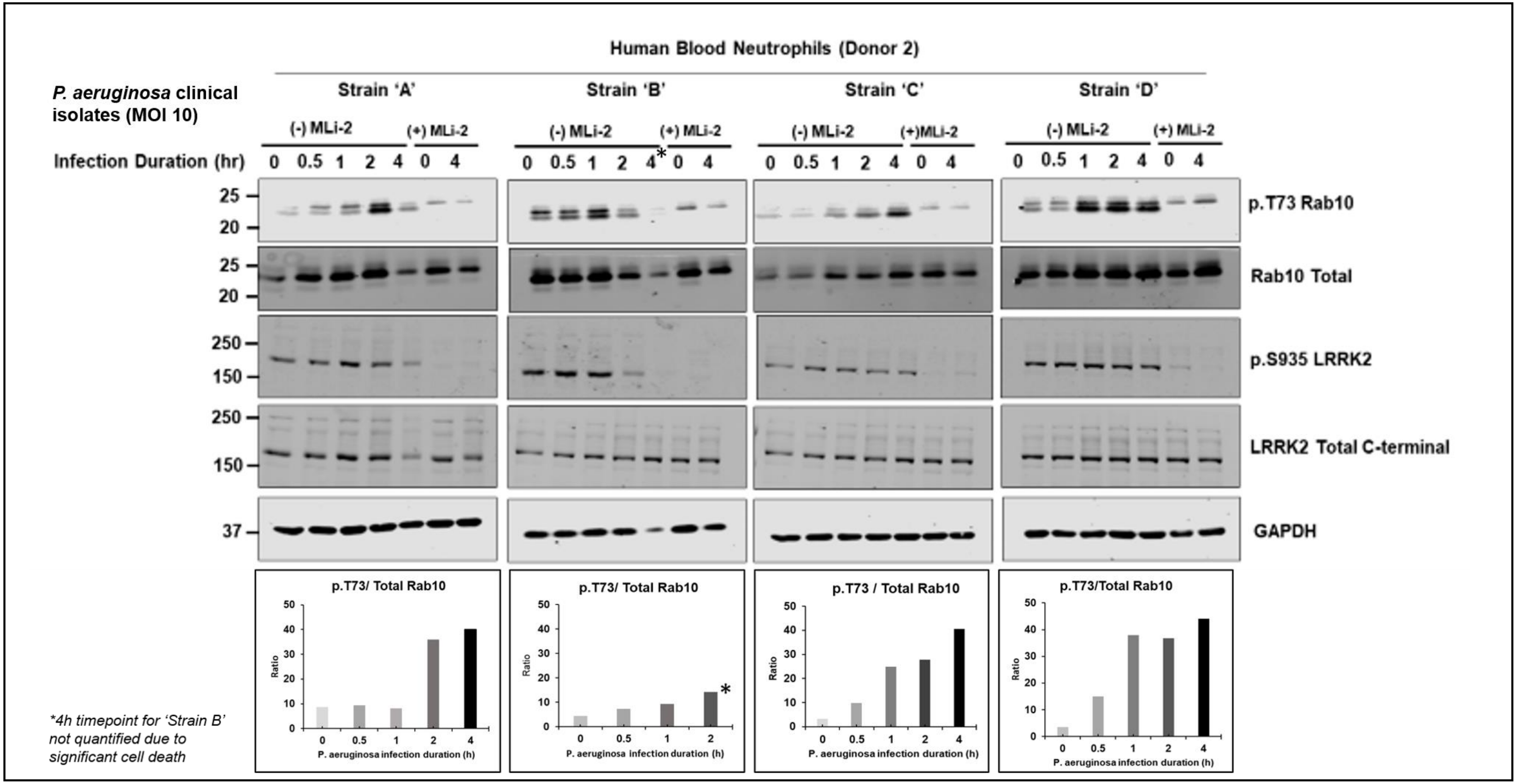

FIGURE 3.3: Increased LRRK2-dependent Rab10 phosphorylation following infection of human peripheral blood neutrophils (Donor 2) with *P. aeruginosa* clinical isolates (uncharacterised Strains 'A-D')

Methodology as described above in **FIGURE 3.2 legend** for top and bottom panels. Similar cell death at 4h using *P. aeruginosa* 'Strain B' was also observed in neutrophils isolated from Donor 2, hence was not included in the pT73-Rab10/Total Rab10 quantification.

3.2 Investigating LRRK2 activity within sputum neutrophils from cystic fibrosis (CF) patients with chronic *P. aeruginosa* infections

Given that increased LRRK2-dependent Rab10 phosphorylation at Thr73 was observed in peripheral blood neutrophils infected with *P. aeruginosa* strains, I next investigated whether LRRK2 activation can be observed in neutrophils isolated from the sputum of CF patients, who are frequently infected with *P. aeruginosa*, and thus harbour the pathogen in their sputum. To achieve this, I directly isolated neutrophils from sputum samples provided from multiple CF patients with recent infective exacerbations (with prior *P. aeruginosa* infection), and obtained un-infected control samples of a) sputum neutrophils isolated from the sputum of a patient with Primary Ciliary Dyskinesia (PCD), and b) peripheral blood neutrophils from a healthy blood donor. All isolated neutrophils were pre-treated with/without 200nM MLi2 and levels of pThr73-Rab10 analysed within the lysates by immunoblotting. Thus, the aim of this experiment was to provide useful initial insight into the role of LRRK2 activity during chronic infection in CF patients, which could be carried forward for future work.

3.2.1 Increased Rab10 phosphorylation observed within sputum neutrophils from CF patients

Figure 3.4A reveals data from the initial experiment analysing LRRK2 activity in sputum neutrophils isolated from 5 infected CF patients (Donors 2-7), compared with 2 non-CF un-infected sputum (Donor 8) and blood (Donor 1) neutrophil controls. Notably, all CF sputum neutrophil lysates demonstrated elevated pThr73-Rab10/Total Rab10 signal compared to control sputum/blood neutrophil lysates, of which pThr73-Rab10 signal was confirmed to be LRRK2 dependent through its elimination with MLi2 treatment. This suggests considerably high LRRK2 activity occurring within CF neutrophils. Quantification of Rab10 phosphorylation normalised to Total Rab10 revealed large variation in Rab10 phosphorylation between CF donors **(Figure 3.4B, upper band)**, with Donor 5 exhibiting the highest increase in Rab10 phosphorylation. Moreover, levels of total Rab10 also appeared to differ between CF donors, which could point to alterations in expression following infection. However, from the small number of CF infected sputum samples alongside un-infected controls, the current work could not demonstrate statistically significant differences in Rab10 phosphorylation between samples, or investigate for key expression differences in Rab10 between individual samples.

Immunoblotting against p.p38 revealed variability in levels observed between CF sputum samples, suggesting differences in the amount of infection present in each sputum sample. This variability could be due to several factors including the chronicity of infection during which samples were taken, or the type or number of pathogens present in the samples. Interestingly, whilst CF Donor 5 exhibited the highest level of Rab10 phosphorylation, levels of p.p38 appeared the lowest compared to other CF samples. Reduced p.p38 signal could be due to chronic rather than acute infection, or due to a reduced level of infection itself. Thus, future work would require sputum culture analysis from each donor to confirm the type and number of pathogens present within the samples, and to then make correlations between p.p38/Total p38 and pThr73-Rab10/Total Rab10 ratios.

Between the uninfected blood/sputum control donors, sputum neutrophils from Donor 8 demonstrated a higher pThr73-Rab10/Total Rab10 signal ratio than that from peripheral blood neutrophils isolated from Donor 1, however this ratio was lower than all other sputum neutrophil samples from CF patients. p.p38 levels appeared low in both Donor samples, suggesting low levels of infection. It should also be noted that levels of total Rab10 were lower in Donor 8 compared to all other samples, in which the pThr73-Rab10 phosphorylation signal was also slightly reduced. Further work using more samples from PCD patients are needed to investigate whether these patients exhibit overall lower total Rab10 levels.

As previously demonstrated for peripheral blood neutrophils in **Figures 3.2 and 3.3**, use of the LRRK2 antibody recognising the C-terminal domain of LRRK2 revealed that the 170kDa truncated form of LRRK2 appeared in higher abundance in sputum neutrophils compared to the full length 250kDa form. Quantification of LRRK2 phosphorylation at Ser935 normalised to Total LRRK2 for each donor revealed that Ser935 phosphorylation was reduced upon MLi2 treatment in both full length **(Figure 3.4B, middle band)** and 170kDa N-terminally truncated LRRK2 species **(Figure 3.4B, lower band)**, albeit to varying extents. Interestingly, Donor 5 demonstrated the highest level of Rab10 phosphorylation compared to all other donors, however had one of the lowest levels of LRRK2 phosphorylation at Ser935, in both LRRK2 species. Conversely, Donor 1 (blood neutrophil control) showed the highest LRRK2 phosphorylation at Ser935 compared to all other donors in both species, despite having the lowest Rab10 phosphorylation. A similar finding had been previously noted in peripheral blood neutrophils from a PD patient possessing a G2019S mutation, who had relatively high levels of LRRK2 Ser935 phosphorylation, despite having low levels of Rab10 phosphorylation[79]. Together, my findings may illustrate that using LRRK2 Ser935 phosphorylation to investigate LRRK2 activity is not a reliable biomarker.

FIGURE 3.4A

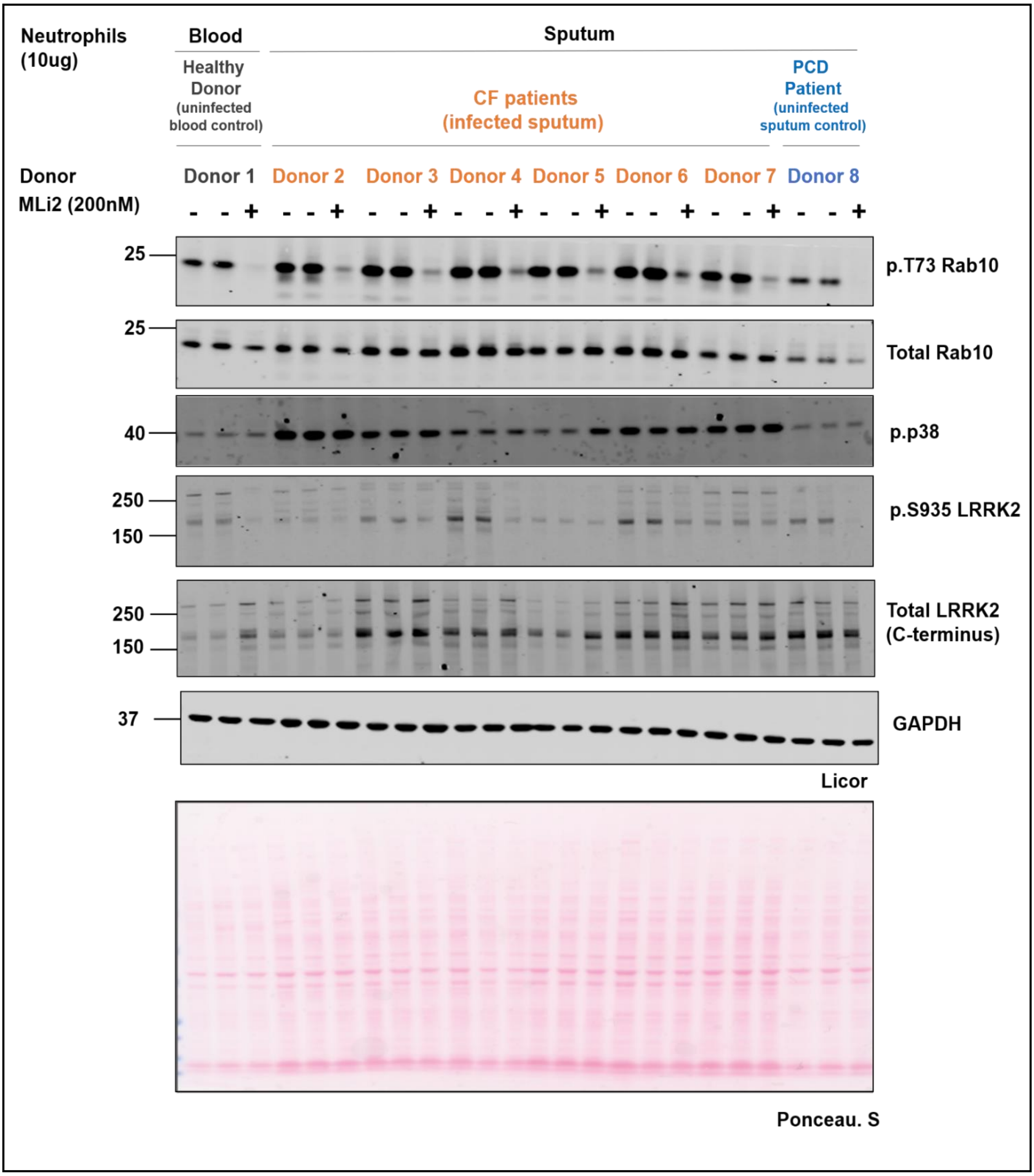

FIGURE 3.4A: Preliminary data of increased Rab10 phosphorylation indicative of LRRK2 activity within sputum neutrophils isolated from infected cystic fibrosis (CF) patients

Immunoblot analysis of sputum neutrophils (pre-treated with/without 200nM MLi2 for 30 minutes) isolated from: 6 different cystic fibrosis (CF) patients (Donor 2-7), a patient with primary ciliary dyskinesia (PCD, Donor 8), and peripheral blood neutrophils isolated from a healthy donor (Donor 1). Membranes were probed with antibodies (1µg/ml antibody); pT73-Rab 10 and Total Rab10 to investigate LRRK2 activity. GAPDH was used as an internal loading control, and Ponceau stain demonstrating equal loading of samples.

FIGURE 3.4B

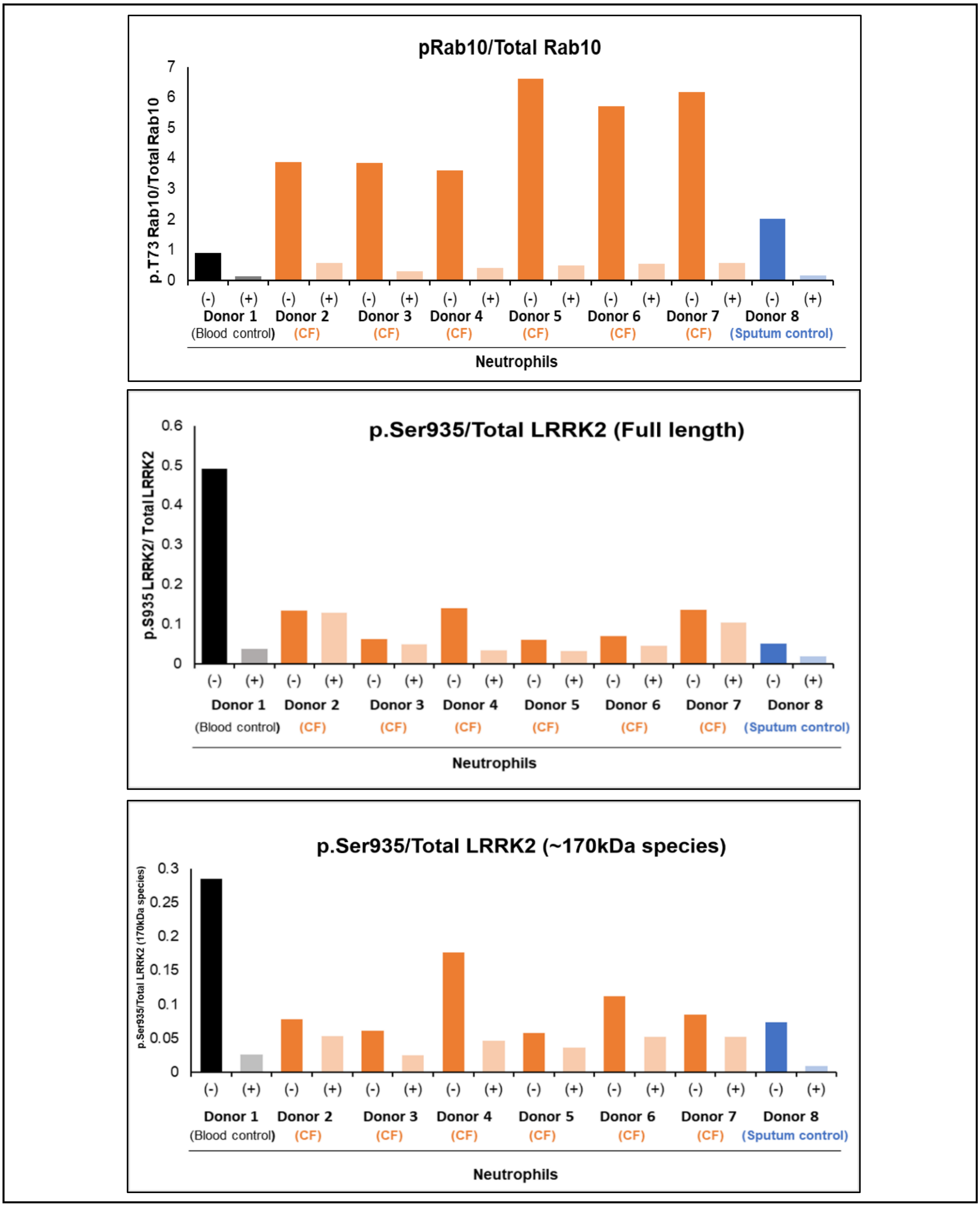

FIGURE 3.4B: Quantification of pRab10/Total Rab10 (Upper bands) and pSer.935/Total LRRK2 full length and 170kDa species (Middle, Lower bands)

(Upper) Quantification of immunoblot results from **Figure 3.4A** reveal that pThr-Rab10/Total Rab10 ratio is highest in sputum neutrophils isolated from CF patients (Donors 2-7), with Donor 5 revealing the highest increase in ratio. **(Middle, Lower bands)** Contrastingly, peripheral blood neutrophils isolated from Donor 1 (control) demonstrated the highest pS935-LRRK2/Total LRRK2 ratios compared to all other neutrophil donors, of both full-length and 170kDa species.

3.3 Investigating LRRK2 activity within mouse BMDMs infected with *P. aeruginosa*

Previously published work has investigated LRRK2 activation in response to infection in mouse bone marrow derived macrophages (BMDMs) with several intracellular pathogens[44,53], however LRRK2 activation following *P. aeruginosa* infection does not yet appear to have been explored. As discussed in **1.1.2**, previous work within the Alessi lab revealed that activation of immune signalling pathways using MyD88-dependent pathway agonists resulted in LRRK2 Ser935 phosphorylation, which was shown to be mediated by the IKK kinase family[49] (**Figures 1.4 and 1.5**). Other published work has revealed that LPS and flagellin produced by *P. aeruginosa* respectively stimulate TLR 2/4 and TLR 5 in mouse alveolar macrophages[59].

Thus, I hypothesised that *P. aeruginosa* infection in mouse BMDMs would similarly lead to LRRK2 Ser935 phosphorylation through activation of MyD88-dependent pathways, and if so, I investigated whether this was also due to IKK kinase control. Additionally, I investigated whether *P. aeruginosa* infection would lead to an increase in LRRK2-dependent Rab10 phosphorylation in mouse BMDMs, which previous work has not yet explored.

3.3.1 Increased LRRK2 Ser935 phosphorylation following PAO1 infection in WT BMDMs

As hypothesised, infection of mouse BMDMs with *P. aeruginosa* PAO1 resulted in a progressive increase in LRRK2 phosphorylation at Ser935 (pSer935-LRRK2) over a 0.5 - 4 hours infection time-course (**Figure 3.5**). PAO1 infection at 50 MOI resulted in a more rapid increase in pSer935-LRRK2 levels compared to 10 MOI, however phosphorylation levels were reduced by 4 hours of infection. Significantly, whilst basal pSer935-LRRK2 in uninfected WT BMDMs was abolished following 1 hour of 200nM MLi2 treatment, pSer935-LRRK2 was restored in MLi2 treated cells in the presence of 4 hours of PAO1 infection. The presence of Penicillin-Streptomycin (P/S) antibiotics within the culture medium of BMDMs with PAO1 infection (4-hour duration) revealed no change in LRRK2 Ser935 phosphorylation at either MOI 10 or 50. MLi2 or P/S treatments at other timepoints (0.5-2h) in this initial experiment shown in **Figure 3.5** were not assessed.

Despite the progressive increase in pSer935-LRRK2 levels, PAO1 infection at either MOI 10 or 50 appeared to have no effect on pThr-Rab10 levels in BMDMs, despite high expression levels of total Rab10 protein observed. In contrast, BMDMs treated with CNF3, a cytotoxic necrotising factor produced from pathogenic *E. coli*, produced a clear signal for Rab10 phosphorylation. Experiments confirming CNF3 in inducing Rab10 phosphorylation in mouse BMDMs has been previously demonstrated by Dr Ying Fan in unpublished work conducted within the Alessi lab, hence was used as a control to assess Rab10 phosphorylation in my experiment. The mechanism of how CNF3 induces Rab10 phosphorylation in BMDMs is not yet understood, however it is likely to activate a different upstream pathway of LRRK2 compared to *P. aeruginosa*.

Interestingly, immunoblotting against p.p38 in infected WT BMDMs revealed that p.p38 activation was highest at early timepoints (0.5 and 1 h) and reduced over the remaining 2 and 4 hour infection durations, which was seen at both MOI 10 and 50. This could be explained by a rapid activation response of the p38 MAPK signalling pathway upon infection in BMDMs, which reduces in intensity with increasing infection duration. This could explain the reduced p.p38 level despite high pThr-Rab10/Total Rab10 ratio observed in Donor 5, who may have had a longer duration of chronic infection compared to other CF donors (**Figure 3.4**).

3.3.2 Increased LRRK2 Ser935 phosphorylation following PAO1 infection in Rab29 KO BMDMs

Following recent work conducted within the Alessi lab which suggested that Rab29 may regulate basal phosphorylation of LRRK2 serine biomarker sites[35], I investigated whether LRRK2 Ser935 phosphorylation can still be induced in Rab29 knockout (KO) mouse BMDMs cells by PAO1 infection. The use of Rab29 knockout BMDMs was confirmed through immunoblotting for Rab29 with the Rab29 total antibody, which was detected only in the WT BMDM control.

Interestingly, progressively increasing levels of pSer935-LRRK2 were still observed within PAO1 infected Rab29 KO BMDMs, which was not eliminated with MLi2 treatment **(Figure 3.6)**. Furthermore, no observable Rab10 phosphorylation was observed in PAO1 infected Rab29 KO BMDMs, however was observed in Rab29 WT/KO control cells treated with 20 hours CNF3. As observed in WT BMDMs, immunoblotting with p.p38 was highest at earlier timepoints (0.5 and 1 h). Collectively, these results demonstrate that Rab29 is not required for *P. aeruginosa* induced LRRK2 Ser935 phosphorylation, or for CNF3-induced Rab10 phosphorylation.

FIGURE 3.5

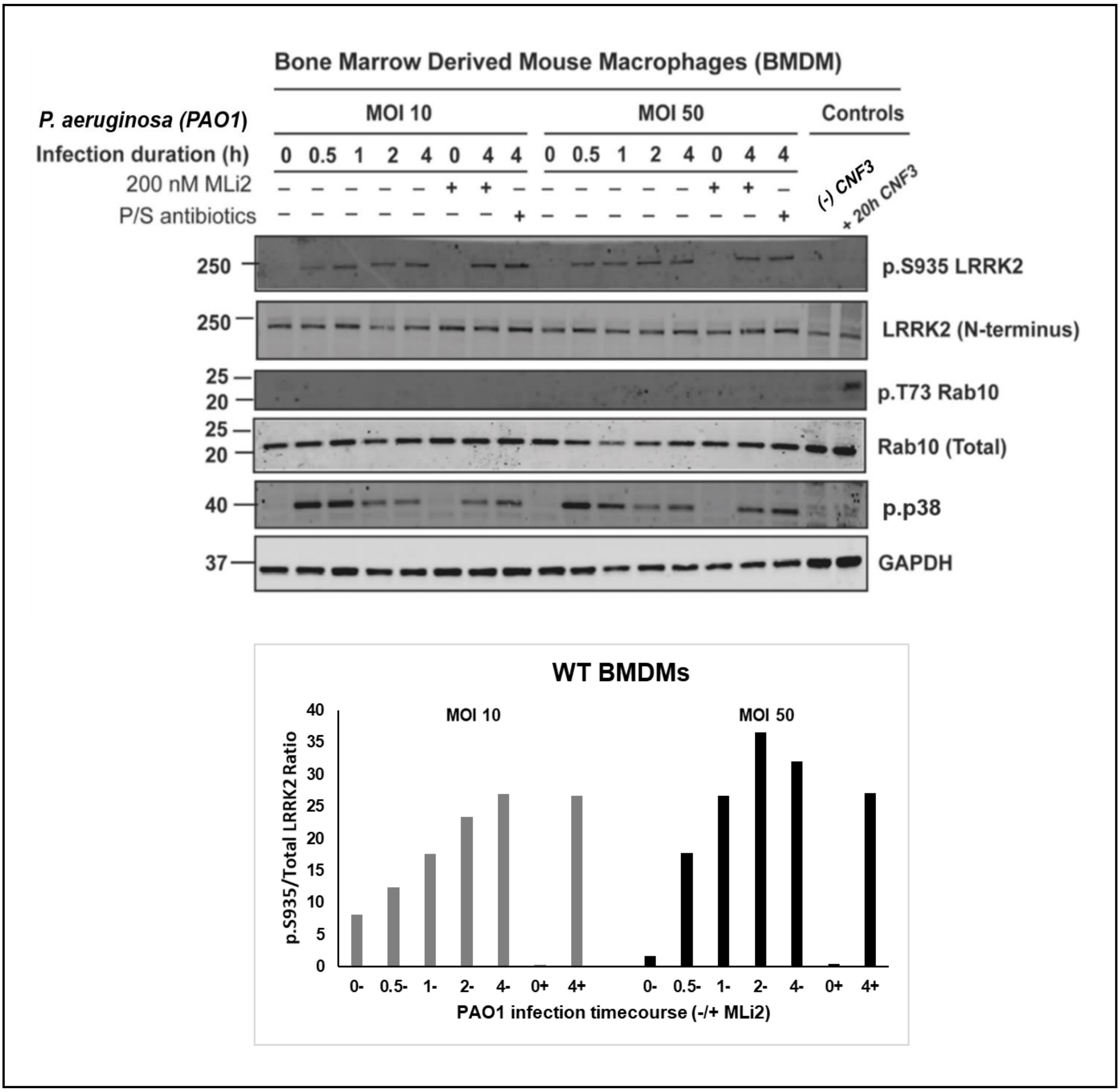

FIGURE 3.5: Increased LRRK2 Ser935 phosphorylation following *P. aeruginosa* PAO1 infection in wild-type (WT) BMDMs

(Top) Primary BMDMs were infected with PAO1 strain (MOI 10 or MOI 50) lasting for 0.5-4 hours. BMDMs were treated either with DMSO or 200nM MLi2 for 1 hour prior to infection, of which 0 and 4 hour infection was used in MLi2 treated cells. In addition, BMDMs cultured in media containing Penicillin/Streptomycin (P/S) were infected with PAO1 for 4 hours. Membranes were probed with the indicated antibodies (1µg/ml antibody), with GAPDH used as an internal loading control. WT BMDMs treated with +/- CNF3 for 20 hours were used as controls. **(Bottom)** Quantification of immunoblots analysed through pS935-LRRK2/Total LRRK2 for both MOI 10 and MOI 50 experiments.

FIGURE 3.6

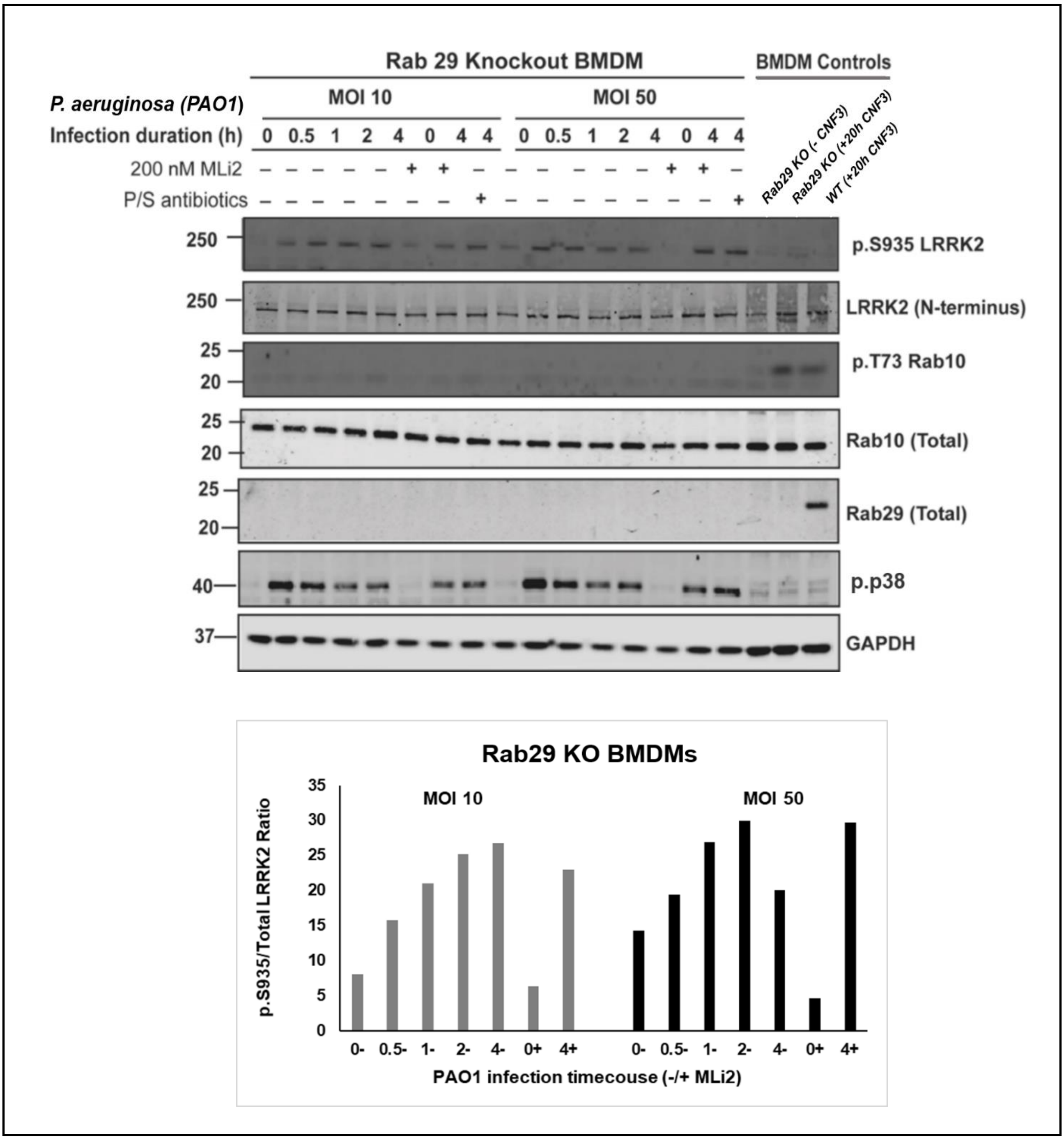

FIGURE 3.6: Increased LRRK2 Ser935 phosphorylation following *P. aeruginosa* PAO1 infection in Rab29 knockout (KO) BMDMs (7B)

(Upper) Experiment design as described in **Figure 3.5**, but using Rab29 KO BMDMs, with Rab29 KO and WT BMDMs treated +/- CNF3 for 20 hours were used as controls. (**Lower**) Quantification of immunoblots analysed through pS935-LRRK2/Total LRRK2 for both MOI 10 and MOI 50 experiments.

3.3.3 LRRK2 Ser935 phosphorylation following PAO1 infection in BMDMs is mediated by ‘canonical’ and ‘non-canonical’ IKK kinases

Following the results obtained in **Figures 3.5 and 3.6**, I set out to investigate whether both ‘canonical’ and ‘non-canonical’ IKK kinases were responsible for the LRRK2 Ser935 phosphorylation observed with PAO1 infection. Previous work from the Alessi lab demonstrated that to block LRRK2 Ser935 phosphorylation in mouse BMDMs treated with various MyD88-dependent agonists, it was necessary to pre-treat cells with a pharmacological inhibitor of TAK1 (Oxozeaenol), in conjunction with inhibitors of TBK1/ IKKε (MRT77307) (**Figure 1.5**)[49]. Thus, I followed the same experimental procedure by pre-treating mouse BMDMs for 1 hour with NG25 (alternative TAK1 inhibitor) and MRT77307, either in isolation or in combination, prior to infection with PAO1 for 0.5-4 hour time durations. Additionally, I assessed the impact of MLi2 treatment in BMDMs to investigate whether LRRK2 plays a role in controlling infection-induced Ser935 phosphorylation.

As previously observed, a progressive increase in LRRK2 phosphorylation at Ser935 following increasing durations of PAO1 infection was demonstrated in DMSO controls **(Figure 3.7)**. However, upon combined use of NG25+MRT77307 IKK kinase inhibitors at 1 and 2 hours, Ser935 phosphorylation was markedly reduced to below uninfected levels, which was a considerably stronger reduction compared with their individual use **(Figure 3.7, lower right)**. This mirrors what has been previously demonstrated for combined use of TAK1/TBK1 and IKKε inhibitors (**Figure 1.5**)[49]. Immunoblotting for p.p38 revealed an increased signal upon PAO1 infection (uninfected compared to 0.5h infection), however the intensity of p.p38 signal decreased over the length of infection, as seen in **Figures 3.5** and **3.6.** Use of the TAK1 inhibitor abolished p.p38 signal, which was demonstrated in previous work (**Figure 1.5**)[49]. 4 hours of infection in the presence of TAK1 inhibitors was lethal to BMDMs, shown by the significant reduction of GAPDH signal in these lanes.

Interestingly, a Ser935 phosphorylation reduction was observed with MLi2 treatment during 0.5, 1 hour and 2- hour PAO1 infection in BMDMs, although to not the same extent of combined inhibitor treatment. However, by 4 hours of PAO1 infection, Ser 935 phosphorylation was restored to untreated levels, as observed in **Figure 3.7.** Interestingly, in MLi2 treated cells, p.p38 signal gradually re-appeared at longer time durations (2-4 hours) of PAO1 infection. Collectively, these findings could suggest that LRRK2 kinase maintains some control over basal Ser935 phosphorylation during early infection.. However, with increasing infection duration, LRRK2 control over Ser935 phosphorylation appears to weaken, either by being overpowered by TAK1/TBK1 and IKKε control, or through *P. aeruginosa* inhibition of LRRK2 phosphatases that control Ser935 dephosphorylation. These possibilities will be further explored in the discussion below (**5.2.4**)

3.3.4 LRRK2 Ser935 phosphorylation following *P. aeruginosa* clinical isolate 'Strain A' infection in BMDMs is also mediated by canonical and 'non' canonical IKK kinases

In order to investigate whether other strains of *P. aeruginosa* also resulted in LRRK2 Ser935 phosphorylation, I infected WT BMDMs as above, but used the *P. aeruginosa* clinical isolate 'Strain A' for 1 and 2 hour durations. Given that the data from **Figure 3.7** revealed significant BMDM cell death following TAK1 inhibition in the presence of *P. aeruginosa* for over 4 hours, this time-point was not included for infection experiments using 'Strain A'.

Figure 3.8 demonstrates that *P. aeruginosa '*Strain A' causes a marked increase in Ser935 phosphorylation at both 1 and 2 hour infection durations compared to uninfected samples. However, in the presence of both NG25+MRT77307 IKK kinase inhibitors, Ser935 phosphorylation was significantly reduced, showing a greater reduction at 2 hours of infection. MLi2 appears to show some reduction in Strain A induced Ser935 phosphorylation, however has a less reductive effect compared to its use in BMDMs with 2 hours of PAO1 infection.

Comparing 'Strain A' with PAO1 infection, 2 hour infection with PAO1 produced a lower Ser935 phosphorylation signal compared to that with 'Strain A', which was lower than even 1 hour infection with Strain A. This suggests that 'Strain A' may enhance LRRK2 Ser935 phosphorylation to a greater degree than PAO1, potentially through activating other kinases that have not been inhibited. Indeed, whilst dual NG25+MRT77307 inhibitor use also resulted in a significant reduction of Ser935 phosphorylation (by ~75% at 2 hours of infection) in 'Strain A' treated BMDMs, residual Ser935 phosphorylation remained compared to in uninfected BMDMs. Overall, understanding how different *P. aeruginosa* strains may be controlled by a different balance of kinases would be interesting for future work to explore.

FIGURE 3.7

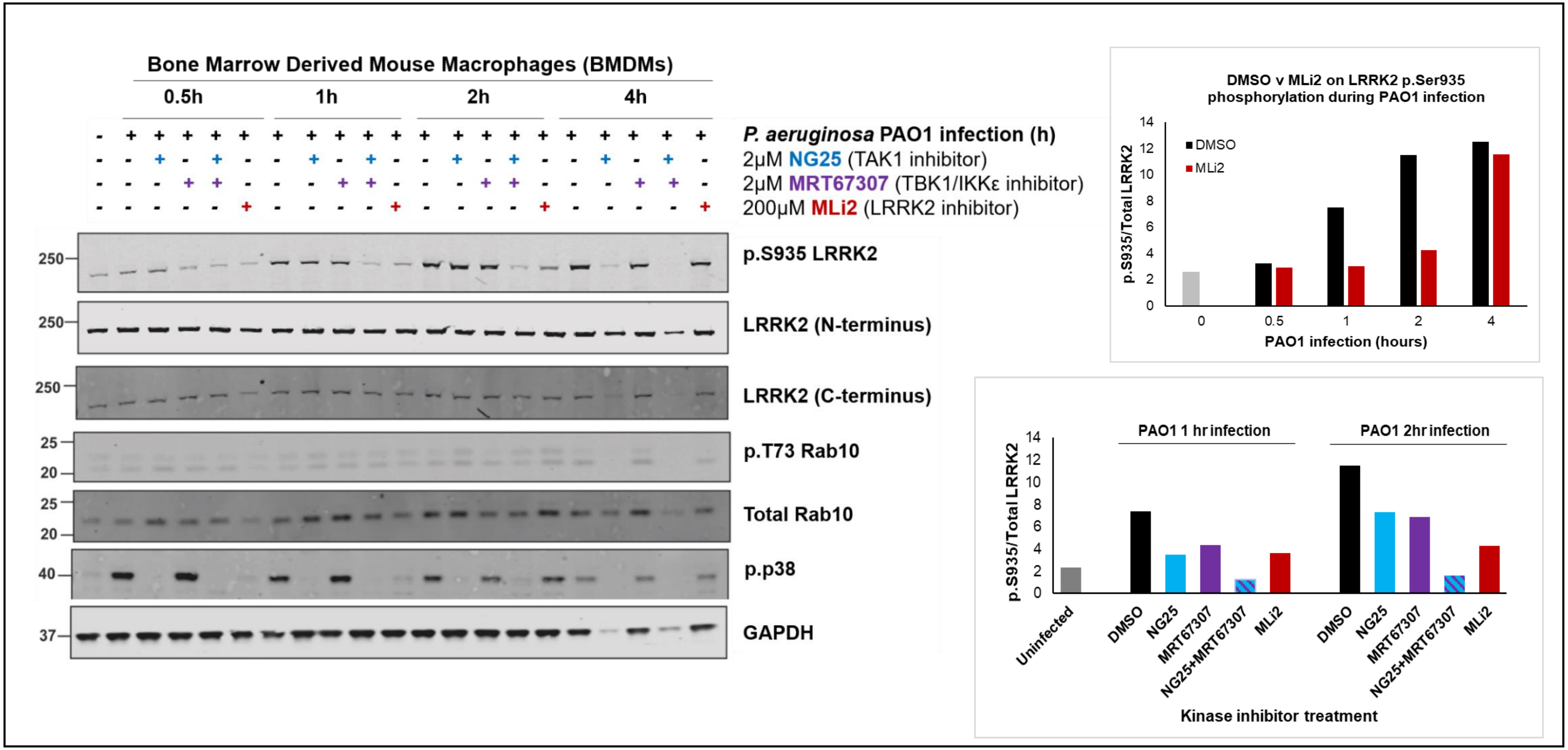

FIGURE 3.7: IkappaB kinases (TAK1 and TBK1/IKKε) contribute to LRRK2 Ser935 phosphorylation following *P. aeruginosa* PAO1 infection in primary mouse bone marrow derived macrophages (BMDMs)

Primary mouse BMDMs were treated with either DMSO, 2μM NG25 (TAK1 inhibitor), 2μM MRT67307 (TBK1/IKKε inhibitor), 200nM MLi2 alone or in the indicated combinations for 1 hour before infection with PAO1 strain (MOI 10) lasting for 0.5,1,2,4 hour durations. Cell lysates were subjected to immunoblot analysis with the indicated antibodies. **(Upper Right)** Quantification of immunoblots analysed for pS935-LRRK2/Total LRRK2 ratios in DMSO compared to MLi2 treated BMDMs at each infection time-course. **(Lower Right)** Quantification of immunoblots analysed for p.S935/Total LRRK2 ratios using all inhibitors at 1 hour and 2 hour PAO1 infection.

FIGURE 3.8

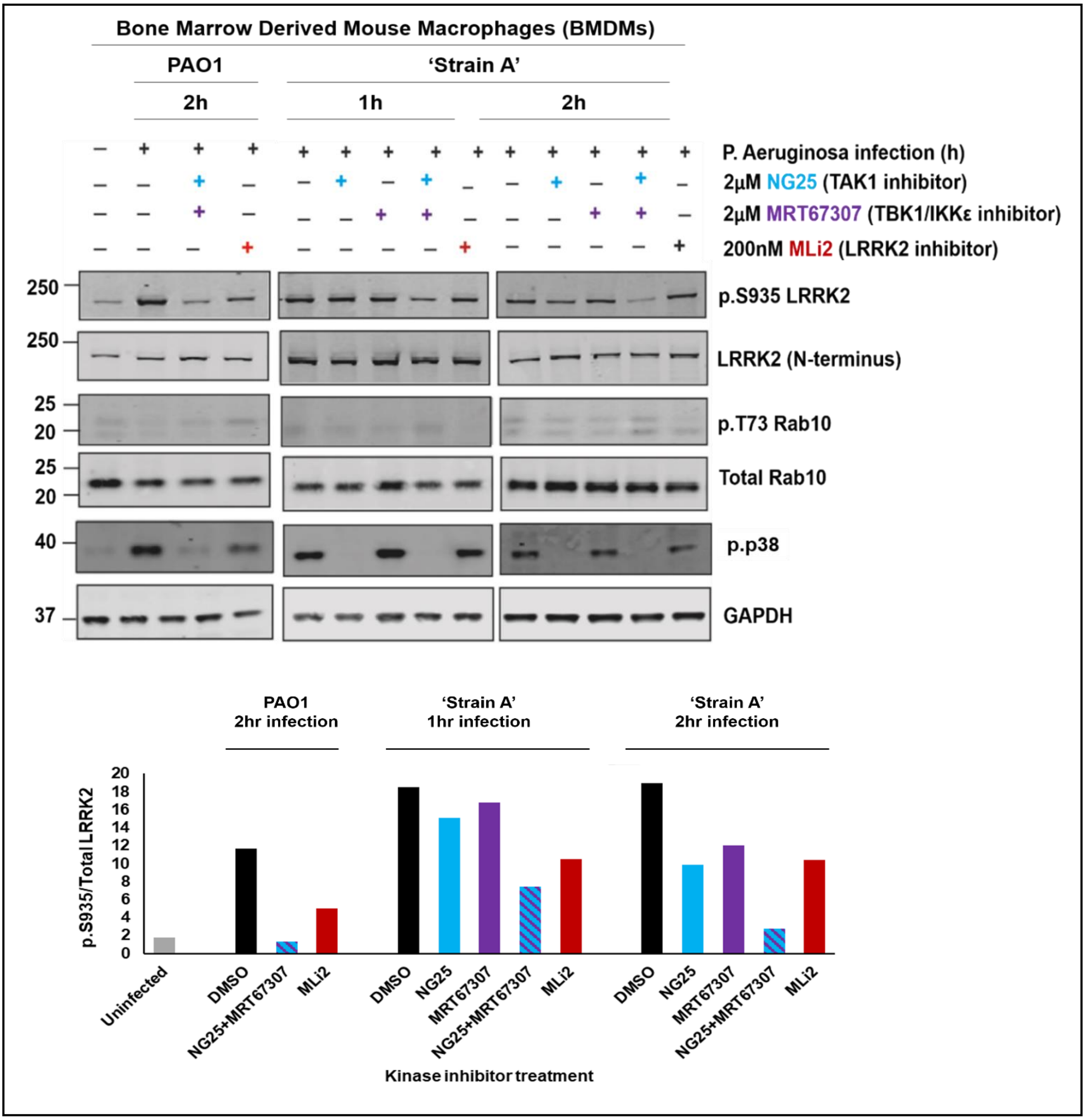

FIGURE 3.8: IkappaB kinases (TAK1 and TBK1/IKKε) contribute to LRRK2 Ser935 phosphorylation following *P. aeruginosa* clinical isolate 'Strain A' infection in primary mouse BMDMs

(Upper) As in **Fig. 3.7**; mouse BMDMs were treated with either DMSO, 2µM NG25 (TAK1 inhibitor), 2µM MRT67307 (TBK1/IKKε inhibitor), 200nM MLi2 alone or in the indicated combinations for 1 hour before infection with *P. aeruginosa* uncharacterised clinical isolate 'Strain A' (MOI 10) lasting for 1 or 2 hour durations. WT BMDMs treated with either DMSO, 2µM NG25+MRT67307 (combination TAK1 and TBK1/ IKKε inhibitor) and MLi2 for 1 hour were infected in parallel with PAO1 strain for 2 hours. Cell lysates were subjected to immunoblot analysis with the indicated antibodies.

(Lower) Quantification of immunoblots analysed for pS935-LRRK2/Total LRRK2 ratios using all inhibitors at 1 hour and 2 hour 'Strain A' infection compared with PAO1 infection.

4. *CHAPTER 4* - PROJECT B RESULTS

For **Project B**, the primary aim was to investigate whether I could detect stabilised PINK1 within human peripheral blood neutrophils. If achievable, these cells could henceforth be recommended as a valuable human cell source to directly investigate the PINK1/Parkin pathway, and compare levels of activity between PD patients and healthy individuals.

Before conducting the relevant experiments, I investigated for existing published evidence of mRNA expression of PINK1 within human peripheral blood neutrophils. Microarray and RNA-sequencing data available on the Expression Atlas database revealed that PINK1 mRNA expression is present within several human neutrophil sources, albeit to a much lower level than that of LRRK2, Rab10 and Rab8A (**Figure 4.1**). Parkin expression was found to be very minimal, and only minutely present in mature neutrophils. Therefore, given evidence of some PINK1 mRNA expression in human neutrophils, I began to conduct experiments to observe if activated PINK1 can be detected in human peripheral blood neutrophils following CCCP treatment. PINK1 activation would be detected either through the presence of stabilised PINK1 protein, or through detection pUb as a readout of PINK1 activity; using antibodies targeted to these proteins for immuno-blotting and immuno-precipitation analysis.

FIGURE 4.1

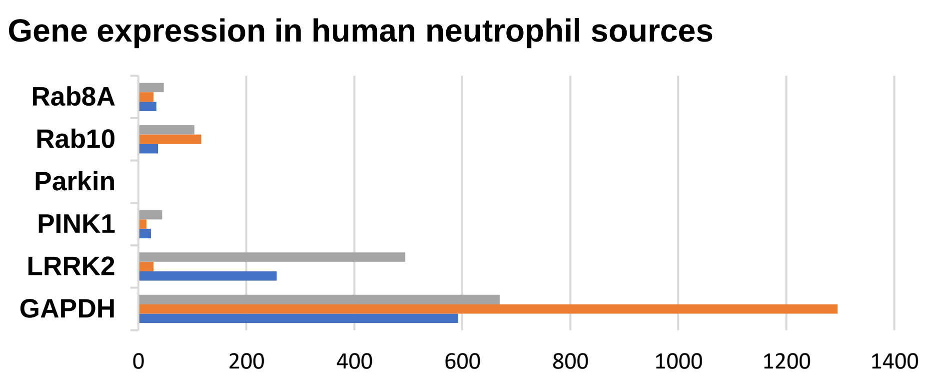

Transcripts per million (TPM):	GAPDH	LRRK2	PINK1	Parkin	Rab10	Rab8A
Segmented neutrophil of bone marrow	669	494	44		104	47
Neutrophillic metamyelocyte	1295	28	15		116	28
Mature neutrophil	592	256	23	0.7	36	33

FIGURE 4.1: Graphical expression of gene expression for Rab8A, Rab10, Parkin, PINK1, LRRK2, GAPDH in several human neutrophil sources

Gene expression, according to transcripts per million, was collected from the online database Expression Atlas (https://www.ebi.ac.uk/gxa/home). GADPH was used as a gene expression standard. PINK1 expression is present in all human neutrophil sources, albeit considerably lower in segmented bone marrow neutrophils compared to LRRK2 and GAPDH, as well as Rab10 and Rab8A. Parkin expression was not present in these cell types.

FIGURE 4.2

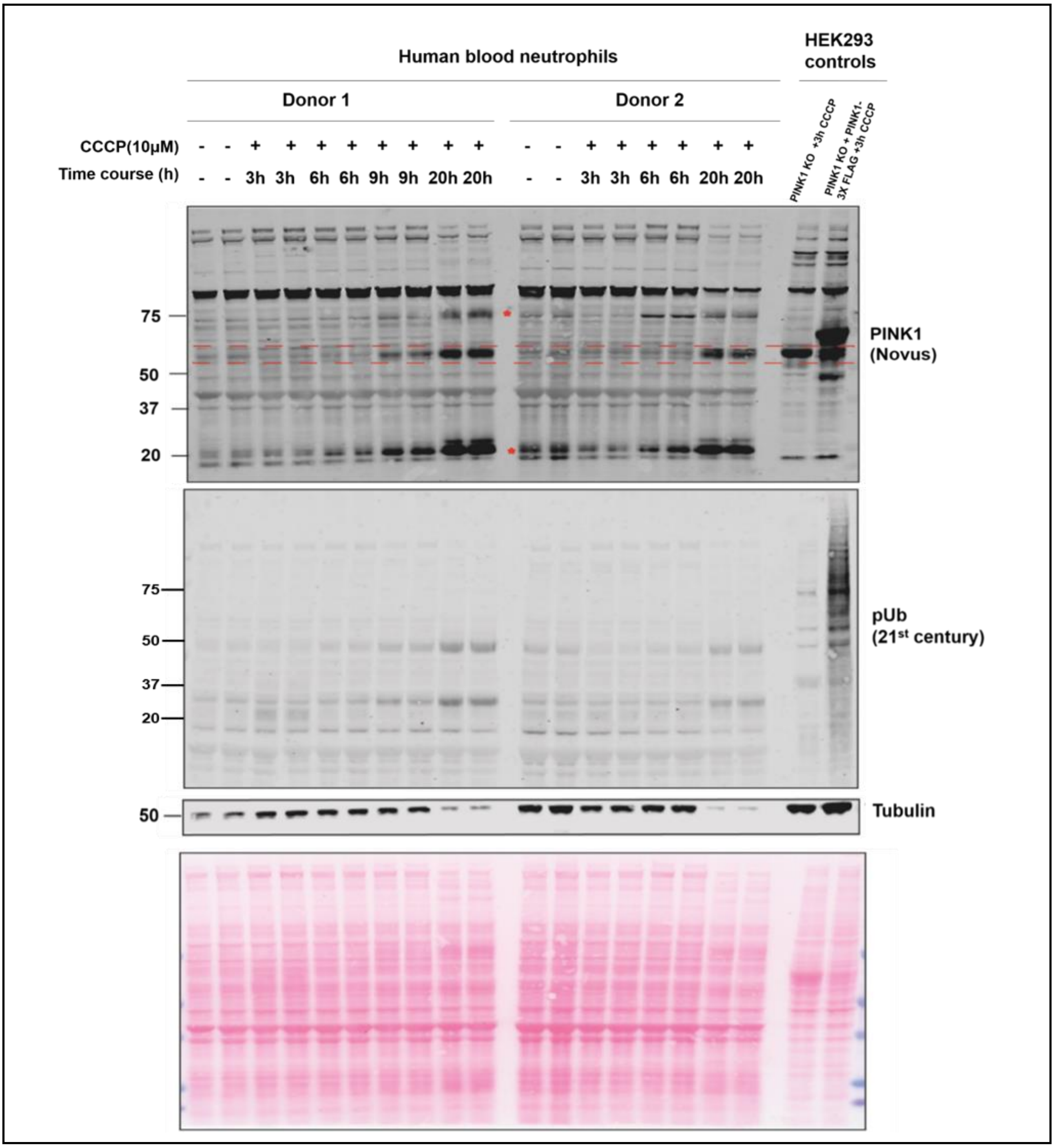

FIGURE 4.2: Interrogating for PINK1 activity following CCCP stimulation in peripheral blood neutrophil whole cell lysates.

Immunoblot analysis of peripheral blood neutrophils stimulated with 10μM CCCP over 3-20h time course, using HEK293 PINK1 knockout and PINK1 knockout cells re-expressing PINK1-3X FLAG (3h CCCP) as controls. Of note, 9h time-course was not used for Donor 2. **(Upper)** Probing the membrane with the anti-PINK1 (Novus Biologicals) antibody revealed presence of 3 species increasing at molecular weights of 75, ~60 (red box) and 20 with increasing CCCP durations. The ~60kDa species was originally considered as potentially activated PINK1, but deemed unlikely due to the similar weighted band in PINK1 KO control. (**Middle**) Probing with pUb antibody did not show any notable smear for pUb at any time point, compared to in the stimulated PINK1 control. (**Lower**) Probing with anti-Tubulin antibody demonstrated reduced protein lysate for both neutrophil donors at 20-hour CCCP treatment, suggesting significant cell death. (**Bottom**) Ponceau stain of membrane also provided.

FIGURE 4.3

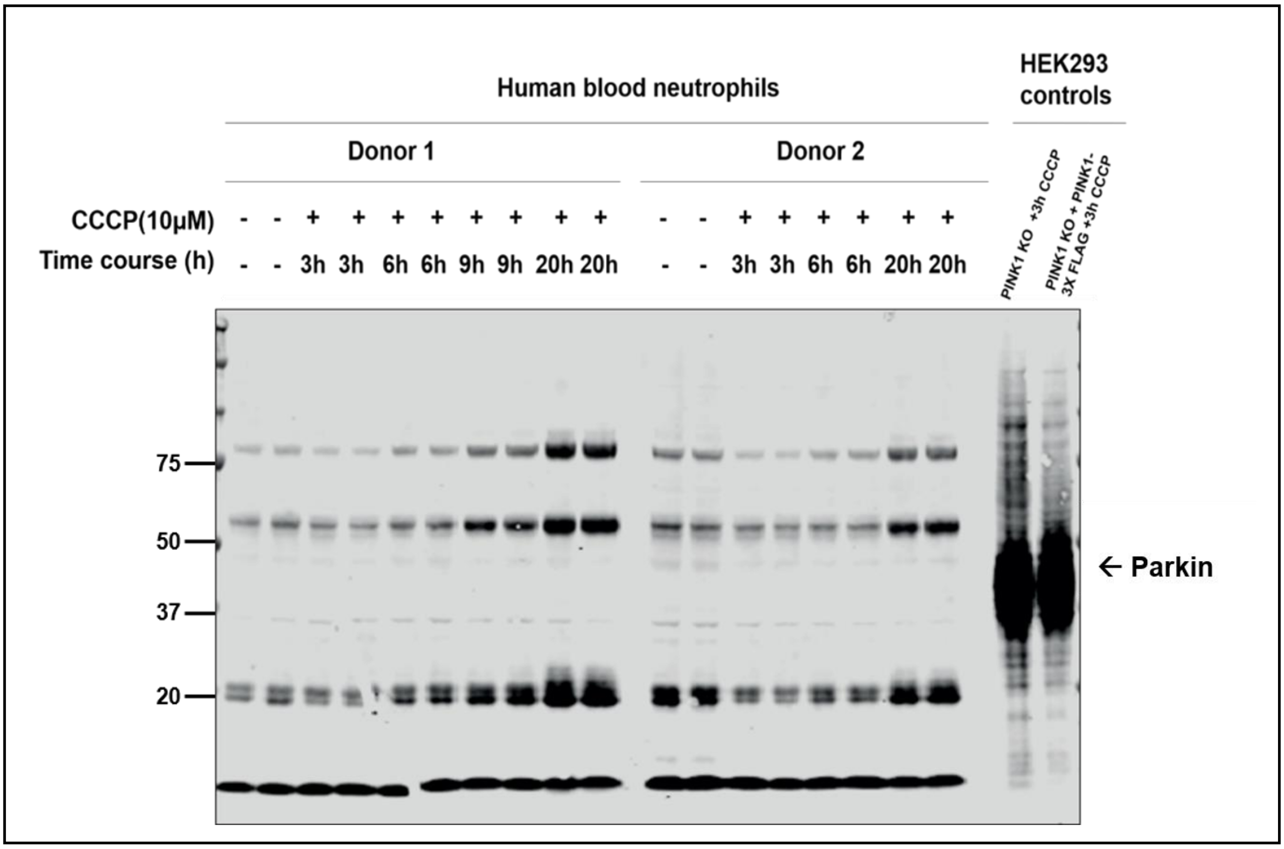

FIGURE 4.3: Interrogating for Parkin expression following CCCP stimulation in peripheral blood neutrophils

As above in **Figure 4.2**, the membrane was probed with the anti-Parkin (SantaCruz) antibody which did not reveal evidence of Parkin expression at the expected molecular weight (52kDa), however was strikingly observed as a larger smear in the PINK1 positive and negative HEK293 controls. 3 species increasing at molecular weights of 75, ~60 and 20 with increasing CCCP durations was also observed, which is likely to be due to non-specific binding as observed in **Figure 4.2** with the PINK1 (Novus) antibody.

4.1 Immunoblot analysis of peripheral blood neutrophils treated with CCCP

Initial immunoblot analysis of peripheral blood neutrophil lysates treated with 10µM CCCP and probed with the PINK1 polyclonal (Novus) antibody revealed 3 species migrating at 75kDa, ~60kDa and 20kDa, which appeared in a time-dependent manner after 9 or 20 hours CCCP treatment in both donors **(Figure 4.2).** Whilst the band around 60kDa appeared near the molecular weight expected for stabilised PINK1 (~63kDa, red box) a similar weight band was also seen in both HEK293 PINK1 knockout and PINK1 knockout cells re-expressing PINK1-3X FLAG wild-type (WT) (PINK1 positive control) lysates, suggesting it may be a non-specific band caused by cross-reactivity of the anti-PINK1 antibody with any degradation proteins present within neutrophils. Indeed, a larger isolated band appearing above the 60kDa species is only present within the HEK293 PINK1 positive control lysate, which is suggestive of over-expressed PINK1. Probing the membrane with anti-pUb antibody also did not show any characteristic signal smear in either donor at any time point, in contrast to the strong pUb signal seen in the HEK293 PINK1 positive control (**Figure 4.2**).

Upon probing the membranes for Parkin (**Figure 4.3**), no evidence of Parkin at the predicted molecular weight (52kDa) could be observed at any timepoint, which corroborates with previous Expression Database findings of minimal Parkin mRNA expression in human neutrophil sources (**Figure 4.1**). This is in contrast to the high intensity Parkin bands observed in both HEK293 PINK1 positive and negative controls, which both contain high Parkin expression. Interestingly, 3 species migrating above 75kDa, ~60kDa and 20kDa which increased in a time-dependent manner was observed in stimulated peripheral neutrophils probed for Parkin, similar to those seen when probing for PINK1 in **Figure 4.2**.

Collectively, the results suggest a lack of identifiable PINK1 or substrate activation in peripheral blood neutrophils following CCCP stimulation, and appear to demonstrate non-specificity in the bands recognised by antibody probing. Thus, in order to assess PINK1 activation in neutrophils following CCCP stimulation in account for potential low-expression, I subsequently conducted PINK1-immunoprecipitation experiments. Given that 20h stimulation with 10µM CCCP did not appear to be tolerated by neutrophils, evidenced by the reduced anti-Tubulin levels despite loading consistent levels of protein for each sample in **Figure 4.2**, the CCCP time-course for later neutrophil experiments was reduced to 12h**.**

FIGURE 4.4

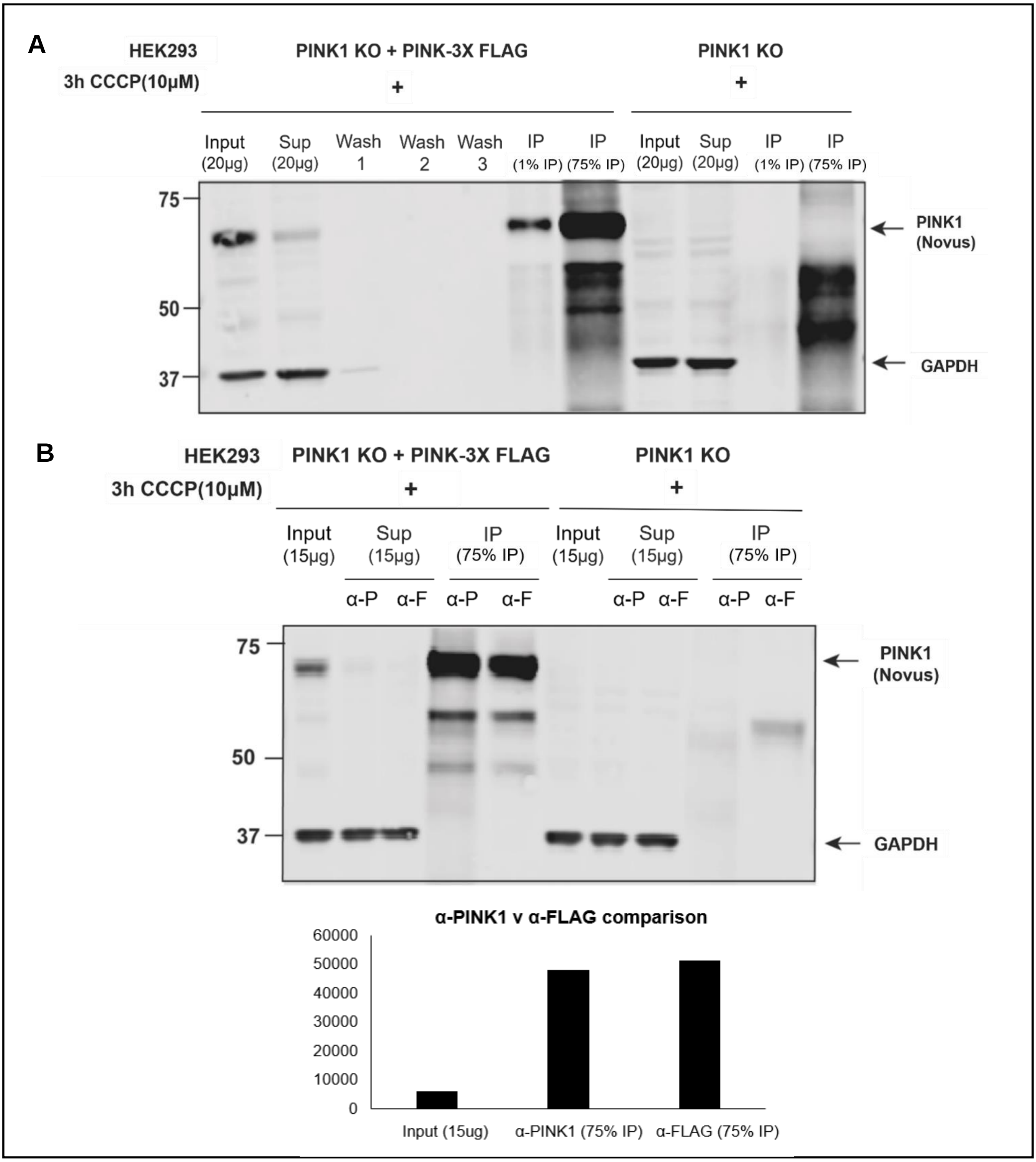

FIGURE 4.4: Immuno-precipitation of PINK1 from HEK293 PINK1 knockout cells and PINK1 knockout cells stably re-expressing PINK1-3X FLAG cells (24h doxycycline, 3h CCCP)

(A) 1mg of whole cell lysates were stimulated with CCCP and subjected to immunoprecipitation (IP) with PINK1 antibody (S085D) covalently coupled to protein G Sepharose beads. 75% of the IP was immunoblotted with anti-PINK1 (Novus) antibody, alongside 20µg of both whole cell lysate (input) and IP supernatant. **(B)** Western blot of PINK1 IP demonstrating comparable efficiency of PINK1 (S085D) coupled to protein G Sepharose beads (α-P) against anti-FLAG agarose beads (α-F), immunoblotted with anti-PINK1 (Novus), with quantification of PINK1 signal below **(B, lower panel)**. GAPDH was used as an internal loading control.

4.2 Optimisation of PINK1 immuno-precipitation and endogenous PINK1 expression control experiments

Prior to investigating PINK1 activation in peripheral blood neutrophils through immuno-precipitation (IP) experiments, I first optimised PINK1 IP based detection in cells with high PINK1 expression. **Figure 4.4A** shows initial testing of PINK1 (in-house S085D, 3rd bleed) antibody coupled with Protein G Sepharose beads in HEK293 FLP-In T-rex PINK1 knockout stably re-expressing PINK1-3X FLAG cell lysates (3h CCCP), confirming successful IP of PINK1 protein on Western blot. **Figure 4.4B** demonstrates that the PINK1 S085D IP beads were comparable in efficiency to commercially available anti-FLAG agarose beads, validating their subsequent use on stimulated whole cell neutrophil lysates **(Figure 4.6).**

In order to compare the detection of endogenous, rather than oxer-expressed, PINK1 in cell lysates to that in peripheral blot neutrophils, I used WT/PINK1 KO HeLa cells as controls for final experiments. Western blot analysis of whole cell HeLa WT/KO lysates treated with 10µM CCCP or combination 10µM Antimycin/1µM Oligomycin for 22 hours revealed that endogenous PINK1 can be detected in WT treated samples when probed with the anti-PINK1 (Novus) antibody (**Figure 4.5**). Use of CCCP as a mediator of mitochondrial depolarisation produced a stronger PINK1 band than the Antimycin/Oligomycin treatment combination, henceforth WT/PINK1 KO HeLa cells treated with CCCP were used for final neutrophil IP experiments as positive endogenous PINK1 controls **(Figure 4.6).** Several other PINK1 antibodies were also trialled (data not shown), however the anti-PINK1 Novus antibody produced the strongest signal that was both sensitive and specific for PINK1 detection in whole cell lysates, hence was used for remaining PINK1 IP experiments.

FIGURE 4.5

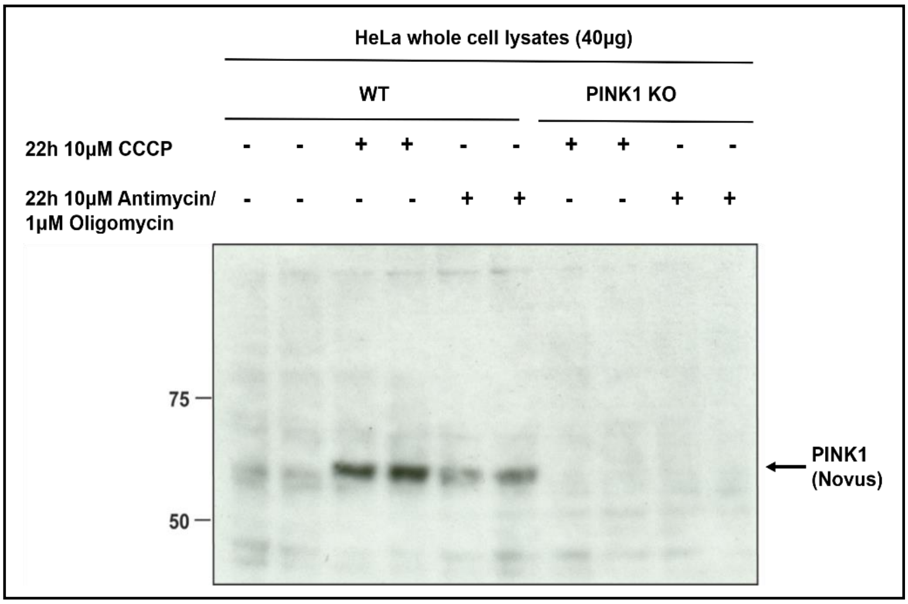

FIGURE 4.5: Western blot demonstrating PINK1 activation in endogenous wild-type (WT) and PINK1 knock-out (KO) HeLa whole cell lysates

WT and PINK1 KO HeLa cells were treated with +/- 10µM CCCP or +/- combination 10µM Antimycin/1uM Oligomycin (A/O) for 22 hours. 40µg whole cell lysates were immunoblotted and probed using the anti-PINK1 (Novus) antibody. A stronger band at 55kDa indicative of stabilised PINK1 appears using 22h CCCP compared to A/O.

FIGURE 4.6

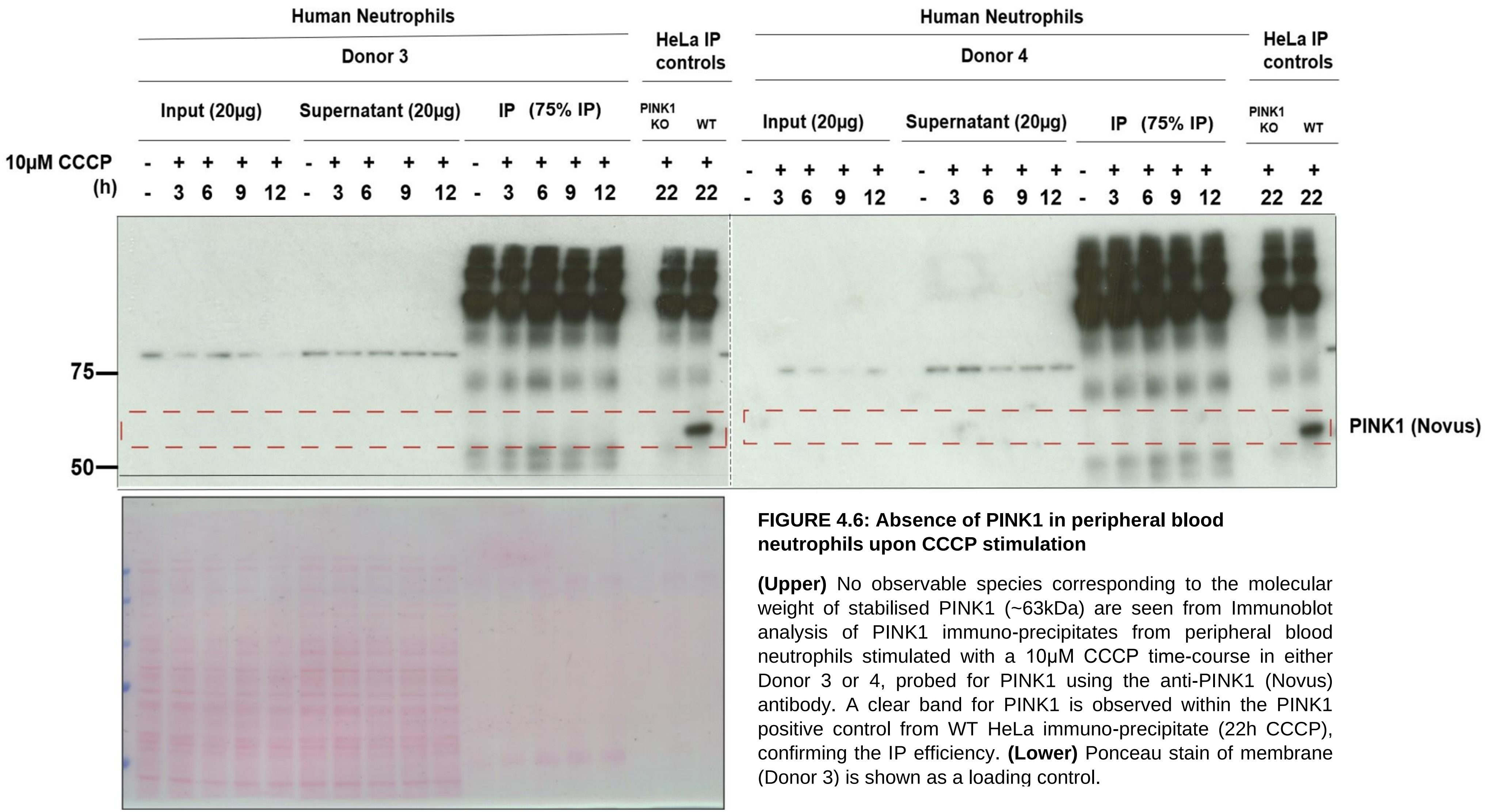

FIGURE 4.6: Absence of PINK1 in peripheral blood neutrophils upon CCCP stimulation

(Upper) No observable species corresponding to the molecular weight of stabilised PINK1 (~63kDa) are seen from Immunoblot analysis of PINK1 immuno-precipitates from peripheral blood neutrophils stimulated with a 10µM CCCP time-course in either Donor 3 or 4, probed for PINK1 using the anti-PINK1 (Novus) antibody. A clear band for PINK1 is observed within the PINK1 positive control from WT HeLa immuno-precipitate (22h CCCP), confirming the IP efficiency. **(Lower)** Ponceau stain of membrane (Donor 3) is shown as a loading control.

4.3 Final investigation of PINK1 activation within stimulated peripheral blood neutrophils through IP experiments

Having optimised IP PINK1 detection, I undertook a time-course of neutrophil stimulation with 10μM CCCP for 3-12 hours in neutrophils isolated from two donors (Donor 3 and 4), and then performed IP experiments of the lysates. Immunoblot analysis of 750μg neutrophil PINK1 immuno-precipitates probed with the anti-PINK1 antibody (Novus) did not show any bands suggestive of endogenous PINK1 presence at any timepoint, in either donor **(Figure 4.6).** In comparison, a strong band for endogenous PINK1 could be visualised from an equivalent amount of 750μg Hela WT PINK1 immuno-precipitate, stimulated with 22 hours of CCCP.

Collectively, the results support previous data from **Figure 4.2**, that endogenous PINK1 cannot be detected in peripheral blood neutrophils following 10μM CCCP stimulation of up to 12 hours. Suggestion future experiments to continue on from the current experiments will be explored within the **Project B 5.3** discussion chapter below.

5. *CHAPTER 5* –DISCUSSION

5.1 Results overview

The following paragraphs focus on the key findings and mechanistic possibilities from my results in **Project A and B** in the context of current literature, upon which I discuss further improvements of each project for future work.

Overall, my findings within **Project A** add to the growing body of research connecting LRRK2 with infection. In accordance with the main aims of **Project A**, I explored the impact of ex-vivo *P. aeruginosa* infection on LRRK2 activity within human peripheral blood neutrophils and mouse BMDMs. Interestingly, I found that *P. aeruginosa* infection in human peripheral blood neutrophils led to an increase in LRRK2-dependent Rab10 phosphorylation, but not in mouse BMDMs, despite both cell types expressing high levels of the LRRK2 protein (**Figure 5.2**). I also observed variable differences in cytotoxicity and the level of Rab10 phosphorylation induced in neutrophils depending on the *P. aeruginosa* strain utilised, including strain PAO1 and clinical isolate strains (‘A-D’) from chronically infected CF patients. Moreover, I demonstrated that *P. aeruginosa* infection in mouse BMDMs resulted in a steady increase in LRRK2 Ser935 phosphorylation, and confirmed that this was mediated through the IKK kinases. In my preliminary experiments using neutrophils isolated from sputum samples of infected CF patients with previous *P. aeruginosa* infection, I also found considerably high levels of LRRK2-dependent Rab10 phosphorylation, suggesting high levels of LRRK2 activity occurring within these cells.

My findings within **Project B** demonstrated that PINK1 stabilisation could not be detected in peripheral blood neutrophils following treatment with CCCP for up to 12 hours. Given that previous work has revealed that neutrophils have a low expression of PINK1 mRNA, these cells may not be a beneficial cell type to observe PINK1/Parkin activity, despite being a readily accessible human cell source.

5.2 Project A Discussion

5.2.1 Influence of *P. aeruginosa* strains on LRRK2-dependent Rab10 phosphorylation within infected peripheral blood neutrophils

My results in **Figures 3.1-3.3** revealed that infection of human peripheral blood neutrophils with different strains of *P. aeruginosa* led to increased LRRK2-dependent Rab10 phosphorylation at Thr73 (pThr73-Rab10), suggesting that the *P. aeruginosa* strains I used may have similar mechanisms of enhancing LRRK2 activity. However, there were notable differences in the rate of Rab10 phosphorylation induced between the strains, as well as in their cytotoxicity. For example, significant neutrophil death in both Donor 1 and 2 was uniquely seen following 4-hour infection with Strain B (**Figures 3.2-3.3**). Furthermore, a band-shift in several Rab proteins including Rab10, Rab 7 and Rab8A was only observed with the PAO1 strain (**Figure 3.1**)

Collectively, these observed differences could be due to distinct host-dependent adaptions of *P. aeruginosa* strains according to the unique lung environments of each CF individual from which they were isolated, including differential antibiotic use and poly-microbial exposure. As discussed in **1.3.1**, *P. aeruginosa* strains have shown to alter their phenotypic and genotypic properties over the time-course of colonization within CF individuals, whereby isolates from chronically infected CF patients more readily form biofilms and overexpress the exopolysaccharide alginate than strains isolated from the same patients at earlier timepoints[97]. Interestingly, later strains appear less inflammatory and cytotoxic; they lack key inflammatory bacterial features, such as flagella and pili, and have a downregulated type 3 secretion system (T3SS)[98]. Hence, it is possible that Strain B was isolated from a less-chronically infected CF patient compared to others, thus had higher cytotoxic properties when used within neutrophils.

Exploring whether adaptions in the inflammatory and cytotoxic properties of different *P. aeruginosa* strains can influence LRRK2-dependent immune signalling pathways necessitates further experimentation. For example, mass spectrometry analysis could investigate for LRRK2 interactors upregulated in neutrophils with each strain infection, as well as investigation for the types, amounts and rates of inflammatory markers or cytokines produced. Moreover, to assess whether changes within the same *P. aeruginosa* strain over time could influence LRRK2 activity, a future experiment design could isolate *P. aeruginosa* strains at different time-points from the same infected CF individual (such as through sputum collections from regular CF clinic appointments), and then investigate differences in the level or rate of LRRK2-dependent Rab10 phosphorylation induced upon infection of immune cells with these time-coursed strains. These experiments would provide useful observations over how evolutionary changes in *P. aeruginosa* could alter key cellular signalling pathways.

In order to assess for specific time-points of the band-shifts or cell toxicity induced by different strains, use of narrower infection duration margins (e.g. between 2-4 hours, when key changes appear to occur), would also be useful for future experiments. In addition, differences in the rate and amount of Rab10 phosphorylation observed per strain (**Figures 3.2-3.3)** may have been due to innate differences between the neutrophils themselves, such as in LRRK2/Rab10 mRNA and protein expression. Therefore, greater numbers of neutrophil donors and biological replicates are also required in future work.

5.2.2 Findings and future investigations of LRRK2 activity in CF sputum neutrophils during natural course of *P. aeruginosa* infection

My results within **Figure 3.4** revealed a novel finding that LRRK2-dependent Rab10 phosphorylation was considerably elevated in sputum neutrophils isolated from CF patients with recent acute infective exacerbations (Donors 2-7), compared to levels within uninfected peripheral blood and sputum neutrophil control samples (Donors 1 and 8). Given that all CF patients had suffered from previous *P. aeruginosa* infections, it is likely that *P. aeruginosa* was present in the collected sputum samples. Based on the results of **Figures 3.1-3,** *P. aeruginosa* presence within CF sputum neutrophils can thus be hypothesised to have influenced the levels of Rab10 phosphorylation observed. Alternatively, the results could point to a unique role of LRRK2/Rab10 phosphorylation in CF sputum neutrophils themselves, where their expression and function may be different.

Further exploration from these findings requires improvements of some of the current limitations within this experiment. Firstly, there may be generalised differences between sputum and peripheral blood neutrophils, including in LRRK2/Rab10 mRNA expression, hence the current comparison between the healthy peripheral blood neutrophil control (Donor 1) with sputum neutrophil samples from CF patients is not optimal. Therefore, future work should isolate both sputum and peripheral blood neutrophils from each CF patient, and subsequently compare any differences in LRRK2/Rab10 mRNA expression, as well as resultant Rab10 phosphorylation. In addition, an equal number of peripheral blood neutrophils should be isolated from healthy blood donors, to compare Rab10 expression and phosphorylation levels between healthy and CF donors.

Secondly, whilst sputum from a patient with PCD (Donor 8) was used as an uninfected ‘sputum’ neutrophil control, it is possible that their sputum sample may also have contained some bacterial pathogens remaining from previous/latent infection, despite not having an ‘acute’ exacerbation. Thus, to create more accurate sputum neutrophil comparisons in future work, an equal amount of sputum samples from non-CF patients and CF patients should be collected, with sputum cultures obtained from all samples to confirm the presence and type of pathogens present. This would enable future experiments to assess LRRK2-dependent Rab10 phosphorylation only in the presence of select organisms, including *P. aeruginosa*.

Bearing these improvements in mind, my findings within **Figure 3.4** pave the way for a future clinical study to investigate LRRK2 activation during the natural time course of *P. aeruginosa* infection within CF patients. A schematic of the proposed study plan is outlined within **Figure 5.1**. As a summary, sputum and blood samples would be collected from CF patients with chronic *P. aeruginosa* infection at a series of timepoints; a) at the start of an infective exacerbation prior to or within 48 hours of commencing antibiotic treatment, b) midway through antibiotic treatment, c) after the completion of antibiotic treatment and/or clinical improvement of patient symptoms. Samples would be respectively recorded as 'acute', 'mid-acute' or 'post-acute' as a generalised description of their infection status. In parallel, blood samples would be taken from age and gender matched healthy donors (e.g. relatives of CF patients), and sputum and culture samples from non-CF uninfected individuals. Routine microbiological culture and sensitivity testing would be performed for all sputum samples, in which only sputum samples without *P. aeruginosa* presence would be used as control samples. Investigation into other organisms frequently cultured in the sputum of CF patients, and comparison of their effect on LRRK2 activity, could also form a subsection of the study.

Following blood/sputum sample collection, all neutrophils would be directly isolated at each timepoint using the existing established protocols (described in **Methods 2.3.1 and 2.3.2**), treated with 200nM of MLi2/DMSO for 30 minutes, and lysates analysed together through immunoblotting to observe any change in LRRK2 activity over the infection time-course per donor. In addition, LRRK2 and Rab10 mRNA expression in both sputum and blood neutrophils from CF and non-CF patients at each collection would be assessed, in order to investigate for changes in transcription during the infection time-course.

Based on my results obtained in **Figures 3.1-3.4**, it could be hypothesised that CF sputum neutrophil samples collected at the start of *P. aeruginosa* infection would contain the highest levels of LRRK2-dependent Rab10 phosphorylation; when LRRK2 activation in response to infection is greatest, and gradually decrease as infection reduces following antibiotic treatment (**Figure 5.1**). Alternatively, given that CF patients are frequently infected with several pathogens, LRRK2 levels may remain considerably higher compared to non-CF individuals suffering from intermittent and resolvable infections, and may even remain elevated for longer than the acute infection time-course itself. Hence, evaluation of these future results will provide key insights into understanding LRRK2 activity during the natural infection time-course.

FIGURE 5.1

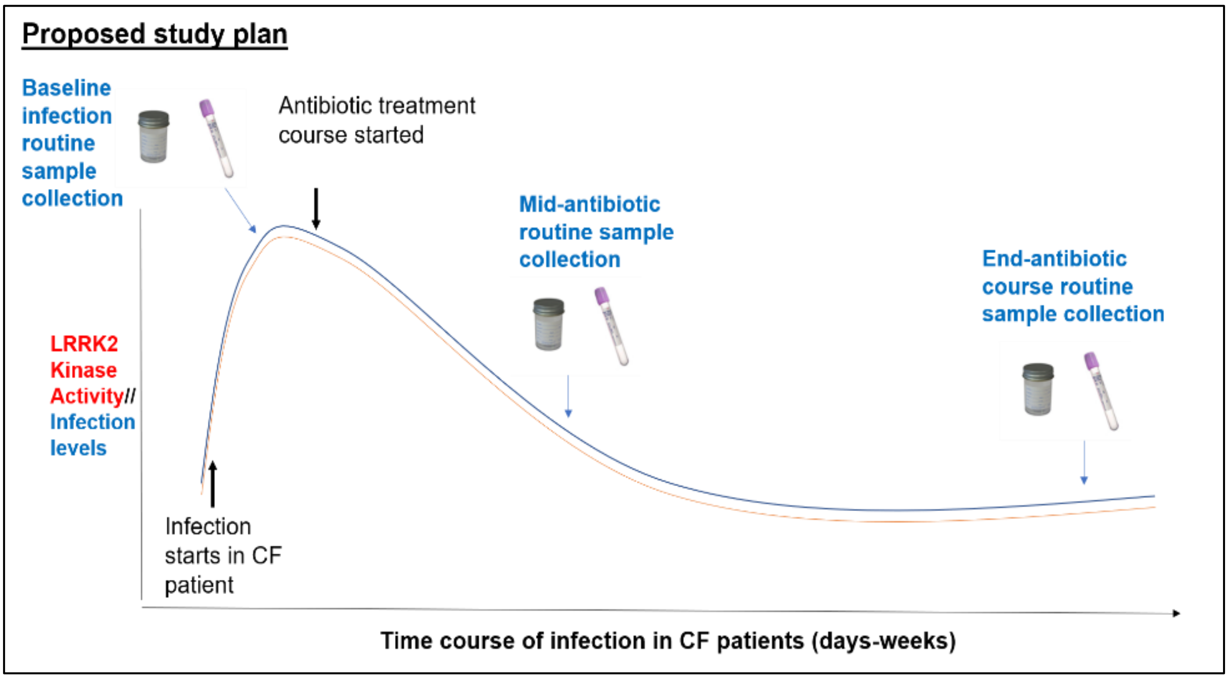

FIGURE 5.1: Schematic of proposed large-scale clinical study plan to investigate LRRK2 activity following in-vivo *P. aeruginosa* infection in CF patients.

Sputum and peripheral blood neutrophils would be collected from infected CF patients at 3 separate time-points over the typical infection time-course (days-weeks) and recorded as 'acute', 'mid-acute' and 'post-acute'. Sputum/blood neutrophil lysates obtained from each donor would be assessed for changes in LRRK2 activity through immunoblotting for levels of LRRK2-dependent Rab10 phosphorylation at Thr73 over the time-course of infection. In addition, control blood and sputum samples would be obtained from non-infected control individuals.

Based on current results, it could be hypothesised that LRRK2 activity would be highest at the start of infection prior to treatment, and then reduce as the infection subsides following antibiotic treatment. However, other LRRK2 patterns are possible, and thus would shed light on LRRK2 role and activation during infection.

Original image

5.2.3 Possible mechanisms behind LRRK2-dependent Rab10 phosphorylation in neutrophils during *P. aeruginosa* infection

There are several possible mechanisms behind how *P. aeruginosa* infection in human neutrophils promotes LRRK2-dependent Rab10 phosphorylation. Firstly, *P. aeruginosa* infection in neutrophils may directly activate LRRK2 through production of a specific LRRK2 activator, which could promote LRRK2 dimerization and localisation to the cell membrane. Alternatively, *P. aeruginosa* may act indirectly through activating an existing upstream activator of the LRRK2 signalling pathway, or promote the loss of/suppress the action of an upstream inhibitor of LRRK2. Either mechanism of LRRK2 activation would be expected to result in an increase of LRRK2-dependent Rab10 phosphorylation. Alternatively, *P. aeruginosa* infection may inhibit currently elusive Rab phosphatases specifically acting on

LRRK2-phosphorylated Rab proteins. Several members of the Alessi lab are currently exploring potential Rab phosphatase candidates, thus once confirmed, would be useful to include in future experiments to investigate whether there are changes to their upregulation during *P. aeruginosa* infection.

Alternatively, *P. aeruginosa* infection within neutrophils could result in alterations to Rab proteins themselves, which could potentially have negative-feedback effects on LRRK2 activation. Indeed, the band-shifts of Rab proteins after 4 hours of PAO1 infection in peripheral blood neutrophils revealed in **Figure 3.1** may be suggestive of post-translational modifications (PTMs) induced by *P. aeruginosa*. PTMs include the addition of various groups (phosphate, acetyl, methyl) onto specific amino acids, or proteolytic cleavage of protein chains[99], which can collectively alter the activity, localization or interactions of modified proteins. In the context of Rab proteins, previous research in macrophages revealed that *P. aeruginosa* utilises its T3SS exotoxin ExoS to modify and downregulate Rab5 activity through ADP-ribosylation, enabling it to avoid destruction[100]. Specifically, Rab5 has been reported to play a critical role during the early stages of *P. aeruginosa* invasion in macrophages[101], which controls epithelial junctions and phagocytosis, and is targeted for subversion. Future work could investigate whether *P. aeruginosa* causes PTMs in other Rab proteins known to be phosphorylated by LRRK2, and investigate potential residues on which these modifications may occur. Additionally, infection experiments utilising inactive *P. aeruginosa* strains or those with impaired/absent T3SS secretion systems could reveal the importance of these factors in the observed LRRK2 activation/ Rab phosphorylation.

Crucially, it would be important to investigate whether possible PTMs induced by *P. aeruginosa* affect the ability of LRRK2 to phosphorylate Rab proteins. Interestingly, whilst an overall increase in Rab10 phosphorylation during *P. aeruginosa* infection was observed with most strains (**Fig. 3.1-3.3**), there was a slight dip in the levels of phosphorylated Rab10 by 4 hours of PAO1 infection in neutrophils (**Fig. 3.1**), during which the band-shift of Rab proteins was also observed. This could potentially indicate a reduction in the ability of LRRK2 to phosphorylate *PAO1*-modified Rab10. Indeed, a type of PTM named ‘eliminylation’ leads to the irreversible removal of phosphate groups from proteins, which has been shown to be mediated by the ‘OspF’ family of type III effectors, including *Pseudomonas* HopAI1 effectors[102]. Thus, certain *P. aeruginosa* effectors could harbour phosphatase activity which permanently reverses LRRK2-phosphorylation of Rab proteins, leading to irreversibly inactive Rab proteins and thus potential LRRK2 inactivation. Therefore, future experiments could also consider longer infection time-points to observe whether LRRK2-dependent Rab10 phosphorylation alters with time, and if so, consider mass spectrometry analysis of the Rab proteins for any observable differences in phosphorylation of specific residues.

5.2.4 Future investigations and potential mechanisms of IKK mediated LRRK2 Ser935 phosphorylation in mouse BMDMs during *P. aeruginosa* infection

Regarding the *P. aeruginosa* infection experiments I conducted within mouse BMDMs, **Figures 3.5-3.6** built on previous work from the Alessi lab[49] by demonstrating that LRRK2 Ser935 phosphorylation could be induced through infection of mouse BMDMs with *P. aeruginosa* (**Figure 3.5)**. Ser935 phosphorylation was also induced in Rab29 KO BMDMs (**Fig.3.6**), providing evidence towards a Rab29-independent LRRK2 phosphorylation pathway induced by TLR agonists. An earlier study revealed that LRRK2 phosphorylation at its serine residues was followed by LRRK2 dimerization and membrane translocation in multiple mouse monocyte cell lines treated with the TLR4 agonist lipopolysaccharide (LPS)[103]. Specifically, whilst peak LRRK2 Ser935 phosphorylation was achieved by 4 hours of LPS treatment, significant dimerization and membrane translocation were only observed by 16 hours[103]. Hence, future work could also use longer time courses of *P. aeruginosa* infection in BMDMs to establish the time-point of peak LRRK2 Ser935 phosphorylation, alongside cellular fractionation and dimerization experiments to observe for changes in LRRK2 dimerization and membrane recruitment.

Furthermore, **Figures 3.7 and 3.8** revealed that LRRK2 Ser935 phosphorylation was controlled by the IKK kinases, whereby Ser935 phosphorylation was considerably reduced through dual inhibition of TAK1 with NG25 and TBK1/ IKKε with MRT67307 during both PAO1 and clinical isolate 'Strain A' infection in BMDMs (**Fig. 3.7 and 3.8**). Interestingly, MLi2 appeared to cause an initial reduction in LRRK2 Ser935 phosphorylation at early PAO1 infection durations, however by 4 hours of infection had minimal effect, which is consistent with previous results (**Figures 3.5 and 3.6**). Understanding the specific relationship between LRRK2 and the IKK kinases during infection in other cell types would be useful for future work to explore.

Collectively, my results may suggest that basal phosphorylation of LRRK2 at Ser935 in BMDMs is controlled by both LRRK2 kinase and IKK kinase activity, of which the latter is LRRK2 independent. Thus, basal phosphorylation can be eliminated by use of LRRK2 kinase inhibitors, such as MLi2, as well as IKK kinase inhibitors. However, upon activation of Toll-like receptors by *P. aeruginosa* ligands, Ser 935 phosphorylation may be gradually shifted towards IKK kinase control, which could explain the reduced ability of MLi2 to induce Ser935 dephosphorylation with increasing infection durations, compared to dual IKK kinase inhibition.

Another possible hypothesis is that *P. aeruginosa* inhibits the protein phosphatase which interacts with LRRK2 and promotes Ser935 dephosphorylation in mouse BMDMs, of which some studies have suggested protein phosphatase 1 (PP1) as a key phosphatase[31].

Therefore, potential mechanisms of *P. aeruginosa* could involve novel protein-protein interactions between the regulatory subunits of PP1 with a specific *P. aeruginosa* effector, which could reduce the accessibility and interaction of PP1 with LRRK2. To investigate this possibility, mass spectrometry analysis for specific protein-protein interactors following *P. aeruginosa* infection in BMDMs should be assessed. However, it is possible that *P. aeruginosa* could inhibit interaction of PP1 with LRRK2 through a currently unknown mechanism. In addition, the IKK kinase pathway may not be regulated by *P. aeruginosa*, thus maintaining LRRK2 Ser935 phosphorylation unless the kinases themselves are inhibited.

5.2.5 Differential LRRK2 activation between immune and host cell types

It is intriguing that increased Ser935 phosphorylation of LRRK2 following *P. aeruginosa* infection was only observed in BMDMs, however not in neutrophils, where there was instead increased Rab10 phosphorylation (**Figure 5.2**). This raises an interesting possibility that LRRK2 has distinct forms or activation pathways within different immune cell types. For example, there may be cell-type specific LRRK2 differential splicing, whereby different cell types could express different LRRK2 isoforms according to their specific cellular functions. Alternatively, there may be different downstream pathways following from LRRK2 phosphorylation or activation with immune cells, which could result in differential immune cell host responses to infection.

Different signalling pathways upstream of LRRK2 may also operate between neutrophils and macrophages. Interestingly, previous work has revealed that human neutrophils exclusively use the “MyD88-dependent” pathway following activation of TLR4 by LPS, compared to monocytes which can utilise both MyD88 streams[104]. Given that LRRK2 Ser935 phosphorylation was abolished in infected peripheral blood neutrophils pre-treated with MLi2 (**Figures 3.1-3.3**), this could suggest that the MyD88-dependent pathway is regulated by LRRK2 activity. In contrast, the MyD88-independent pathway may be LRRK2-independent or additionally controlled by other kinases, which could explain why Ser935 phosphorylation was still preserved in BMDMs pre-treated with MLi2 **(Figures 3.5-3.8),** in which both MyD88-dependent and independent pathways are functional in these cells**.**

Another important factor to consider is that BMDMs and peripheral blood neutrophils were obtained from mice and humans respectively, thus differences in LRRK2 activation may be due to dissimilar mechanisms of *P. aeruginosa* infection in each species. Indeed, previous research involving *Salmonella Typhi* (*S. Typhi*) revealed significant host-specificity which was restricted to humans, whereby *S. Typhi* was unable to survive within mouse macrophages compared to human macrophages[105]. Although *P. aeruginosa* has shown to be capable of infecting a broad spectrum of species[106], it would be useful for future experiments to similarly investigate the survival and impact on LRRK2 activity of *P. aeruginosa* infection in human monocyte-derived macrophages, compared to in mouse BMDMs. This would provide further clarity of any species-specific differences of *P. aeruginosa* activation of LRRK2 activity, which could be utilised to further dissect differences between immune cell types.

FIGURE 5.2

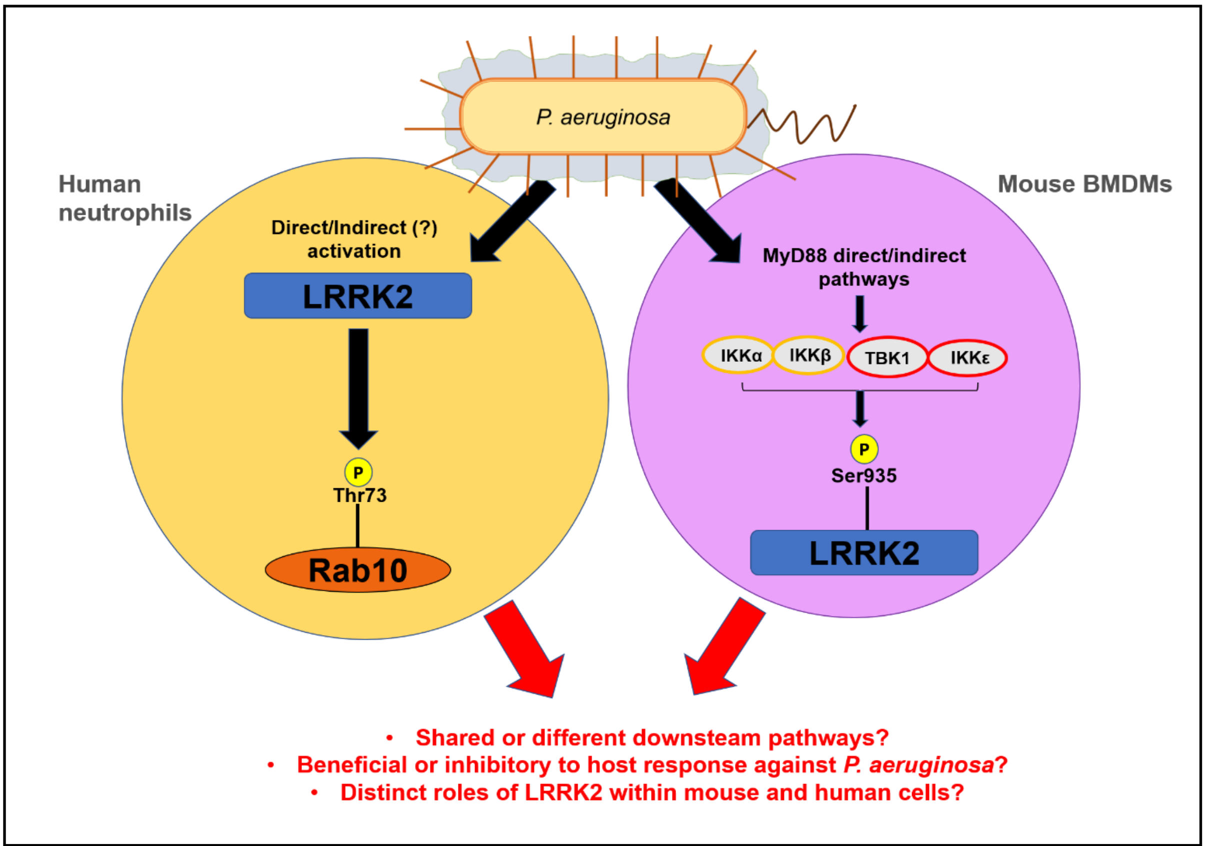

FIGURE 5.2: Summary schematic of LRRK2 response to *P. aeruginosa* infection in experiments utilizing human peripheral blood neutrophils (left) and mouse BMDMs (right).

P. aeruginosa infection in human neutrophils led to increased LRRK2-dependent Rab10 phosphorylation at Thr73, of which the mechanism is currently unknown. Conversely, *P. aeruginosa* infection within mouse BMDMs led to increased LRRK2 phosphorylation at Ser935, which was mediated through activation of IKK canonical and non-canonical kinases downstream of the MyD88 dependent and independent pathways.

Understanding the downstream pathways following from Rab10 phosphorylation and LRRK2 Ser935 phosphorylation within each immune cell, investigating for any cell or host specific differences in LRRK2 response, and clarifying the overall beneficial or inhibitory response of LRRK2 to *P. aeruginosa* infection, are key questions remaining for future work.

Original image

5.2.6 The role of LRRK2 in immune cells during *P. aeruginosa* infection

The fundamental question remaining from all experiments conducted within **Project A** is whether LRRK2 plays a beneficial or deleterious role in the host immune response against *P. aeruginosa*. As discussed within **1.1.2,** several studies utilising different pathogens have revealed complex and contrasting roles for LRRK2 in the immune response[51,53], which are indeed likely to be immune cell and host cell dependent.

On the one hand, given that neutrophils are vital for host defence against *P. aeruginosa* in healthy and immuno-competent individuals, the increase in Rab10 phosphorylation seen following *P. aeruginosa* infection in human peripheral blood and sputum neutrophils (**Figures 3.1-3.4**) could be a beneficial host mechanism induced by LRRK2; such as through activating downstream signalling pathways involved in pathogen localisation to lysosomes and degradation. Interestingly, previous research has revealed that Rab10 is a positive regulator of TLR4 complex signalling, which is involved in activating an inflammatory response against LPS present on the outer membrane of Gram-negative bacteria[107]. Specifically, Rab10 co-localises with TLR4 and promotes its transport from the Golgi to the plasma membrane upon exposure to LPS, replenishing TLR4 membrane receptors and thus enhancing host cell defence. Given that LPS produced by *P. aeruginosa* has shown to act as a ligand for TLR4[108], future work could consider immuno-fluorescence (IF) experiments to explore Rab10 localisation with TLR4 following *P. aeruginosa* infection, and investigate if LRRK2-dependent Rab10 phosphorylation results in any specific changes.

Alternatively, it is possible that LRRK2 activation by *P. aeruginosa* is detrimental to the host cell response. By example, previous research involving infection of mouse macrophages with the Gram-negative intracellular pathogen *S. Typhimurium* revealed that LRRK2 promoted activation of the NLRC4-inflammasome, which enabled host defence through resultant caspase-1 and IL-1 β secretion[51]. Mechanistically, LRRK2 formed a complex with NLRC4, leading to NLRC4 phosphorylation at Ser533. However, whilst the NLRC4-inflammasome is key to the clearance of intracellular pathogens, other studies surprisingly found that NLRC4-inflammasome activation by *P. aeruginosa*, an extracellular pathogen, decreased its clearance within mouse macrophages[109]. This was later revealed to be mediated through enhanced secretion of the pro-inflammatory cytokine IL-18, resulting in lung injury through excess neutrophil recruitment, and repression of beneficial IL-17 antimicrobial host response[110]. Thus, exploring the interaction of LRRK2 with the NLRC4-inflammasome during *P. aeruginosa* infection in both macrophages and neutrophils may provide important insights into understanding whether its role is beneficial or deleterious in the host cell response.

Finally, based on my findings of increased LRRK2-dependent Rab10 phosphorylation in CF sputum neutrophils (**Figure 3.4)**, it is important to consider that LRRK2 'hyperactivation' could be involved in the maintenance of chronic inflammatory states. Indeed, recent research revealed that LRRK2 expression was positively correlated with the severity of systemic lupus erythematosus (SLE), a chronic autoimmune disease, and LRRK2-deficient mice showed attenuated lupus-like pathology[47]. Given that CF patients have elevated hyperinflammatory states which uniquely predispose them to frequent infections and ineffective clearance of *P. aeruginosa*, exploration into whether this is maintained by LRRK2 activity could be ground-breaking. Interestingly, some evidence has suggested that the defective CFTR channel protein in CF can itself induce inflammation in the absence of infection[111], thus investigation into whether LRRK2 normally interacts with this protein, and how it could be affected by mutation, may be of interest. It would also be interesting to understand whether LRRK2 plays a distinct role in CF neutrophils, particularly concerning their altered migration and impaired phagocytic properties. Thus, novel insights of LRRK2 in CF pathobiology could open new ideas for CF treatment, such as trialling LRRK2 inhibitors in CF patients to observe if their intractable upper airway inflammation and pathogen burden can be reduced. Nevertheless, before these exciting possibilities can be considered further, increased research as well as better understanding of the safety profile of LRRK2 inhibitors are required.

5.3 Project B Discussion

5.3.1 Endogenous PINK1 could not be detected in peripheral blood neutrophils following CCCP activation

For **Project B**, my overall aim was to investigate if I could stabilise and visualise endogenous PINK1 within peripheral blood neutrophils from healthy blood donors in immunoblotting/immuno-precipitation (IP) experiments following 10µM CCCP treatment. My main experimental outcome was that endogenous PINK1 could not be detected in either whole cell lysates or PINK1 immuno-precipitates of healthy human peripheral blood neutrophils following up to 12 hours 10µM CCCP stimulation **(Figure 4.6)**. Whilst my initial experiments with whole cell lysates revealed a band around the expected molecular weight for full length PINK1 (~63kDa) that emerged with increasing CCCP time-course (**Figure 4.2**), this band was also observed in HEK293 PINK1 knockout cells, suggesting it as a non-specific band detected by cross-reaction of other abundant proteins activated in peripheral blood neutrophils with the PINK1 Novus antibody.

Recent work investigating PINK1 expression in CCCP-treated mouse platelets similarly revealed that multiple bands around the predicted molecular weight of PINK1 were seen in both WT and KO PINK1 platelet lysates using several different PINK1 antibodies, including the PINK1 Novus used within this project[112]. However, whilst PINK1 protein expression could be detected through IP experiments in WT PINK1 mouse platelets treated with CCCP for 6 hours, I was unable to achieve this in the experiments I conducted **(Fig. 4.6).** This could be explained by potential expression level differences in PINK1 between blood cell type (platelet versus neutrophils), as well as PINK1 expression between species (mouse versus human). Indeed, it could be hypothesised that PINK1 mRNA expression is much lower in human neutrophils compared to mouse platelets, and hence more drastic and longer time-courses of mitochondrial depolarisation may be needed to detect any observable changes in PINK1 protein activation in human neutrophils.

5.3.1 Project B limitations and future work

Although my results from **Project B** suggest that human peripheral blood neutrophils are not an ideal cell type to visualise endogenous PINK1 activation, further experiments are required to overcome existing project limitations and validate findings. Firstly, one of the limitations of my work was not independently establishing whether PINK1 mRNA transcripts were present within the neutrophil lysates isolated from human peripheral blood. Although previous experiments published within the Expression Atlas database revealed that PINK1 mRNA is expressed in several types of human neutrophils (**Fig. 4.1**), quantitative RT-PCR experiments on both untreated/CCCP treated peripheral blood neutrophils to assess PINK1 mRNA expression should be considered for future experiments. In addition, it would be interesting to investigate for any time-dependent changes in PINK1 mRNA transcription following CCCP treatment in neutrophils. Whilst previous research showed that PINK1 transcription was not increased in HeLa cells treated with CCCP for 1 hour compared to DMSO controls[81], it is possible that PINK1 transcription and expression is controlled differently between cell types, and may require longer CCCP treatment for any observable changes in PINK1 transcription.

Another limitation of my work was not being able to confirm that CCCP induced mitochondrial membrane depolarisation, despite observing significant cell death in neutrophils treated with CCCP for 20 hours (**Figure 4.2**). Immunoblotting for OPA1 as an indirect readout of mitochondrial membrane depolarisation is used for many cell models, whereby cleaved forms of OPA1 can be detected upon mitochondrial damage. However, in initial experiments involving OPA1 immunoblotting in CCCP-treated neutrophils, I did not obtain clearly cleaved bands, potentially due to non-specific binding with other proteins in the same molecular weight region (data not shown). Using a different OPA1 antibody that recognises a different epitope of OPA1, or using a different marker of mitochondrial depolarisation, such as ATP5A, may therefore be worth assessing for future experiments. Alternatively, flow cytometry analysis

(FACS) using Mitotracker as used in previous work[113] could also be considered, in which mitochondrial depolarisation following CCCP treatment can be directly visualised based on the intensity of a fluorescent dye taken up by neutrophils, which will be reduced in depolarised mitochondria.

It is also possible that the length of CCCP treatment I used for mitochondrial depolarisation was not sufficient to stabilise endogenous PINK1 for detection with the current available tools, if present, in neutrophils. Hence, repeating the experiment with CCCP time-courses between 12-20 hours would provide assessment for optimal PINK1 activation balanced with maintaining cell integrity. Using other mitochondrial inhibitors, such as Antimycin/Oligomycin, may also be more appropriate given that their action is targeted to the mitochondrial respiratory chain, rather than CCCP which creates generalised cellular membrane damage and thus may be too harsh on neutrophils. However, previous experimentation using 10µM Oligomycin in human peripheral blood neutrophils was reported to result in a small increase in apoptosis (~5%) after 20 hours of treatment (personal communication), hence may still present similar issues as observed with CCCP use.

The experiments I conducted in this project only investigated for PINK1 activation in whole cell neutrophil lysates. Importantly, the amount of PINK1 present within the mitochondria itself is crucial for study of the PINK1/Parkin pathway in neutrophils, as it is here that its stabilisation and activation is being measured. Hence, future work could consider mitochondrial fractionation of stimulated neutrophil lysates, which would enrich integral mitochondrial proteins and thus reduce the amount of non-specific proteins present detected by PINK1 antibody for Western blotting.

Whilst I utilised the best currently available antibody tools to detect PINK1/Parkin activity for my experiments within **Project B**, it is possible that they were not sensitive enough to detect the low levels of PINK1/pUb in stimulated peripheral blood neutrophils, which may have been below the threshold of detection. Although other commercial and in-house mouse monoclonal PINK1 antibodies trialled on HeLa cell control lysates did not prove superior in PINK1 detection compared to use with the PINK1 Novus (data not shown), there may be different sensitivities in the PINK1 Novus antibody in detecting endogenous PINK1 in peripheral blood neutrophils. Previous data from the Expression database also indicated that Parkin mRNA expression was significantly low (**Fig 4.1**), which was corroborated with the results in **Figure 4.3** which could not detect Parkin in stimulated neutrophil lysates upon probing with the anti-Parkin antibody. However, using other readouts of Parkin E3 ligase activity in activated neutrophils could be considered for future work, such as antibodies against ubiquitylated forms of CISD1 or Miro1. More excitingly, future work should consider using the Rab8A Ser111 antibody recently developed by members of the Muqit lab, which is anticipated to provide a highly sensitive and specific readout of PINK1/Parkin pathway activity based on the indirect phosphorylation of Rab8A at Ser111 by PINK1.

Finally, it is possible that neutrophils have distinct mechanisms independent of the PINK1/Parkin pathway which regulate mitophagy, hence mitochondrial stimulation may not activate the pathway to the same extent as observed in other control cell types. Supportively, previous research revealed that healthy human peripheral blood neutrophils do not complete mitophagy upon mitochondrial damage, but instead have two complementary pathways involving 1) the extrusion of inner mitochondrial components, including mtDNA, which is devoid of oxidized residues, followed by 2) mtDNA targeting to lysosomes for degradation after it is oxidised and dissociated from transcription factor A mitochondria (TFAM)[114]. Indeed, 1hr CCCP treatment in peripheral blood neutrophils was shown to increase mtDNA extrusion with a concomitant reduction of TFAM intracellular levels. Interestingly, in monocytes but not neutrophils, CCCP treatment promoted the upregulation of several transcripts related to autophagy activation (ULK2), autophagosome trafficking (Rab27a and Rab4a), fusion (NSF, SNAP23, SNAP29, STX2, and LAMP2) and lysosome activation (Presenilin-1)[114]. In contrast, TOM1, which participates in autophagosome maturation, was significantly reduced in neutrophils following CCCP treatment. Surprisingly, the authors of this study did not investigate for any changes in the gene or protein expression of PINK1 or Parkin, where it is possible that their role in mitophagy is overshadowed by upregulation of other transcripts relevant for other parallel pathways in peripheral blood neutrophils. This would be interesting for future work to assess, as well comparing for any differences in the activation of the PINK1/Parkin pathway in human derived monocytes or macrophages, given that mitochondrial depolarisation appears to cause differential autophagic transcript upregulation in these cells.

6. *CHAPTER 6* - CONCLUSIONS

To conclude, my work for **Project A and B** presented within this thesis explored key aspects of the PD associated LRRK2 and PINK1/Parkin signalling pathways within immune cells.

With regards to **Project A,** my results revealed differential effects of LRRK2 activation in response to *P. aeruginosa* infection, whereby LRRK2-dependent Rab10 phosphorylation and LRRK2 Ser935 phosphorylation was induced in human peripheral blood neutrophils and mouse BMDMs following infection, respectively. Furthermore, my preliminary investigation into LRRK2 activity within sputum neutrophils isolated from infected CF patients revealed high levels of LRRK2-dependent Rab10 phosphorylation, providing a supportive basis for a large clinical study in CF patients to investigate changes in LRRK2 activity during the natural time-course of infection. Exploring upstream and downstream immune signalling pathways from Rab10 phosphorylation or LRRK2 Ser935 phosphorylation may also help piece together relevant cell-specific or host-specific roles of LRRK2, and thus provide novel insights into the relationship between *P. aeruginosa* infection and LRRK2 cellular function.

Crucially, the key question remaining is whether LRRK2 kinase activation is beneficial or detrimental to the host response during infection. As explored in my project, the answer is likely to be complex; based on pathogen, cell and host specific factors, as well as potential differences in LRRK2 function existing between healthy individuals and those with conditions impairing the immune system. Thus, whilst improved understanding of LRRK2 function in the context of infection and inflammation will provide benefits for understanding PD pathobiology, it may also open up novel opportunities for treating chronic and inflammatory diseases, like CF, if LRRK2 activation is also revealed to play a role in its pathogenesis.

With regards to **Project B**, my findings revealed that PINK1 protein activation or expression following CCCP treatment of human peripheral blood neutrophils could not be visualised through either immunoblotting or immuno-precipitation experiments. Whilst my results therefore do not promote peripheral blood neutrophils as a useful human cell resource for investigating the PINK1/Parkin activation pathway, future experiments adapted to use different mitochondrial depolarisers, treatment timings, mitochondrial fractionation experiments or antibody readouts are required to confirm the current findings. Ultimately, finding appropriate cell sources to directly monitor endogenous PINK1/Parkin pathway activation in humans will provide better knowledge on its overall functioning and regulation, and engender greater insight into how its dysfunction can precipitate PD pathology. Importantly, this knowledge could enable stratification for appropriate PD patients that may benefit from elusive future drugs that aim to re-activate the damaged PINK1/Parkin pathway, and thus provide a direct way of measuring drug response.

7. REFERENCES

1. Kim, S. D., Allen, N. E., Canning, C. G. & Fung, V. S. C. Parkinson disease. *Handb. Clin. Neurol.* **159,** 173–193 (2018).

2. Farrer, M. J. Genetics of Parkinson disease: Paradigm shifts and future prospects. *Nature Reviews Genetics* (2006). doi:10.1038/nrg1831

3. Cohen, P. The origins of protein phosphorylation. *Nat. Cell Biol.* (2002). doi:10.1038/ncb0502-e127

4. Hernandez, D. G., Reed, X. & Singleton, A. B. Genetics in Parkinson disease: Mendelian versus non-Mendelian inheritance. *Journal of Neurochemistry* 59–74 (2016). doi:10.1111/jnc.13593

5. Obeso, J. A. *et al.* Past, present, and future of Parkinson's disease: A special essay on the 200th Anniversary of the Shaking Palsy. *Movement Disorders* (2017). doi:10.1002/mds.27115

6. Przedborski, S. The two-century journey of Parkinson disease research. *Nature Reviews Neuroscience* (2017). doi:10.1038/nrn.2017.25

7. Dauer, W. & Przedborski, S. Parkinson's disease: Mechanisms and models. *Neuron* (2003). doi:10.1016/S0896-6273(03)00568-3

8. Berg, D. *et al.* MDS research criteria for prodromal Parkinson's disease. *Movement Disorders* (2015). doi:10.1002/mds.26431

9. Schapira, A. H. V., Chaudhuri, K. R. & Jenner, P. Non-motor features of Parkinson disease. *Nature Reviews Neuroscience* (2017). doi:10.1038/nrn.2017.62

10. Deuschl, G. & de Bie, R. M. A. New therapeutic developments for Parkinson disease. *Nat. Rev. Neurol.* (2019). doi:10.1038/s41582-019-0133-0

11. Kogan, M., McGuire, M. & Riley, J. Deep Brain Stimulation for Parkinson Disease. *Neurosurgery Clinics of North America* (2019). doi:10.1016/j.nec.2019.01.001

12. Kim, S. D., Allen, N. E., Canning, C. G. & Fung, V. S. C. in *Handbook of Clinical Neurology* (2018). doi:10.1016/B978-0-444-63916-5.00011-2

13. Alcalay, R. N. *et al.* Frequency of known mutations in early-onset Parkinson disease: Implication for genetic counseling: The consortium on risk for early onset Parkinson disease study. *Arch. Neurol.* (2010). doi:10.1001/archneurol.2010.194

14. Chang, D. *et al.* A meta-analysis of genome-wide association studies identifies 17 new Parkinson's disease risk loci. *Nat. Genet.* (2017). doi:10.1038/ng.3955

15. Zimprich, A. *et al.* Mutations in LRRK2 cause autosomal-dominant parkinsonism with pleomorphic pathology. *Neuron* (2004). doi:10.1016/j.neuron.2004.11.005

16. Valente, E. M. *et al.* Hereditary early-onset Parkinson's disease caused by mutations in PINK1. *Science (80-.).* (2004). doi:10.1126/science.1096284

17. Johnson, L. N. & Lewis, R. J. Structural basis for control by phosphorylation. *Chemical Reviews* (2001). doi:10.1021/cr000225s

18. Cohen, P. The regulation of protein function by multisite phosphorylation - A 25 year update. *Trends in Biochemical Sciences* (2000). doi:10.1016/S0968-0004(00)01712-6

19. Paisán-Ruíz, C. *et al.* Cloning of the gene containing mutations that cause PARK8-linked Parkinson's disease. *Neuron* (2004). doi:10.1016/j.neuron.2004.10.023

20. Martin, I., Kim, J. W., Dawson, V. L. & Dawson, T. M. LRRK2 pathobiology in Parkinson's disease. *Journal of Neurochemistry* (2014). doi:10.1111/jnc.12949

21. Domingo, A. & Klein, C. in *Handbook of Clinical Neurology* (2018). doi:10.1016/B978-0-444-63233-3.00014-2

22. Alessi, D. R. & Sammler, E. LRRK2 kinase in Parkinson's disease. *Science* **360,** 36–37 (2018).

23. Lill, C. M. Genetics of Parkinson's disease. *Molecular and Cellular Probes* **30,** 386–396 (2016).

24. Billingsley, K. J., Bandres-Ciga, S., Saez-Atienzar, S. & Singleton, A. B. Genetic risk factors in Parkinson's disease. *Cell and Tissue Research* (2018). doi:10.1007/s00441-018-2817-y

25. Marras, C. *et al.* Phenotype in parkinsonian and nonparkinsonian LRRK2 G2019S mutation carriers. *Neurology* (2011). doi:10.1212/WNL.0b013e318227042d

26. Li, J. Q., Tan, L. & Yu, J. T. The role of the LRRK2 gene in Parkinsonism. *Molecular neurodegeneration* (2014). doi:10.1186/1750-1326-9-47

27. Trinh, J. *et al.* A comparative study of Parkinson's disease and leucine-rich repeat kinase 2 p.G2019S parkinsonism. *Neurobiol. Aging* (2014). doi:10.1016/j.neurobiolaging.2013.11.015

28. Kang, U. B. & Marto, J. A. Leucine-rich repeat kinase 2 and Parkinson's disease. *Proteomics* (2017). doi:10.1002/pmic.201600092

29. Doggett, E. A., Zhao, J., Mork, C. N., Hu, D. & Nichols, R. J. Phosphorylation of LRRK2 serines 955 and 973 is disrupted by Parkinson's disease mutations and LRRK2 pharmacological inhibition. *J. Neurochem.* (2012). doi:10.1111/j.1471-4159.2011.07537.x

30. Deak, M. *et al.* 14-3-3 binding to LRRK2 is disrupted by multiple Parkinson's disease-associated mutations and regulates cytoplasmic localization. *Biochem. J.* (2010). doi:10.1042/bj20100483

31. Beullens, M. *et al.* Identification of protein phosphatase 1 as a regulator of the LRRK2 phosphorylation cycle. *Biochem. J.* (2013). doi:10.1042/bj20121772

32. Steger, M. *et al.* Systematic proteomic analysis of LRRK2-mediated rab GTPase phosphorylation establishes a connection to ciliogenesis. *Elife* (2017). doi:10.7554/eLife.31012

33. Steger, M *et al.* Phosphoproteomics reveals that Parkinson's disease kinase LRRK2 regulates a subset of Rab GTPases. *Elife* (2016). doi:10.7554/eLife.12813

34. Cherfils, J. & Zeghouf, M. Regulation of Small GTPases by GEFs, GAPs, and GDIs. *Physiol. Rev.* (2013). doi:10.1152/physrev.00003.2012

35. Purlyte, E. *et al.* Rab29 activation of the Parkinson's disease-associated LRRK2 kinase. *EMBO J.* (2018). doi:10.15252/embj.201798099

36. Wightman, M. *et al.* Rab29 activation of the Parkinson's disease-associated LRRK2 kinase. *EMBO J.* (2017). doi:10.15252/embj.201798099

37. Pylypenko, O., Hammich, H., Yu, I. M. & Houdusse, A. Rab GTPases and their interacting protein partners: Structural insights into Rab functional diversity. *Small GTPases* (2018). doi:10.1080/21541248.2017.1336191

38. Gao, Y. *et al.* The emerging role of Rab GTPases in the pathogenesis of Parkinson's disease. *Mov. Disord.* (2018). doi:10.1002/mds.27270

39. Lis, P. *et al.* Development of phospho-specific Rab protein antibodies to monitor in vivo activity of the LRRK2 Parkinson's disease kinase. *Biochem. J.* BCJ20170802 (2017). doi:10.1042/BCJ20170802

40. Dzamko, N. L. LRRK2 and the immune system. In *Advances in Neurobiology* **14,** 123–143 (2017).

41. Cook, D. A. *et al.* LRRK2 levels in immune cells are increased in Parkinson's disease. *npj Park. Dis.* **3,** 11 (2017).

42. Rideout, H. J. & Re, D. B. Leucine Rich Kinase 2 (LRRK2). In *Advances in Neurobiology* (2017). doi:10.1007/978-3-319-49969-7_10

43. Hakimi, M. *et al.* Parkinson's disease-linked LRRK2 is expressed in circulating and tissue immune cells and upregulated following recognition of microbial structures. *J. Neural Transm.* (2011). doi:10.1007/s00702-011-0653-2

44. Balzola, F., Bernstein, C., Ho, G. T. & Lees, C. LRRK2 is involved in the IFN-gamma response and host response to pathogens: Commentary. *Inflammatory Bowel Disease Monitor* (2011).

45. Zhang, F.-R. *et al.* Genomewide association study of leprosy. *N. Engl. J. Med.* (2009). doi:10.1056/NEJMoa0903753

46. Liu, Z. & Lenardo, M. J. The role of LRRK2 in inflammatory bowel disease. *Cell Res.* (2012). doi:10.1038/cr.2012.42

47. Hou, P. *et al.* Autophagy-related gene *LRRK2* is likely a susceptibility gene for systemic lupus erythematosus in northern Han Chinese. *Oncotarget* (2017). doi:10.18632/oncotarget.14631

48. Saunders-Pullman, R. *et al.* LRRK2 G2019S mutations are associated with an increased cancer risk in Parkinson disease. *Mov. Disord.* (2010). doi:10.1002/mds.23314

49. Dzamko, N. *et al.* The IkappaB kinase family phosphorylates the Parkinson's disease kinase LRRK2 at Ser935 and Ser910 during Toll-Like Receptor signaling. *PLoS One* (2012). doi:10.1371/journal.pone.0039132

50. Iwasaki, A. & Medzhitov, R. Control of adaptive immunity by the innate immune system. *Nature Immunology* (2015). doi:10.1038/ni.3123

51. Liu, W. *et al.* LRRK2 promotes the activation of NLRC4 inflammasome during Salmonella Typhimurium infection . *J. Exp. Med.* (2017). doi:10.1084/jem.20170014

52. Zhang, Q. *et al.* Commensal bacteria direct selective cargo sorting to promote symbiosis. *Nat. Immunol.* (2015). doi:10.1038/ni.3233

53. Härtlova, A. *et al.* LRRK2 is a negative regulator of Mycobacterium tuberculosis phagosome maturation in macrophages. *EMBO J.* e98694 (2018). doi:10.15252/embj.201798694

54. Silby, M. W., Winstanley, C., Godfrey, S. A. C., Levy, S. B. & Jackson, R. W. Pseudomonas genomes: Diverse and adaptable. *FEMS Microbiol. Rev.* (2011). doi:10.1111/j.1574-6976.2011.00269.x

55. Holloway, B. W. Genetic Recombination in Pseudomonas aeruginosa. *Microbiology* (2009). doi:10.1099/00221287-13-3-572

56. Bernut, A., Belon, C., Soscia, C., Bleves, S. & Blanc-Potard, A.-B. Intracellular phase for an extracellular bacterial pathogen: MgtC shows the way. *Microb. Cell* (2015). doi:10.15698/mic2015.09.227

57. Belon, C. & Blanc-Potard, A.-B. Intramacrophage Survival for Extracellular Bacterial Pathogens: MgtC As a Key Adaptive Factor. *Front. Cell. Infect. Microbiol.* (2016). doi:10.3389/fcimb.2016.00052

58. Wilson, J. W. *et al.* Mechanisms of bacterial pathogenicity. *Postgraduate Medical Journal* (2002). doi:10.1136/pmj.78.918.216

59. Raoust, E. *et al.* Pseudomonas aeruginosa LPS or flagellin are sufficient to activate TLR-dependent signaling in murine alveolar macrophages and airway epithelial cells. *PLoS One* (2009). doi:10.1371/journal.pone.0007259

60. Zolfaghar, I., Evans, D. J., Ronaghi, R. & Fleiszig, S. M. J. Type III secretion-dependent modulation of innate immunity as one of multiple factors regulated by Pseudomonas aeruginosa RetS. *Infect. Immun.* (2006). doi:10.1128/IAI.01891-05

61. Hauser, A. R. The type III secretion system of Pseudomonas aeruginosa: Infection by injection. *Nature Reviews Microbiology* (2009). doi:10.1038/nrmicro2199

62. Sawa, T. *et al.* Active and passive immunization with the Pseudomonas V antigen protects against type III intoxication and lung injury. *Nat. Med.* (1999). doi:10.1038/7391

63. Kerr, K. G. & Snelling, A. M. Pseudomonas aeruginosa: a formidable and ever-present adversary. *Journal of Hospital Infection* (2009). doi:10.1016/j.jhin.2009.04.020

64. Accurso, F. J. Update in Cystic Fibrosis 2005. *Am. J. Respir. Crit. Care Med.* (2006). doi:10.1164/rccm.2601006

65. Cohen, T. S. & Prince, A. Cystic fibrosis: A mucosal immunodeficiency syndrome. *Nature Medicine* (2012). doi:10.1038/nm.2715

66. Simon, R., Mallory, G. & Hoppin, A. Cystic fibrosis: Treatment of acute pulmonary exacerbations. *UptoDate* (2017).

67. Folkesson, A. *et al.* Adaptation of Pseudomonas aeruginosa to the cystic fibrosis airway: An evolutionary perspective. *Nature Reviews Microbiology* (2012). doi:10.1038/nrmicro2907

68. Zhao, J. *et al.* Decade-long bacterial community dynamics in cystic fibrosis airways. *Proc. Natl. Acad. Sci.* (2012). doi:10.1073/pnas.1120577109

69. Hancock, R. E. W. & Speert, D. P. Antibiotic resistance in Pseudomonas aeruginosa: Mechanisms and impact on treatment. *Drug Resist. Updat.* (2000). doi:10.1054/drup.2000.0152

70. Oliver, A., Cantón, R., Campo, P., Baquero, F. & Blázquez, J. High frequency of hypermutable Pseudomonas aeruginosa in cystic fibrosis lung infection. *Science (80-.).* (2000). doi:10.1126/science.288.5469.1251

71. Friedman, L. & Kolter, R. Genes involved in matrix formation in Pseudomonas aeruginosa PA14 biofilms. *Mol. Microbiol.* (2004). doi:10.1046/j.1365-2958.2003.03877.x

72. Rosenfeld, M. *et al.* Early pulmonary infection, inflammation, and clinical outcomes in infants with cystic fibrosis. *Pediatr. Pulmonol.* (2001). doi:10.1002/ppul.1144

73. Paulsen, I. T. *et al.* Pseudomonas aeruginosa Cell Membrane Protein Expression

from Phenotypically Diverse Cystic Fibrosis Isolates Demonstrates Host-Specific Adaptations . *J. Proteome Res.* (2016). doi:10.1021/acs.jproteome.6b00058

74. Cassatella, M. A. in (2008). doi:10.1016/s0065-2776(08)60791-9

75. Gifford, A. M. & Chalmers, J. D. The role of neutrophils in cystic fibrosis. *Current Opinion in Hematology* **21,** 16–22 (2014).

76. Laval, J., Ralhan, A. & Hartl, D. Neutrophils in cystic fibrosis. *Biological Chemistry* **397,** 485–496 (2016).

77. Brockbank, S., Downey, D., Elborn, J. S. & Ennis, M. Effect of cystic fibrosis exacerbations on neutrophil function. *Int. Immunopharmacol.* **5,** 601–608 (2005).

78. Painter, R. G. *et al.* CFTR expression in human neutrophils and the phagolysosomal chlorination defect in cystic fibrosis. *Biochemistry* (2006). doi:10.1021/bi060490t

79. Fan, Y. *et al.* Interrogating Parkinson's disease LRRK2 kinase pathway activity by assessing Rab10 phosphorylation in human neutrophils. *Biochem. J.* (2017). doi:10.1042/BCJ20170803

80. McWilliams, T. G. & Muqit, M. M. PINK1 and Parkin: emerging themes in mitochondrial homeostasis. *Current Opinion in Cell Biology* **45,** 83–91 (2017).

81. Narendra, D. P. *et al.* PINK1 is selectively stabilized on impaired mitochondria to activate Parkin. *PLoS Biol.* (2010). doi:10.1371/journal.pbio.1000298

82. Yue, Z., Friedman, L., Komatsu, M. & Tanaka, K. The cellular pathways of neuronal autophagy and their implication in neurodegenerative diseases. *Biochimica et Biophysica Acta - Molecular Cell Research* (2009). doi:10.1016/j.bbamcr.2009.01.016

83. Kumar, A. *et al.* Structure of PINK1 and mechanisms of Parkinson's disease-associated mutations. *Elife* (2017). doi:10.7554/elife.29985

84. Sekine, S. & Youle, R. J. PINK1 import regulation; a fine system to convey mitochondrial stress to the cytosol. *BMC Biology* (2018). doi:10.1186/s12915-017-0470-7

85. Greene, A. W. *et al.* Mitochondrial processing peptidase regulates PINK1 processing, import and Parkin recruitment. *EMBO Rep.* (2012). doi:10.1038/embor.2012.14

86. Yamano, K. & Youle, R. J. PINK1 is degraded through the N-end rule pathway. *Autophagy* (2013). doi:10.4161/auto.24633

87. Kondapalli, C. *et al.* PINK1 is activated by mitochondrial membrane potential depolarization and stimulates Parkin E3 ligase activity by phosphorylating Serine 65. *Open Biol.* **2,** (2012).

88. Kazlauskaite, A. *et al.* Phosphorylation of parkin at serine65 is essential for activation: Elaboration of a miro1 substrate-based assay of parkin E3 ligase activity. *Open Biol.* (2014). doi:10.1098/rsob.130213

89. McWilliams, T. G. *et al.* Phosphorylation of Parkin at serine 65 is essential for its activation in vivo. *Open Biol.* (2018). doi:10.1098/rsob.180108

90. Lai, Y.-C. *et al.* Phosphoproteomic screening identifies Rab GTPases as novel downstream targets of PINK1. *EMBO J.* (2015). doi:10.15252/embj.201591593

91. McWilliams, T. G. *et al.* Basal Mitophagy Occurs Independently of PINK1 in Mouse Tissues of High Metabolic Demand. *Cell Metabolism* (2018). doi:10.1016/j.cmet.2017.12.008

92. Taymans, J. M., Van Den Haute, C. & Baekelandt, V. Distribution of PINK1 and LRRK2 in rat and mouse brain. *J. Neurochem.* (2006). doi:10.1111/j.1471-4159.2006.03919.x

93. Blackinton, J. G. *et al.* Expression of PINK1 mRNA in human and rodent brain and in Parkinson's disease. *Brain Res.* (2007). doi:10.1016/j.brainres.2007.09.056

94. Pao, K. C. *et al.* Probes of ubiquitin E3 ligases enable systematic dissection of parkin activation. *Nat. Chem. Biol.* (2016). doi:10.1038/nchembio.2045

95. Lucas, J. S. *et al.* Diagnosis and management of primary ciliary dyskinesia. *Archives of Disease in Childhood* (2014). doi:10.1136/archdischild-2013-304831

96. Gong, X., Ming, X., Deng, P. & Jiang, Y. Mechanisms regulating the nuclear translocation of p38 MAP kinase. *J. Cell. Biochem.* (2010). doi:10.1002/jcb.22675

97. Marvig, R. L., Sommer, L. M., Molin, S. & Johansen, H. K. Convergent evolution and adaptation of Pseudomonas aeruginosa within patients with cystic fibrosis. *Nat. Genet.* (2015). doi:10.1038/ng.3148

98. Fauvart, M., de Groote, V. N. & Michiels, J. Role of persister cells in chronic infections: Clinical relevance and perspectives on anti-persister therapies. *Journal of Medical Microbiology* (2011). doi:10.1099/jmm.0.030932-0

99. Ouidir, T., Jouenne, T. & Hardouin, J. Post-translational modifications in Pseudomonas aeruginosa revolutionized by proteomic analysis. *Biochimie* (2016). doi:10.1016/j.biochi.2016.03.001

100. Stein, M. P., Müller, M. P. & Wandinger-Ness, A. Bacterial pathogens commandeer Rab GTPases to establish intracellular niches. *Traffic* (2012). doi:10.1111/tra.12000

101. Mustafi, S., Rivero, N., Olson, J. C., Stahl, P. D. & Barbieri, M. A. Regulation of Rab5 Function during Phagocytosis of Live Pseudomonas aeruginosa in Macrophages. *Infect. Immun.* (2013). doi:10.1128/IAI.00387-13

102. Li, H. *et al.* The phosphothreonine lyase activity of a bacterial type III effector family. *Science (80-.).* (2007). doi:10.1126/science.1138960

103. Schapansky, J., Nardozzi, J. D., Felizia, F. & LaVoie, M. J. Membrane recruitment of endogenous LRRK2 precedes its potent regulation of autophagy. *Hum. Mol. Genet.* (2014). doi:10.1093/hmg/ddu138

104. Tamassia, N. *et al.* The MyD88-independent pathway is not mobilized in human neutrophils stimulated via TLR4. *J. Immunol.* (2007). doi:10.4049/JIMMUNOL.178.11.7344

105. Spanò, S. & Galán, J. E. A Rab32-dependent pathway contributes to Salmonella typhi host restriction. *Science (80-.).* (2012). doi:10.1126/science.1229224

106. Neves, P. R., McCulloch, J. A., Mamizuka, E. M. & Lincopan, N. in *Encyclopedia of Food Microbiology: Second Edition* (2014). doi:10.1016/B978-0-12-384730-0.00283-4

107. Cao, X. *et al.* Ras-related protein Rab10 facilitates TLR4 signaling by promoting replenishment of TLR4 onto the plasma membrane. *Proc. Natl. Acad. Sci.* (2010). doi:10.1073/pnas.1009428107

108. McIsaac, S. M., Stadnyk, A. W. & Lin, T.-J. Toll-like receptors in the host defense against Pseudomonas aeruginosa respiratory infection and cystic fibrosis . *J. Leukoc. Biol.* (2012). doi:10.1189/jlb.0811410

109. Cohen, T. S. & Prince, A. S. Activation of inflammasome signaling mediates pathology

of acute P. aeruginosa pneumonia. *J. Clin. Invest.* (2013). doi:10.1172/JCI66142

110. Faure, E. *et al.* Pseudomonas aeruginosa type-3 secretion system dampens host defense by exploiting the NLRC4-coupled inflammasome. *Am. J. Respir. Crit. Care Med.* (2014). doi:10.1164/rccm.201307-1358OC

111. Bartlett, J. A. *et al.* Newborn cystic fibrosis pigs have a blunted early response to an inflammatory stimulus. *Am. J. Respir. Crit. Care Med.* (2016). doi:10.1164/rccm.201510-2112OC

112. Walsh, T. G., van den Bosch, M. T. J., Lewis, K. E., Williams, C. M. & Poole, A. W. Loss of the mitochondrial kinase PINK1 does not alter platelet function. *Sci. Rep.* (2018). doi:10.1038/s41598-018-32716-4

113. Barini, E. *et al.* The Anthelmintic Drug Niclosamide and Its Analogues Activate the Parkinson's Disease Associated Protein Kinase PINK1. *ChemBioChem* (2018). doi:10.1002/cbic.201700500

114. Caielli, S. *et al.* Oxidized mitochondrial nucleoids released by neutrophils drive type I interferon production in human lupus. *J. Exp. Med.* (2016). doi:10.1084/jem.20151876